

# Interactions *With* and *Among* the Azobenzene Scaffold in Photoswitches

---

Inauguraldissertation zur Erlangung des Doktorgrades (Dr. rer. nat.)  
der Naturwissenschaftlichen Fachbereiche im Fachgebiet Chemie  
der Justus-Liebig-Universität Gießen

vorgelegt von

**Anne Kunz**

aus Medenbach

Betreuer: Prof. Dr. Hermann A. Wegner

Gießen 2022

## **Versicherung Nach §17 der Promotionsordnung**

Ich erkläre: Ich habe die vorgelegte Dissertation selbstständig und ohne unerlaubte fremde Hilfe und nur mit den Hilfen angefertigt, die ich in der Dissertation angegeben habe. Alle Textstellen, die wörtlich oder sinngemäß aus veröffentlichten Schriften entnommen sind, und alle Angaben, die auf mündlichen Auskünften beruhen, sind als solche kenntlich gemacht. Ich stimme einer evtl. Überprüfung meiner Dissertation durch eine Antiplagiat-Software zu. Bei den von mir durchgeführten und in der Dissertation erwähnten Untersuchungen habe ich die Grundsätze guter wissenschaftlicher Praxis, wie sie in der „Satzung der Justus-Liebig-Universität Gießen zur Sicherung guter wissenschaftlicher Praxis“ niedergelegt sind, eingehalten.

Anne Kunz

Ort, Datum

Dekan: Prof. Dr. Thomas Wilke

Erstgutachter: Prof. Dr. Hermann A. Wegner

Zweitgutachter: Prof. Dr. Richard Göttlich

SOMETIMES,  
SCIENCE IS MORE ART  
THAN SCIENCE. A LOT OF  
PEOPLE DON'T GET THAT.

**Rick Sanchez**

## Table of Contents

Abstract .....	III
Zusammenfassung .....	V
1 Photoswitches .....	1
1.1 Fundamentals of Photoswitches.....	1
1.2 Classification of Photoswitches .....	2
2 Azobenzenes as Photoswitches .....	5
2.1 Concept and Properties of Azobenzenes .....	5
2.2 Interactions Influencing the Isomerization of Azobenzenes.....	6
2.3 Syntheses of Azobenzenes .....	11
3 Combining Photoswitches .....	14
3.1 Challenges in Multiphotochromic Systems.....	15
3.2 Homo-multinary Photoswitches Containing the Azobenzene Scaffold .....	16
3.3 Hybrid-multinary Photoswitches Containing the Azobenzene Scaffold .....	20
4 Contributions to the Literature .....	23
4.1 1+1 $\geq$ 2? Norbornadiene-Azobenzene Molecules as Multistate Photoswitches	23
4.2 Continuous Flow Synthesis of Azobenzenes via Baeyer-Mills Reaction .....	29
4.3 Azobenzene Substituted Triptycenes – Understanding Exciton Coupling of Molecular Switches in Close Proximity.....	37
4.4 Investigation of Alkyl-Aryl Interactions using the Azobenzene Switch – The Influence of the Electronic Nature of Aromatic London Dispersion Donors.....	44
5 Additional Contributions .....	51
5.1 Electrochemically Triggered Energy Release from an Azothiophene-Based Molecular Solar Thermal System .....	51
Abbreviations.....	I
Acknowledgement .....	iii
References .....	v

## Abstract

Azobenzenes, with their ability to undergo a reversible change from the (*E*)- to the (*Z*)-isomer by irradiation with light, have a wide range of possibilities in various fields of research, including host-guest chemistry, information- or energy storage. To successfully incorporate azobenzenes in the previously mentioned applications it is essential to have a thorough understanding of the effects of the interactions *with* or *among* the azobenzene scaffold. Apart from the interactions of azobenzenes with sensitizers, catalysts or solvent molecules, intramolecular interactions also significantly influence their isomerization behavior. For the latter, the role of substituents and their pattern is crucial, as they can influence the electronics and thermodynamics of those systems. In this context, the stabilizing effects of London dispersion forces on different non-symmetric azobenzenes were examined. The strategic introduction of *meta*-alkyl substituents on one phenyl ring and electron rich or poor *meta*-aryl moieties on the other phenyl unit revealed the decisive factor for the observed stabilization *among* the azobenzene scaffold.

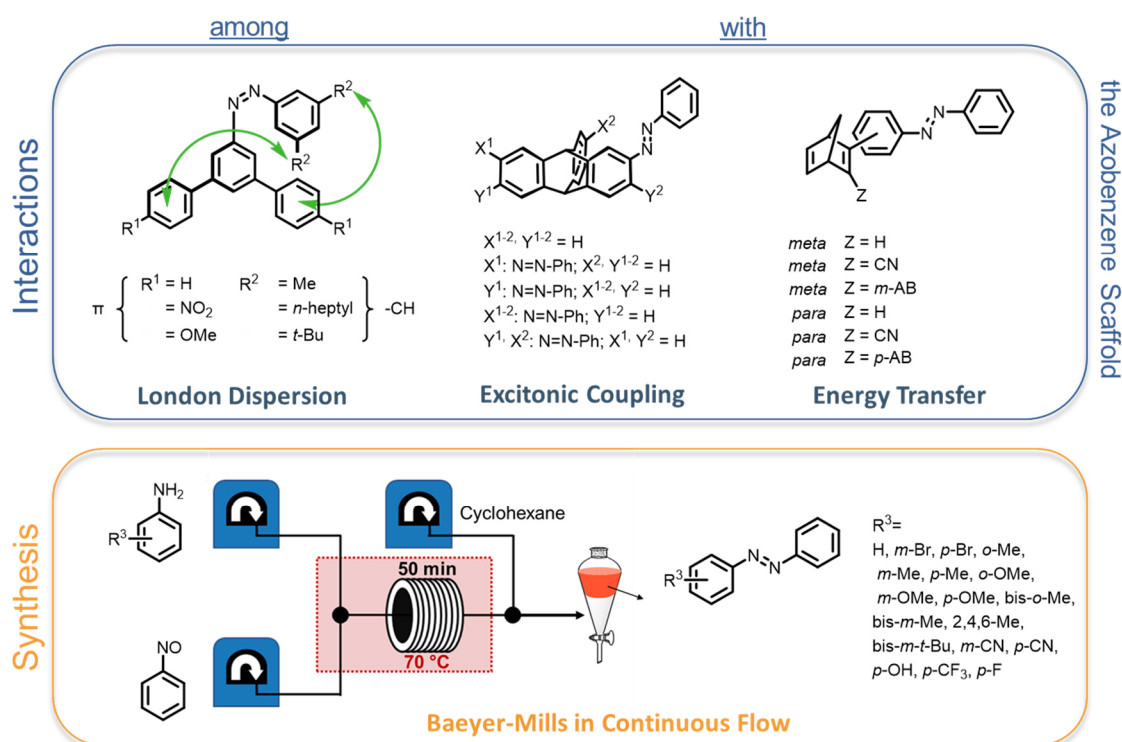


**Figure 1: Possible interactions *with* and *among* azobenzene photoswitches and an azobenzene synthesis strategy in continuous flow setup.**

The addition of one or more photoswitchable units to the azobenzene scaffold as substituent(s), provides multiphotochromic systems with expected increased information and storage density. Nonetheless, complex mixtures can arise, wherein their interplay is still not fully understood. Therefore, the interaction of different photochromic systems *with* the azobenzene scaffold, including the interaction of combined azobenzenes in close proximity, was investigated in this work.

Lastly, the synthesis of azobenzenes was improved by applying the prominent Baeyer-Mills coupling reaction to a continuous flow system. This led to an efficient, reproducible and large scale approach which is essential for future applications of this fascinating compound class.

## Zusammenfassung

Azobenzole eröffnen mit ihrer Fähigkeit, durch Lichteinstrahlung reversibel vom (*E*)- zum (*Z*)-Isomer zu schalten, ein breites Spektrum an Anwendungen in verschiedensten Forschungsbereichen, wie z.B. in der supramolekularen Chemie sowie in der Informations- oder Energiespeicherung. Daher ist es notwendig, die Auswirkungen verschiedener Wechselwirkungen *mit* und *zwischen* dem Azobenzolgerüst im Detail zu verstehen. Abgesehen von den Wechselwirkungen der Azobenzole *mit* Photosensibilisatoren, Katalysatoren oder Lösungsmittelmolekülen haben auch intramolekulare Wechselwirkungen einen erheblichen Einfluss auf ihr Isomerisierungsverhalten. Für Letzteres ist die Rolle der Substituenten und deren relative Position entscheidend. Diese können die elektronischen Eigenschaften sowie die Thermodynamik dieser Systeme beeinflussen. In diesem Zusammenhang wurden die stabilisierenden Effekte der London Dispersion *zwischen* verschiedenen nicht-symmetrischen Azobenzolen untersucht. Durch die Einführung von verschiedenen *meta*-Alkyl-Substituenten an einem Phenylring und elektronenreichen oder -armen *meta*-Aryl-Einheiten am anderen Phenylring, konnte ermittelt werden, welche Faktoren für die beobachtete Stabilisierung des Azobenzols verantwortlich sind.

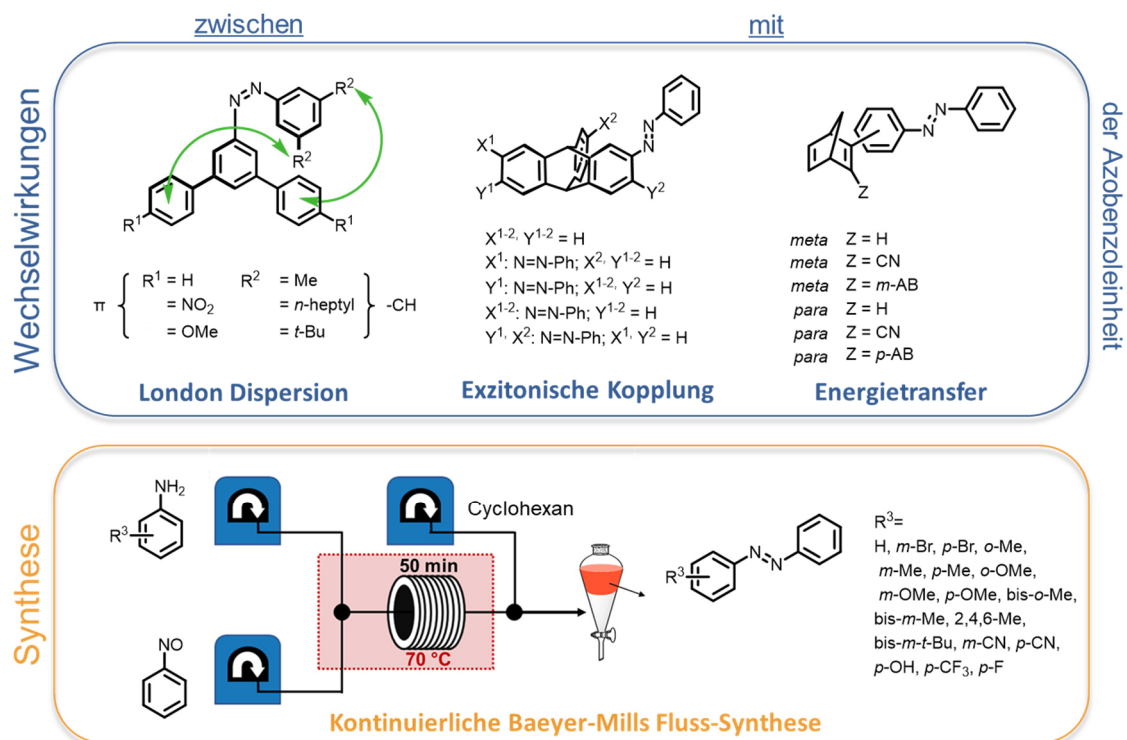


**Abbildung 1: Wechselwirkungen mit und zwischen der Azobenzoleinheit in Photoschaltern, die im Rahmen dieser Arbeit untersucht wurden und die Entwicklung einer kontinuierlichen Fluss Synthese zur Darstellung von Azobenzolen.**

Die Kombination einer oder mehrerer photoschaltbare(n/r) Einheit(en) mit dem Azobenzolgerüst als Substituent(en) führt zu multiphotochromen Systemen mit erwarteter erhöhter Informations- und Speicherdichte. Es können jedoch komplexe Mischungen entstehen, deren Zusammenspiel noch nicht vollständig verstanden ist. Daher wurde in dieser Arbeit die Wechselwirkung verschiedener photochromer Systeme *mit* dem Azobenzolgerüst untersucht, einschließlich der Wechselwirkung von kombinierten Azobenzolen, welche sich in unmittelbarer Nähe befinden.

Außerdem wurde die Synthese von Azobenzolen mit der bekannten Baeyer-Mills-Kupplungsreaktion in ein kontinuierliches Durchflusssystem überführt. Dadurch ist die Reaktion effizient, reproduzierbar und im großen Maßstab möglich und kann für künftige Anwendungen mit dieser faszinierenden Verbindungsklasse genutzt werden.

# 1 Photoswitches

## 1.1 Fundamentals of Photoswitches

Molecules with the ability to reversibly isomerize between a parent molecule (A) and its corresponding photoisomer (B) when applying light as an external stimulus are referred to as photoswitches.<sup>[1]</sup> This takes advantage of the fact that light is a non-embedding energy source that additionally has a high spatial and temporal resolution. It can be simplified for most photochromic molecules, that parent molecule (A) (Figure 2, left), which is typically the most stable isomer, absorbs light in the UV (ultraviolet) or near-UV region and has at least one characteristic absorption maximum at a specific wavelength ( $\lambda_A$ ), while its photoisomer (B) has a different absorption spectrum (Figure 2, right).

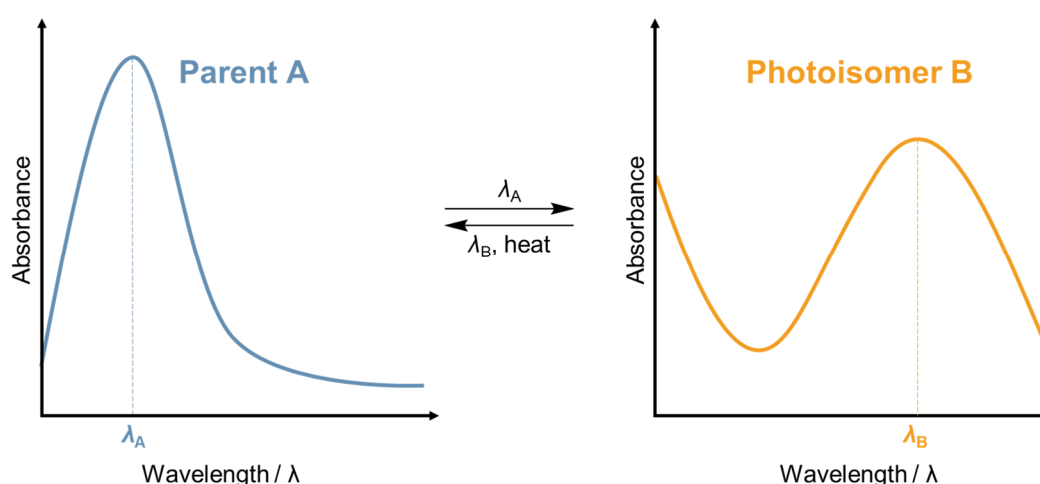


**Figure 2: Schematic absorption spectra of parent molecule (A) and its photoisomer (B).**

When light of this particular wavelength ( $\lambda_A$ ) is shone on the molecule, a photon is absorbed and molecule (A) gets excited from the ground to the excited state. Once this occurs, the molecule has the opportunity to relax back to (A) or convert to its photoisomer (B). For the reversion back from (B) to (A) it can be distinguished between thermal (T-Type) or photo-induced (P-Type) isomerization.<sup>[2]</sup> In general, the performance of a photoswitch can be estimated according to four different parameters:<sup>[3]</sup>

- Quantum yield
- Stability of photoisomers
- Photostationary state
- Reproducibility of photoswitching

The quantum yield is defined as the ratio between photons absorbed and the actual photoisomerization.<sup>[4]</sup> As second parameter, the thermal stability of both photoisomers can be appointed. Depending on the area of application, the respective half-lives ( $t_{1/2}$ ) need to be adjusted, as in some cases, it is beneficial that the photoisomer is present for months or longer; while in other cases shorter half-lives can be favoured. Half-lives are usually measured in solution, which can also have an influence on the stability of the corresponding isomer.<sup>[5,6]</sup> The third parameter is the respective photostationary state (PSS) at a specific wavelength, which describes a constant ratio of photoisomers after exposure to a specific light source (or none). The fourth parameter defines the photoswitchings` reproducibility, which is typically measured in switching cycles. During this experiment, photoisomerization can lead to decomposition or other competing side reactions.<sup>[7-9]</sup>

## 1.2 Classification of Photoswitches

It is therefore not surprising that these molecules get exploited in various fields of research due to their ability to undergo reversible changes, which are expressed in geometry, polarity, electrochemical and optical properties, just to name a few. There are numerous examples of photochromic molecules in organic chemistry, from which a limited selection relevant to this work will be presented. They can be divided into different categories based on the reaction involved in the photoisomerization. Of these categories, proton transfer, (*E*)-(*Z*)-isomerization and cyclization reactions are the most prominent (Figure 3). When we consider the first category, one predominant example is salicylideneanilines (**cis-enol-1**) (Figure 3, a)), also called anils, which are Schiff's bases ( $R_2C=NR'$ ), where R' is a phenyl or substituted phenyl group.<sup>[4]</sup> They can easily be synthesized by condensation of salicylaldehyds with the corresponding anilines. When salicylideneaniline **enol-1** or its derivatives, which are typically yellow, are irradiated with light in the UV region, excited-state intramolecular proton transfer (ESIPT) from the enol to its *cis*-keto form takes place. This *cis*-keto form **cis-keto-1** is subsequently isomerized to its *trans*-keto form **trans-keto-1**. The anil's keto forms usually have a characteristic red color and can be assigned to the T-type, which means they can only be back-isomerized thermally. While the back reaction in solution takes a few milliseconds, it can take seconds up to months in the solid state.<sup>[10-12]</sup>

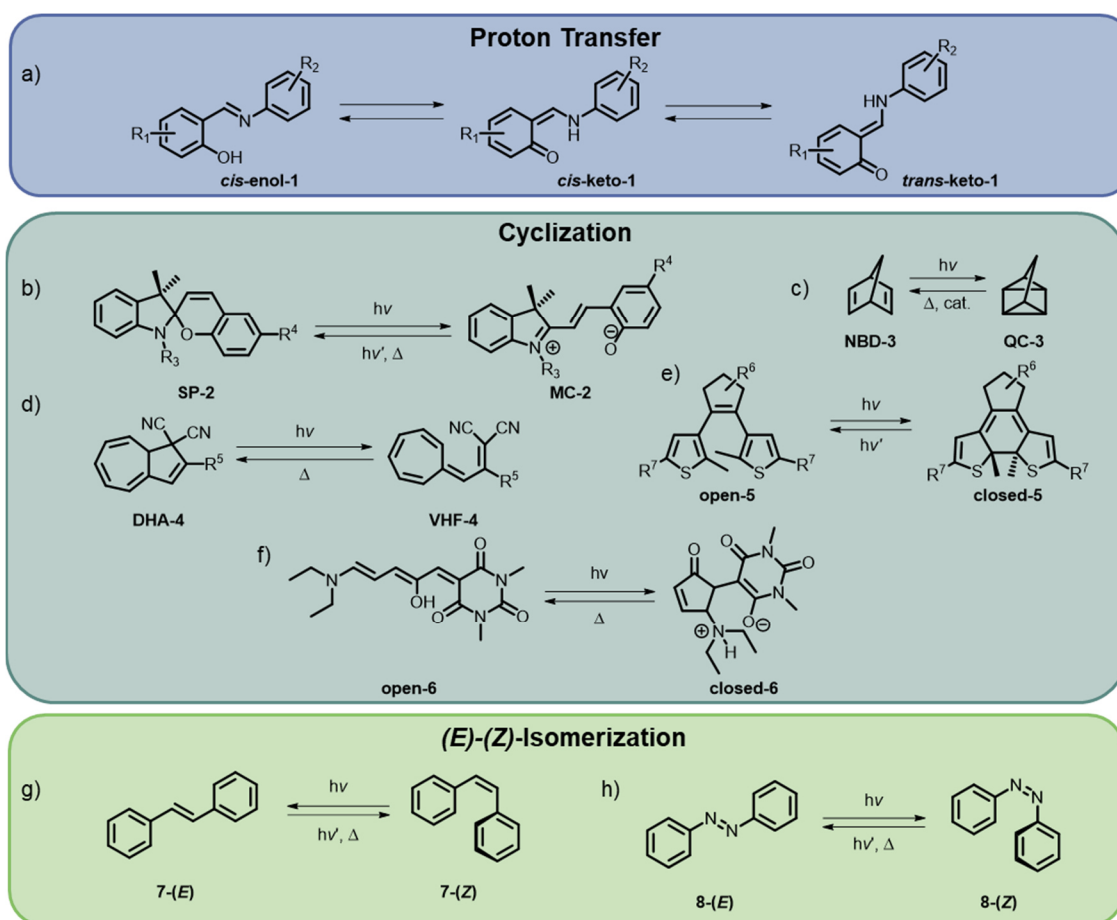


**Figure 3: Classes of photoswitches organized into groups based on their reaction involved in photoisomerization.**

Besides the proton transfer mechanism, several photochromic molecules can be assigned to the cyclization category when separating them by the reaction involved in their photoisomerization. One example of this category is spiropyran (SP) **SP-2**, which can undergo a ring opening reaction by irradiation of UV-light upon C-O cleavage, followed by *cis-trans* isomerization to its merocyanine (MC) form **MC-2**, which is, in contrast to spiropyran **SP-2**, highly conjugated and usually exhibits strong absorption in the visible (VIS) range.<sup>[13–15]</sup> **SP-1** is typically colorless in its closed form due to broken conjugation.<sup>[15]</sup> Merocyanine can be present in its zwitterionic or in its quinonic form.<sup>[15]</sup> The back reaction from merocyanine **MC-2** to spiropyran **SP-2** occurs thermally, classifying them as T-type. Another member of this family is dihydroazulene **DHA-4** (Figure 3, d)). **DHA-4** undergoes a retro-electrocyclization, which involves a carbon-carbon bond cleavage, by irradiation to its photoisomer vinylheptafulvene (VHF) **VHF-4**.<sup>[16]</sup> VHF typically has a redshifted absorption maximum at around 470 nm, which makes it colored compared to its photoisomer DHA. Moreover, it is associated as T-type. While the ring-opening proceeds quite fast,<sup>[17,18]</sup> the ring-closing

takes longer.<sup>[19–21]</sup> Their ability to isomerize completely to both isomers, makes them interesting for applications as solar fuels or information storage systems.

Donor-acceptor Stenhouse-adducts (DASA, Figure 3, f)), which are T-type photoswitches, isomerize with light of the visible or near infrared range from the colored neutral linear isomer **open-6** to colorless zwitterionic cyclic form **closed-6**.<sup>[22–24]</sup> Another photoswitch, which is based on a  $6\pi$ -electrocyclization, is dithienylethene (DTE, Figure 3, e)) **open-5**. By irradiation of UV light, a ring closure occurs to its corresponding photoisomer **closed-5**. Because of  $\pi$ -conjugation in its closed form, this photoisomer has a red shifted absorption maximum in comparison to its open form, where  $\pi$ -conjugation is enabled.<sup>[25]</sup> The open photoisomer is thermally stable and can only be back-isomerized by irradiation of visible light, which classifies them as P-type. Norbornadiene (NBD) has a bicyclic structure with two isolated double bonds and can undergo a [2+2]-cycloaddition to the corresponding metastable quadricyclane (QC) (Figure 3, c)).<sup>[26–29]</sup> In contrast to the previous examples, NBDs experience negative photochromism during the photoisomerization process, by decolorization from yellow NBD to colorless QC, resulting in a hypsochromic shifted spectrum. During this photoisomerization the molecule's ring strain nearly doubles, resulting in an increased energy difference, which can be exploited for the potential use as molecular solar thermal energy storage systems (MOST).<sup>[30–33]</sup> QC can be instantly isomerized back to NBD by an external trigger, e.g. electrochemically or by catalysts.<sup>[34–40]</sup> Although its unsubstituted form **NBD-3** has the advantage of high energy density, it can only be converted to **QC-3** by photosensitizers,<sup>[41,42]</sup> is volatile, air sensitive and prone to polymerization upon irradiation.<sup>[43–45]</sup> Accordingly, the photochemical properties of NBD can be modified by introducing substituents. For example, by introducing electron donating as well as electron withdrawing substituents at C2 and C3, the spectrum of NBD can be redshifted, eliminating the need of a photosensitizer; however, this is at an expense of drastically reduced half-lives (Figure 4).<sup>[46–48]</sup>

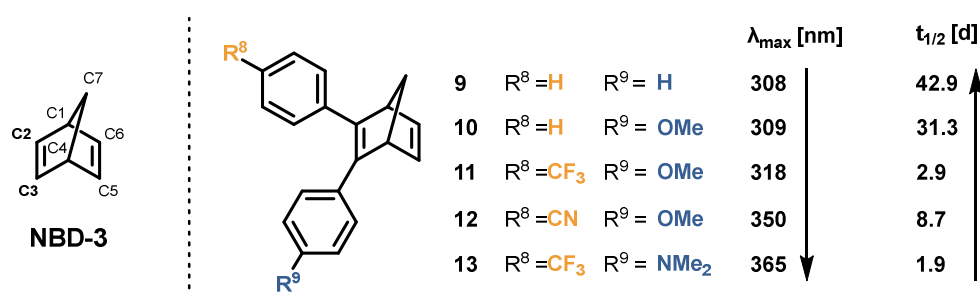


Figure 4: Diaryl-substituted NBDs 9-13 and their absorption maxima and half-lives in toluene.<sup>[46]</sup>

## 2 Azobenzenes as Photoswitches

### 2.1 Concept and Properties of Azobenzenes

Similar to the concept of stilbenes (Figure 3, g)), another class of photoswitches are azobenzenes (AB), which can be assigned to the family of (*E*)-(*Z*) isomerization. ABs typically consist of two phenyl groups connected by a nitrogen-nitrogen double bond (N=N) (Figure 3, h)). Since they were discovered about 190 years ago, they are mostly known for their applications as dyes, pigments and indicators because of their characteristic color and intensity (Figure 5, b)).<sup>[49,50]</sup>



**Figure 5: a) UV-Vis spectra of unsubstituted AB 8 in *n*-decane. Red spectrum: 8-(*E*), black spectrum: 8-(*Z*). b) Solid AB 8. c) Isomerization and characteristics of unsubstituted AB 8.<sup>[6]</sup>**

In recent years, the application areas for ABs have increased dramatically, where their properties are exploited in energy and information storage, organocatalysis, photobiology and photopharmacology, host-guest chemistry, molecular mechanics, molecular machines and other areas of research.<sup>[5,51-62]</sup> These versatile applications can be attributed to the fact that ABs can switch between their energetically favorable (*E*)-isomer and the energetically less favorable (*Z*)-isomer by irradiation of light, which was only reported in 1937 by Hartley several years after their original discovery.<sup>[49,63]</sup> They are synthetically well accessible, exhibit robust handling and moreover, their isomerization process can be followed by UV-Vis spectroscopy (Figure 5, a)).<sup>[6]</sup> While the (*E*)-isomer exhibits a strong  $\pi$ - $\pi^*$  absorption around 300-350 nm, depending on the substitution pattern and solvent, and a weak  $n$ - $\pi^*$  absorption at around 450 nm, the (*Z*)-isomer has a decreased  $\pi$ - $\pi^*$  and a marginally increased  $n$ - $\pi^*$  absorption band (Figure 5, a)).<sup>[64]</sup> By irradiation with light in these characteristic absorption bands, the

AB can be switched photochemically either from (*E*)→(*Z*) with 300-350 nm or from (*Z*)→(*E*) with light of around 450 nm. Additionally, ABs can relax back to their energetically favored isomer thermally or electrochemically.<sup>[65,66]</sup> However, by isomerization not only the photochemical properties change but also their geometry, polarity and electronic properties (Figure 5, c)).<sup>[67-71]</sup> The (*E*)-isomer of ABs follows a  $C_{2h}$ -symmetry and is planar, while the (*Z*)-isomer exhibits a non-planar  $C_2$  symmetry with a distorted arrangement of the phenyl-rings (unsubstituted AB). In this process, the system's geometry changes drastically from 9.1 Å to 6.2 Å, which, among others, makes them extremely interesting for the usage in molecular machines.<sup>[68,72]</sup>

## 2.2 Interactions Influencing the Isomerization of Azobenzenes

This characteristic isomerization behavior of ABs can be influenced by external or internal interactions. For example, the half-life of the corresponding metastable (*Z*)-isomer is drastically dependent on the solvent system. Among other things, it can be explained by the respective mechanism of the thermal back isomerization, which in turn is dependent on the substitution of the AB. When electron donating as well as electron withdrawing substituents are attached on opposing phenyl rings of the AB scaffold, a rotational mechanism of thermal back isomerization is proposed.<sup>[73]</sup> The dipolar transition state of these so-called “push-pull”-systems can be stabilized by polar solvents or solvents with acidic protons, which subsequently leads to a shorter half-life and accelerated isomerization rate of the metastable (*Z*)-AB of test systems in certain cases by a factor of over 3000.<sup>[74]</sup> If the thermal back isomerization is based on an inversion mechanism, the trend for the isomerization rate and half-life is also inverted and accordingly prolonged.<sup>[75,76]</sup> This is due to a stabilization of the (*Z*)-isomer as well as the destabilization of the corresponding transition state of electronically neutral ABs.<sup>[77,78]</sup> There are also various other aspects of the chosen solvents that need to be considered as they can influence the isomerization of AB.<sup>[79]</sup>

Additionally, the isomerization behavior can be influenced by involvement of a catalyst or photosensitizer. It was already shown in 1958 by Schulte-Frohlinde that (*Z*)→(*E*)-a large number of different catalysts can trigger AB thermal back isomerization.<sup>[80]</sup> When for example thiophenol is added, the half-life of (*Z*)-isomer **8** decreases from 16 h to 7.5 h (in benzene). Additionally, different Brønsted or Lewis acids like salicylic acid, hydrochloric acid or tricoordinated phosphorus compounds can be used to decrease half-lives.<sup>[80-84]</sup> An additional approach is the electrocatalytic (*Z*)→(*E*) isomerization.

Hecht and co-workers showed that the isomerization can be initiated either by an oxidative (hole catalysis) or reductive (electron catalysis) reaction channel.<sup>[65,66]</sup> When the reaction is triggered by an oxidative reaction channel, a chemical oxidant or a photosensitizer like methylene blue as an initiator (oxidation or sensitization, respectively) is needed for the formation of a radical cation. Depending on hole or electron catalysis, the radical anion or cation performs  $Z^{\bullet+/-} \rightarrow E^{\bullet+/-}$  isomerization and can subsequently transfer the radical onto other (Z)-8 molecules (Figure 6, a)).<sup>[65,66]</sup> Heteroaryl-AB **14** can be used to avoid oxidized byproducts from initiation (Figure 6, b)).<sup>[85]</sup> Furthermore, thio-AB **15** was isomerized by electron catalysis for potential solar fuel applications, while in this case hole catalysis led to decomposition (Figure 6, c)).<sup>[86]</sup> Photosensitizers are mostly known for sensitizing (Z)→(E)-isomerization, while fewer examples for sensitizing the (E)→(Z)-isomerization are known, which would be especially interesting for applications as solar fuels, where the light of the whole solar spectrum should be exploited.<sup>[87]</sup> Though using a photosensitizer for the (E)→(Z)-isomerization wavelength of over 600 nm can be used to enable the isomerization, this often leads to a smaller quantum yield.<sup>[88,89]</sup>

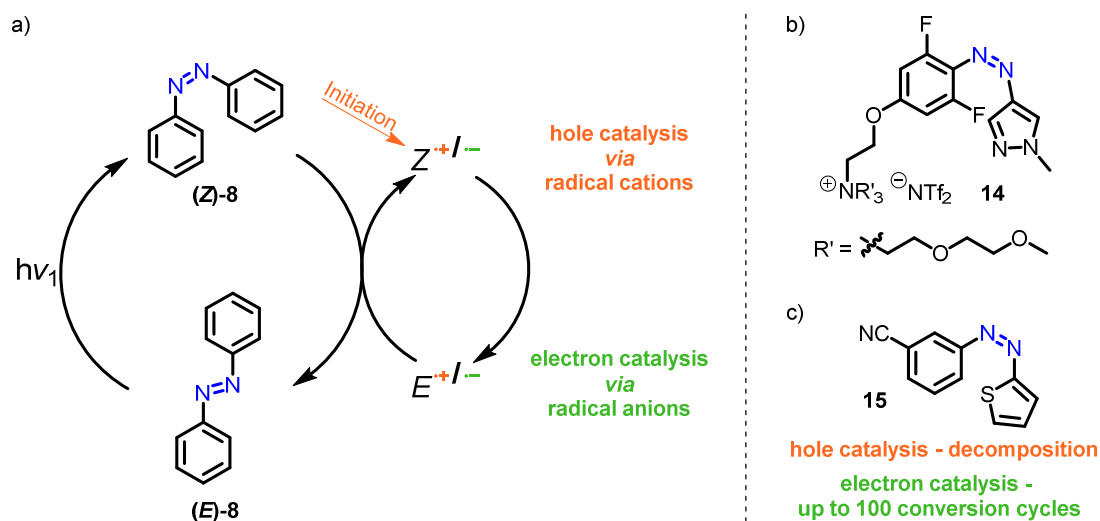


**Figure 6:** a) Principles of electrocatalytic (Z)→(E) isomerization of ABs.<sup>[65,66]</sup> b) Heteroaryl-AB **14** avoiding oxidated products while initiation of electrocatalytic isomerization. c) Candidate thio-AB **15** for electrocatalytic (Z)→(E)-isomerization presented in this work.

### 2.2.1 Influence of Substituents on Azobenzene Derivatives

As previously mentioned, the parameters of AB photoswitches can also be influenced through the attachment of substituents on the corresponding phenyl ring(s). This can drastically affect the parameters of the photoswitch like its absorbance, quantum yield, half-life and electrochemical properties, among others. Based on the different spectroscopic characteristics, Rau divided ABs into three categories: *azobenzenes*,

*aminoazobenzenes* and *pseudo-stilbenes* (Figure 7).<sup>[90]</sup> The first class, *azobenzenes*, consists of unsubstituted AB as well as ABs, which are substituted with alkyl, aryl, halide, carbonyl, amide, nitrile, ester and carboxylic acid substituents. In this class, the  $\pi$ - $\pi^*$  and the  $n$ - $\pi^*$  are well separated and the thermal back reaction is typically in the minute to days range (Figure 7, left). The second class includes ABs with amino, hydroxyl- and alkoxy-groups in *ortho*- or *para*-position (Figure 7, middle). In this class the  $\pi$ - $\pi^*$  absorption maximum can be redshifted, so that it overlaps with the  $n$ - $\pi^*$  absorption maximum. This can result in difficulties in addressing the respective transition and also assigning the quantum yields.<sup>[88,91–95]</sup> Moreover, their half-lives are usually lower than for *azobenzenes*. *Pseudo-stilbenes*, the third class, consist of protonated ABs and “push-pull” systems (Figure 7, right). By introducing a strong electron donor on one phenyl ring and a strong electron acceptor on the other in 4 and 4' position, the energy of the  $\pi$ - $\pi^*$  decreases resulting in a red shifted spectrum. The reason for this is simultaneous destabilization of the HOMO and stabilization of the LUMO.<sup>[5,96–101]</sup> Additionally, these “push-pull”-systems exhibit intermolecular charge transfer (ICT).<sup>[102]</sup> This class can also be characterized by its decreased half-life in the second to millisecond time range, in comparison to the other classes. Because of the electronic as well as their steric effects, the regiochemical substitution of the phenyl rings is also essential. Here it has to be distinguished between *ortho*-, *meta*- and *para*-connection (Section 3.2.1).<sup>[103]</sup>

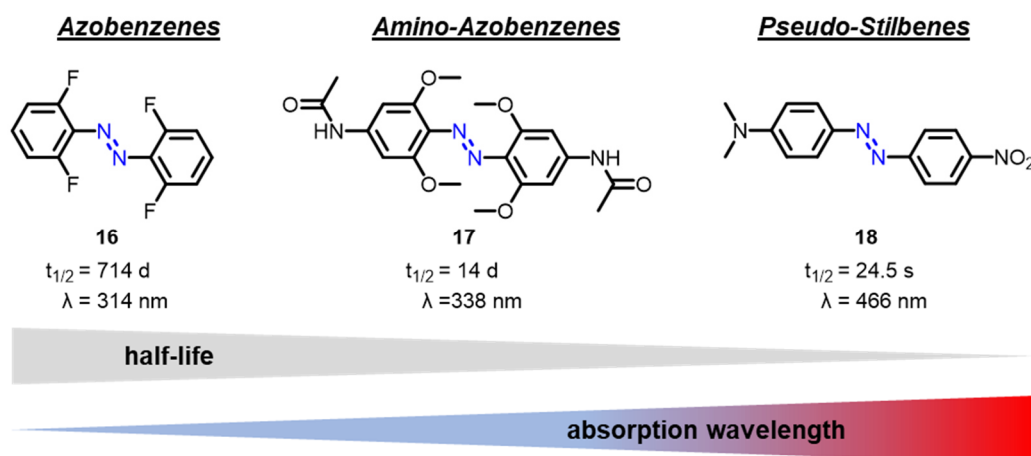


**Figure 7: Representative ABs for the different categories: *azobenzenes*<sup>[104]</sup>, *amino-azobenzenes*<sup>[104]</sup> and *pseudo-stilbenes*<sup>[105]</sup> together with their absorption maxima as well as the half-life of their corresponding (Z)-isomer in DMSO (16, 17) and toluene (18).**

Furthermore, through the buildup of ring strain around the AB scaffold, the thermodynamics can be influenced to such an extent that their (Z)-AB becomes the most stable isomer (Figure 8).<sup>[106–108]</sup> An example for this is bridged-AB (Z)-19,

investigated by Siewertsen *et al.*. It can be switched to ~90% (*E*)-**19** and back with light of 520 nm to its energetically favored (*Z*)-**19** to 100%, which can be explained by good separation of the  $\pi$ - $\pi^*$  and  $n$ - $\pi^*$  absorption bands (Figure 8, left).<sup>[107]</sup> Cyclic (*Z,Z*)-**20**, with the same inverted stability, can be isomerized by laser or Hg-lamp to (*E,E*)-**20**, which has a half-life of 20 days before it converts to its (*E,Z*)-isomer, which is quite unstable due to increased ring strain with a half-life of ~1 s.<sup>[108]</sup> In contrast to the previously mentioned examples, (*Z,Z*)-**21** can only be photoisomerized to the (*E,Z*)-**21**-isomer, which, due to its half-life in the millisecond range, could only be observed through ultrafast spectroscopy measurements.<sup>[109]</sup>

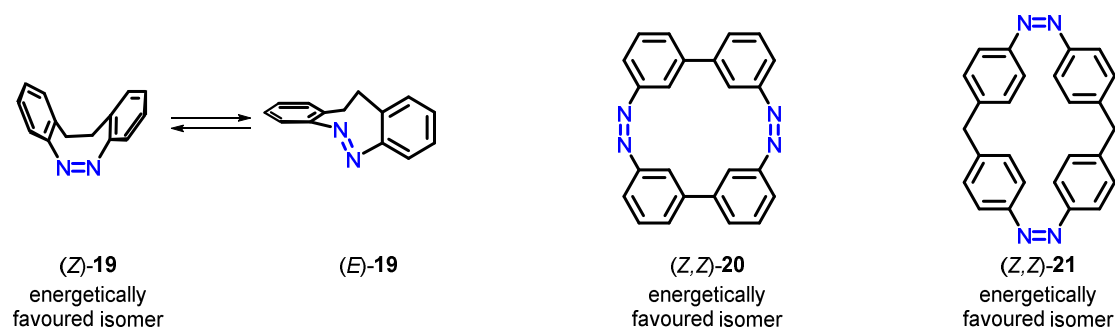
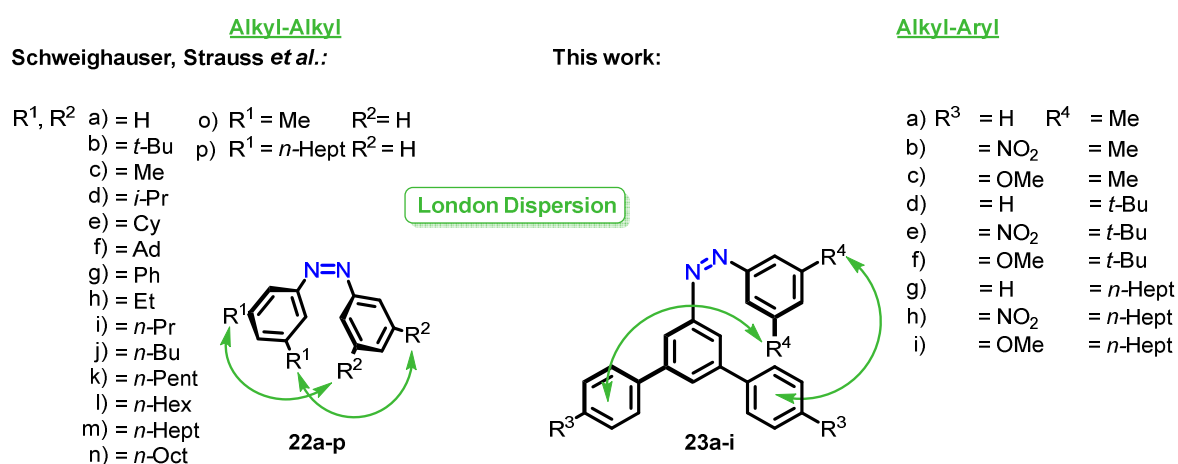


Figure 8: Examples of inverted stability of photoisomers in AB derivatives 19-21.

### 2.2.2 London Dispersion Among the Azobenzene Scaffold

The previous section (2.2.1) showed that substituents can drastically affect the electronic nature of the AB scaffold and thus influence various (photochromic) properties. Nonetheless, influences *among* the AB scaffold through interactions within the substituents can also change the properties of AB. Although the strength of London dispersion, the attractive part of the van der Waals equation, is relatively weak, it increases with increasing sizes of the electron shell of interacting atoms. It can thus affect specific parameters of certain systems.<sup>[110,111]</sup> Those stabilizing effects were demonstrated for example by enabling long C–C bonds in adamantyl dimers,<sup>[112]</sup> stabilizing deoxyribonucleic acid (DNA) helices<sup>[113]</sup> or aiding in the aggregation of rhodium complexes.<sup>[114]</sup> Initially, it seemed counterintuitive that larger groups on both phenyl groups of ABs in *meta*-position did not lead to destabilization due to steric hindrance in the (*Z*)-isomer, but rather to stabilization due to the attractive interactions described above. This in turn, led to a prolonged half-life of the (*Z*)-photoisomers.<sup>[6,76,115]</sup> L. Schweighauser *et al.*<sup>[76]</sup> as well as M. Strauss *et al.*<sup>[6,115]</sup> investigated the photochemical properties of different alkyl-substituted AB derivatives and found that even flexible alkyl chains like *n*-Bu (**22j**) can cause increased half-lives

of the (*Z*)-isomer, which are up to five times prolonged in comparison to their *meta*-Me-substituted AB-derivatives (**22c**) (*n*-decane as solvent, Figure 9). It has to be mentioned that the solvent system also plays an important role when arguing with London dispersion.<sup>[116]</sup> Therefore, for substituted AB derivatives in polar solvents as DMSO for example, solvophobic contributions dominate for alkyl chains longer than *n*-hex. In the work of Schweighauser *et al.* and Strauss *et al.* it was shown that although the stabilizing alkyl-alkyl interactions in the (*Z*)-conformation have the most decisive influence on the increased half-life, alkyl-aryl interactions can also be contributors. To disbar the alkyl-alkyl interactions and put a focus on just the aryl-alkyl interactions as work of this thesis, nine different AB derivatives were synthesized and investigated. They are substituted in *meta*-connection with Me, *t*-Bu and *n*-hept on one phenyl ring and with electron donating (*p*-OMe), electron withdrawing (*p*-NO<sub>2</sub>) and unsubstituted phenyl-rings in *meta*-connection on the opposite phenyl ring relative to the corresponding azo unit (Figure 9).<sup>[117]</sup> To get a deeper understanding of how important the electronic structure of the  $\pi$ -donor is in alkyl-aryl-substituted AB-derivatives **23a-i**, their respective half-lives were measured in *n*-octane (Figure 10). The half-lives for *n*-heptyl as well as for *t*-Bu-substituted ABs **23d-i** are increased, which can be attributed to alkyl-aryl-interactions, independent of their electronic structure on the aryl fragment. <sup>1</sup>H NOESY NMR experiments revealed that these interactions are not present in the Me-substituted derivatives **23a-c**.



**Figure 9:** Reported alkyl-alkyl and aryl-alkyl interactions in different substituted ABs from Strauss, Schweighauser *et al.* (**22a-p**), as well as from current work of this thesis (**23a-i**).

In conclusion, the kinetic data revealed that the strength of the London dispersion donor of the alkyl-substrate is the crucial factor for the observed stabilization and that the substitution at the aryl-fragment has a significantly smaller impact.

These previous examples clearly point out that there is a great variety of parameters that influences the quantum yields, half-lives ( $t_{1/2}$ ) as well as the batho- or hypsochromic shifts of AB derivatives; but it is also shown, that by influencing one parameter often another one changes simultaneously.

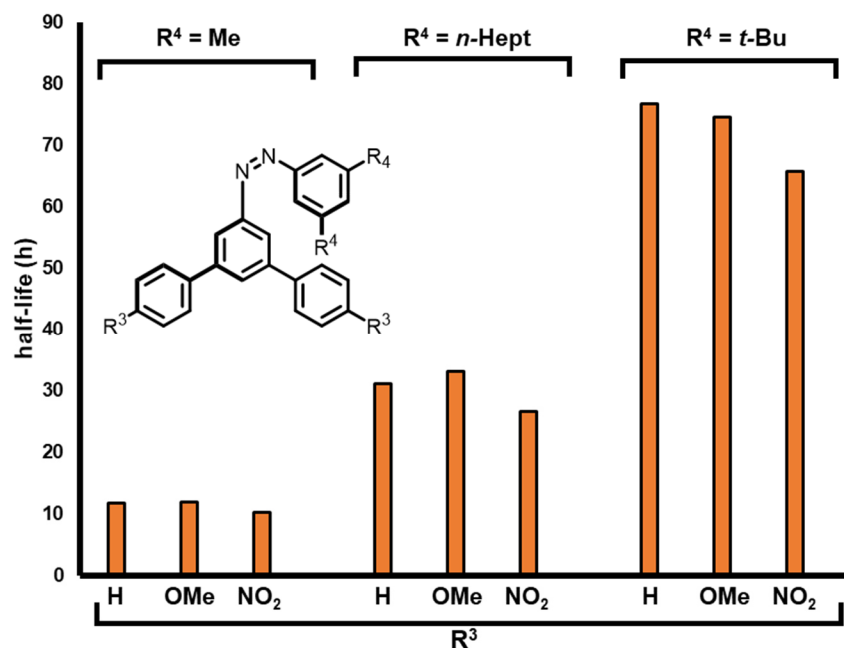
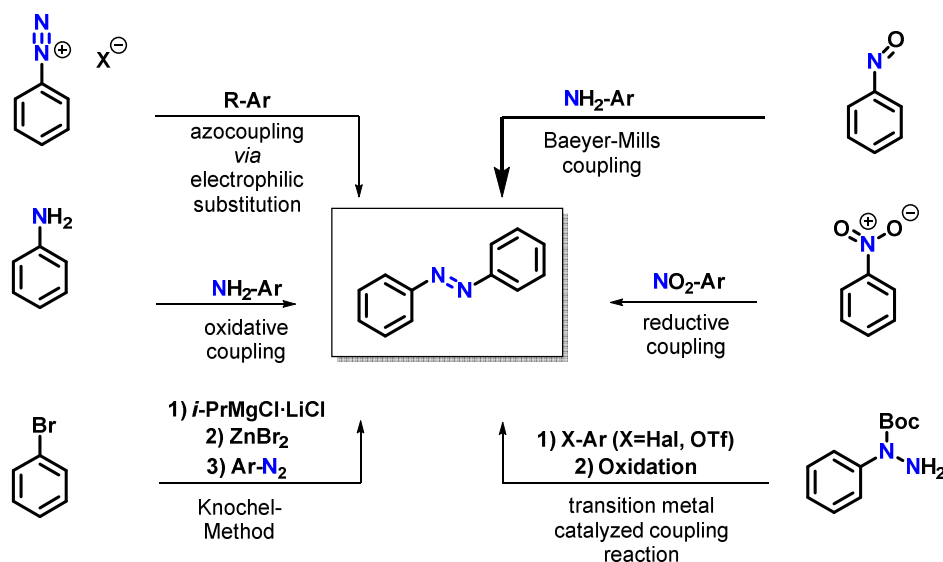


Figure 10: Half-lives of AB-derivatives 23a-i in *n*-octane.<sup>[117]</sup>

### 2.3 Syntheses of Azobenzenes

The previous chapters demonstrated the importance of substitution effects in detail. In order to enable various substitution patterns for the desired properties of the subsequent applications, suitable syntheses options must be accessible. Depending on final compound's design, there are various reactions to choose from, where the best synthesis must be individually selected.<sup>[118]</sup> Here, some elected examples of well-established azocouplings are presented (Scheme 1). Symmetrical ABs, where both phenyl entities are identically substituted, can be constructed by coupling one precursor with itself. In this incident, oxidative or reductive azo coupling can be mentioned as an example, where two anilines or aryl-nitro compounds react with each other.<sup>[118–127]</sup> Although these strategies can also be used to build up non-symmetrical ABs, lower yields are expected, as there can be different coupling results. Azocouplings, like the reaction of diheteroarylzincs with aryldiazonium salts (Knochel-method) or Pd-catalyzed couplings of aryl-halides with hydrazines followed by an oxidation, can be used to build up different substituted non-symmetrical and symmetrical AB derivatives in an effective way.<sup>[128,129]</sup> The classic method for

synthesizing ABs is the azocoupling of diazonium salts with electron-rich aromatics as nucleophiles.<sup>[130]</sup> The substitution takes place in *para*- or *ortho*-position and also hetero-aryl ABs can be built up with this method.<sup>[131]</sup> A well-established synthesis of symmetric, as well as non-symmetric ABs is the so-called Baeyer-Mills coupling reaction. While it was first published by Baeyer in 1874, it was afterwards investigated in further detail by Mills.<sup>[132,133]</sup> This reaction includes the condensation of nitrosobenzenes with anilines. The corresponding ABs are formed by nucleophilic attack of the aniline to the nitrosobenzene in acidic or basic media.<sup>[134,135]</sup> Based on this mechanism, the best results are obtained when the reaction proceeds when using electron-deficient nitrosobenzenes with electron-rich anilines. Nitrosobenzenes can easily be synthesized by oxidation of the corresponding amines with e.g. acetic acid/H<sub>2</sub>O<sub>2</sub>, *meta*-chloroperbenzoic acid or OXONE<sup>®</sup> as oxidation agent in a biphasic system.<sup>[136]</sup> To apply ABs as functional materials, the compounds have to be accessible in a large scale and moreover in a reproducible and effective way. One possibility to overcome the complications of a batch synthesis, such as chemoselectivity, kinetics control, material output, solvent consumption, precise control of T and concentration, flow synthesis can be an option.<sup>[137]</sup>



**Scheme 1: Strategies for synthesizing AB derivatives.**

Even though continuous flow was previously used to synthesize symmetric ABs *via* Cu-catalysis, non-symmetric ABs cannot be efficiently synthesized in this way.<sup>[138,139]</sup> Therefore, the Baeyer-Mills coupling reaction in continuous flow was implemented, considering it is well established for synthesizing non-symmetric ABs in a good yield in batch.<sup>[140]</sup> The applicability of the reaction in continuous flow was confirmed with a

scope of 20 substances, including anilines with electron-donating as well as electron-withdrawing substituents (Figure 11, a)). Moreover, the scalability was demonstrated by synthesizing ~70 g of an azobenzene derivative applied as an energy storage system.

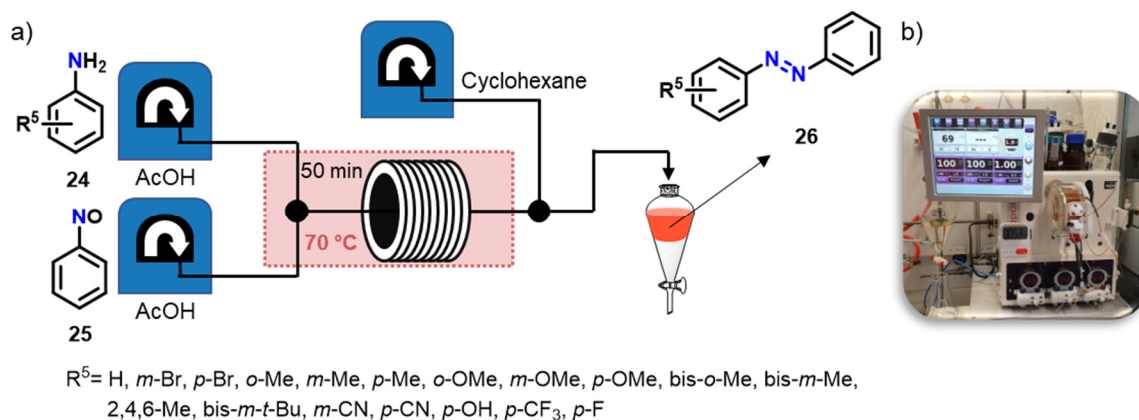


**Figure 11: a) Continuous flow synthesis of substituted anilines 24 with nitrosobenzene 25 to obtain the respective ABs 26. b) Picture of flow apparatus.**

### 3 Combining Photoswitches

As previously described, photoswitchable molecules consisting of just one photoswitchable unit can be rather complex and still show properties that are not examined in its entirety yet. By optimizing one specific factor, another is often changed concurrently; therefore, optimizing the photoswitch for the respective usage can still be challenging, but it is worth examining considering their broad area of possible applications. This area is even broader when photoswitchable units get combined. Combined photoswitches open new possibilities, for example in MOST systems. The ability to store solar energy in the molecule itself by photoisomerization is exploited in these systems. In Figure 12, the general concept of MOST is depicted. In a solar collector the parent molecule (A) is isomerized to its energetically higher lying isomer (B), ideally with light of the solar spectrum. This metastable isomer is then stored in a reservoir. If heat is needed, an external trigger (catalyst etc.) can initiate the back isomerization and the stored energy is released in the form of heat. By combining more than one photoswitchable unit, the energy of the sun can in principle be stored in both photoisomers, increasing the energy density and also gradual release of the energy can be enabled.<sup>[2,141–144]</sup>

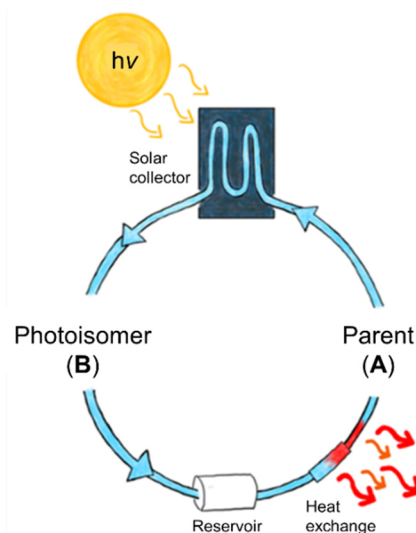


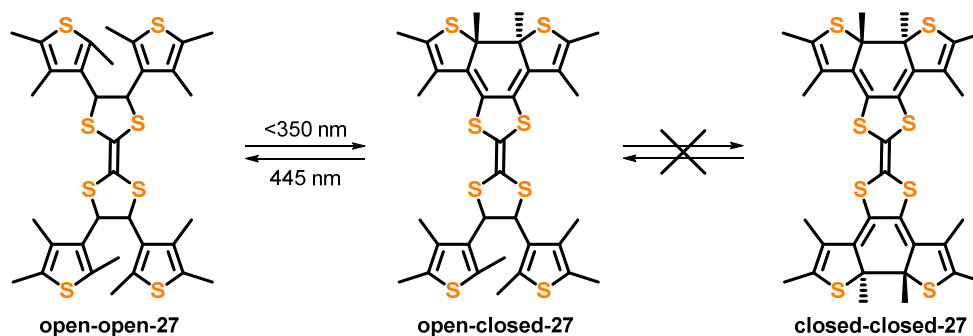
**Figure 12: General concept of a MOST-system.**

Additionally, to the improvement of MOST systems, combining photoswitches also enhances the performance of information storage systems. Due to the ability to switch reversibly between two photoisomers (A/B), they can be considered as logical units with “on/off” or “0/1” behavior.<sup>[2,53]</sup> This information can be read out by analyzing the absorbance of a particular wavelength, which is different for both photoisomers. By linking one or more photoswitches with each other, the information density increases

because of a resulting enlarged number of photoisomers. The number of photoisomers is dependent on the type of linkage (Figure 13). While the number in an acyclic system with  $n$  different photochromic units is maximum  $2^n$ , the number of isomers in a cyclic system can be more complex.<sup>[144]</sup> It can also differ when the multiphotochromic compound consists of the same or different photoswitches. Additionally, combined photoswitches can have additional advantages in host-guest chemistry or molecular machinery.<sup>[57–59]</sup>

### 3.1 Challenges in Multiphotochromic Systems

Besides the advantages of fusing photochromic systems in MOST and information storage systems, there are also challenges which have to be overcome.<sup>[145–147]</sup> Because of the complexity of multiphotochromic systems, it is important that the general ability to isomerize is maintained, while other properties are added or even improved. Depending on the application, the design must be adapted beforehand. For example: for MOST applications or host guest systems it can be useful to isomerize both photoswitchable units simultaneously, while it could be more beneficial for information storage system when both units can be switched independently from each other with light of different wavelengths. Therefore, it is crucial to have a proper energy match of the absorption wavelength of both moieties to ensure switching of either both photochromic units simultaneously, or only one selectively.



**Scheme 2: Dimer photoswitch DTE 27. The intramolecular energy transfer between the open and the closed entities in 27 prevents a second ring closure to closed-closed 27.<sup>[148]</sup>**

Furthermore, the addition of another photochromic unit can affect and reduce the quantum yield of one or both respective processes. Additionally, strong conjugation over the whole system can prevent the switchability of the photochromic entities because of energy transfer between them. An example of that is dimeric dithienylethene **open-open-27**, where one entity undergoes ring closure to **open-closed-27**. Intramolecular energy transfer quenching prevents a second ring closure

to the **closed-closed-27** (Scheme 2).<sup>[148]</sup> Strong conjugation of combined photoswitches can be broken upon introduction of non-conjugative linker between the photochromic moieties or by connectivity in *meta*-position, leading to independent photoswitching (Section 3.2.1).<sup>[103,149,150]</sup>

### 3.2 Homo-multinary Photoswitches Containing the Azobenzene Scaffold

Although the number of novel multinary photoswitches consisting of different photoswitchable entities has increased in the last years,<sup>[103,144,151–155]</sup> the following section focuses particularly on understanding combined ABs in multinary photoswitches. Here, it can be distinguished between directly linked azobenzene multinary photoswitches (AMPs) on the same phenyl ring and AMPs, which are connected by a core unit or linker, which can be conjugative or non-conjugative. Depending on the number and type of linked ABs, there could be linear, branched or macrocyclic AMPs (Figure 13). Due to the enlarged number of AMPs, only selected AMPs will be discussed in the following section. For a detailed description of almost all AMPs see a detailed review article by Venkataramani and co-workers.<sup>[151]</sup>

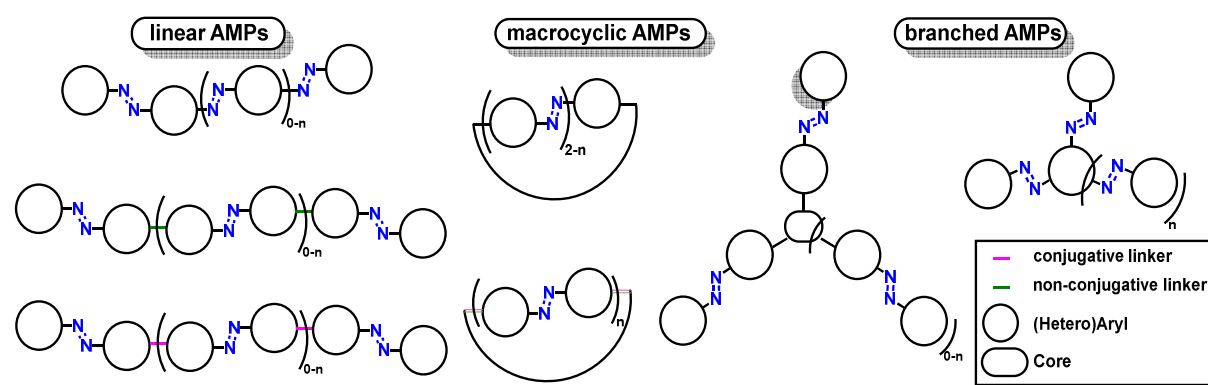
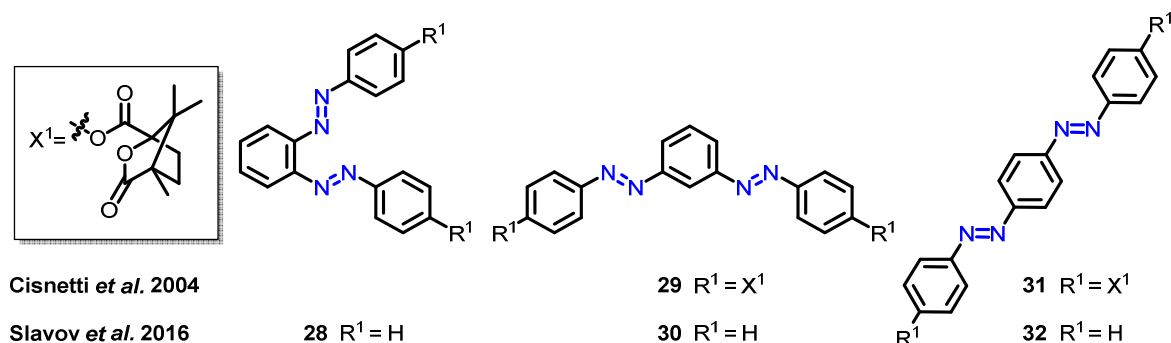


Figure 13: Schematic overview of different types of ABs in homo-multinary photoswitches.

#### 3.2.1 AMPs connected on one Aryl-Unit

When the ABs in AMPs are directly connected on the same phenyl ring, there is always interaction between the two or more photochromic units, either by  $\pi$ -conjugation or excitonic coupling between them. Depending on *ortho*-, *meta*- or *para*-linkage the electronic communication between the units is drastically affected. The importance of the pattern was first demonstrated by Cisnetti *et al.* by combination of two substituted ABs in *meta*- and *para*-connection.<sup>[156]</sup> In this study it was already evident that electronic communication in *para*- was stronger than in *meta*-position.



**Figure 14: Bis-ABs in *ortho*-, *meta*-, as well as *para*-connectivity**<sup>[103,156]</sup>

A more detailed analysis was conducted by combination of two unsubstituted AB-moieties in *ortho*-, *meta*- and *para*-connection by Slavov *et al.* (Figure 14).<sup>[103]</sup> When separated in *ortho*-position (**28**), the spectral properties and also the quantum yield were similar to unsubstituted AB, but its thermal back conversion from (*Z*)- to (*E*)-AB arises in milliseconds due to intramolecular excitonic coupling. Construction of the two ABs in *para*-position (**32**) leads to high  $\pi$ -conjugation between them and therefore, a red-shift of the spectrum from 320 up to  $\sim$ 360 nm was observed, but the quantum yield was drastically decreased. On the contrary, the isomerization behavior of the two AB moieties in *meta*-position (**30**) was almost independent of each other, which can be explained by less  $\pi$ -conjugation between them ("*meta*"-rule).<sup>[103]</sup> If AMPs are desired where all entities isomerize orthogonally, their absorption maxima should at least not completely overlap. Keeping the influence of linkage in mind, the impact of substituents is still crucial. This interplay was demonstrated after Lim *et al.* reported the synthesis of different C<sub>3</sub> symmetrical 1,3,5-tris-ABs in 2004 (Figure 15, a))<sup>[157]</sup> and Yang *et al.* calculated different substitution patterns for these types of AMPs with the goal to shift the absorption bands of each AB individually so that orthogonal switching is possible. Moreover, *meta*-connection was chosen to prevent influences of the ABs with each other in a significant manner (Figure 15, b)).<sup>[158]</sup>

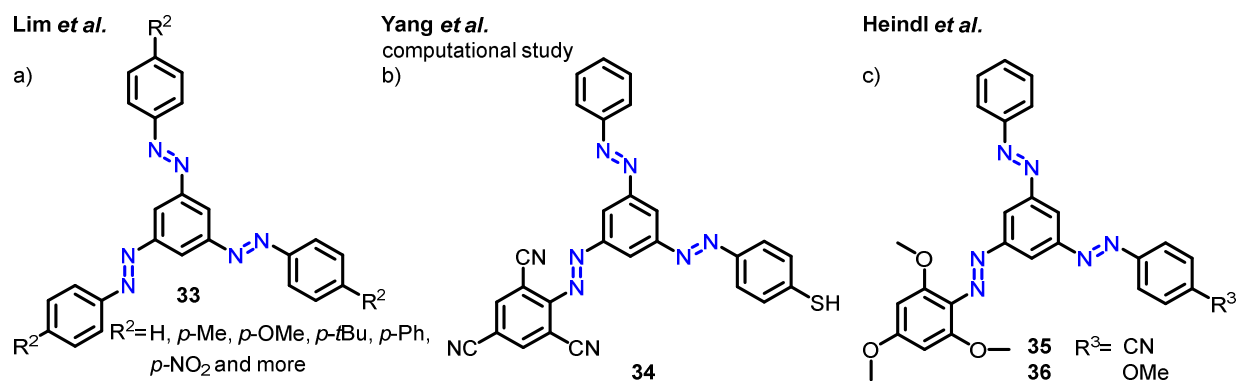
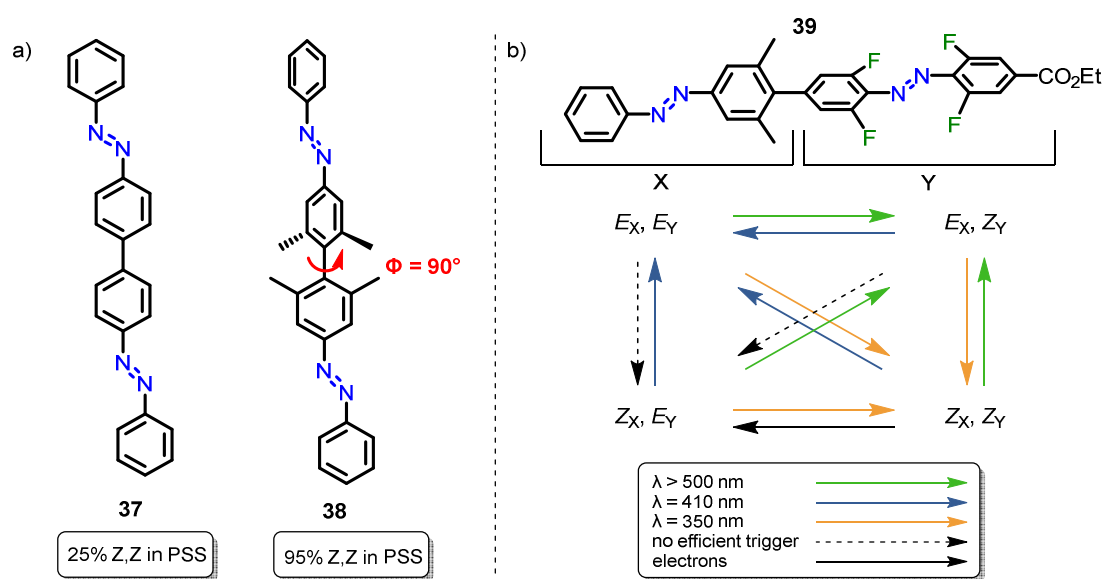


**Figure 15: a) Reported 1,3,5-tris-ABs 33. b) Computational study of independent AB branches. c) Non-symmetric ABs 35 & 36. The entities in 35 & 36 did not isomerize independently.**

Inspired by these computational results, where orthogonal switching in theory was ensured, Heindl *et al.* implemented a synthesis strategy for non-symmetric star shaped compounds (Figure 15, c)). Although those ABs (**35** & **36**) showed no independent switching in preliminary studies, the reported synthesis strategy opens new gateways for future orthogonal switchable ABs.<sup>[159]</sup>

### 3.2.2 Linked AMPs

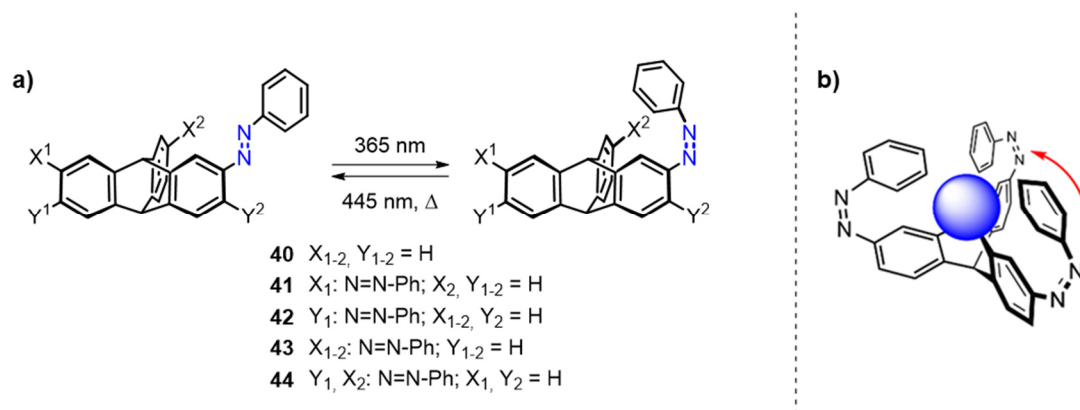
As an additional approach to guarantee orthogonal switching, Bléger *et al.* designed a biphenyl-linked bis-AB photoswitch with *ortho*-Me substitution **38**, which drastically increases the dihedral biphenyl angle up to 90° in comparison to its unsubstituted bis-AB **37**. This leads to a loss in conjugation and an increase of (Z,Z) content from 25% to 95% (Scheme 3, a)).<sup>[160]</sup> By exploiting this principle, bis-AB **39** was designed, which was orthogonally switchable to all four depicted states by light or electrocatalytically (Scheme 3, b)).<sup>[154]</sup>



**Scheme 3:** a) Unsubstituted bis-AB **37** and *ortho*-Me-substituted AB-**38** with an increased torsion angle  $\phi$ , which leads to loss in conjugation and a more efficient switching. b) Based on this principle bis-AB **39** was designed, where all four isomers can be selectively addressed.

When AMPs are separated with non-conjugative linkers in close proximity, even if not directly conjugated, they can influence each other.<sup>[161]</sup> One option was demonstrated by cyclic arrangement of ABs with methylene-linker, where their isomerization behavior is influenced by the formed ring strain already described in section 2.2.1.<sup>[106]</sup> Using the latter principle of non-conjugative linkage, ABs were incorporated into the triptycene scaffold separated by a  $sp^3$  center. This allows investigation of the switching behavior and interactions of multiple ABs in close proximity. Even though the decoupled AB

moieties were efficiently switchable, computational studies determined excitonic coupling effects within the azobenzene units, which might increase the efficiency of multinary photoswitches in the near future (Scheme 4, a)). Additionally, the design can be exploited for future host-guest chemistry due to the cavity formed upon isomerization (Scheme 4, b)).<sup>[162]</sup>



**Scheme 4: a) Synthesized AB-triptycene derivatives 40-44 with one, two and three AB entities. b) Possibility as model for molecular gripper.**

### 3.2.3 Macrocyclic AMPs

As already discussed in Section 2.2.1 there are macrocyclic AMPs, which can also be referred to as azobenzophanes. While the first example of azobenzophanes was introduced by Rau *et al.* in 1982, by now there are various different compounds in this category, which were divided in subclasses by Venkataramani and co-workers.<sup>[64,151]</sup> Their classification is based on shape, charge and symmetry. Two major classes are rigid or flexible macrocyclic AMPs. Rigidity can lead to high ring strain, where even stability of the isomers can be inverted (Section 2.2.1).<sup>[106,108]</sup> Moreover, there can be neutral or charged spacing units, where the resulting charged azobenzophanes can be utilized as hosts for complexations of cations, anions or organic molecules,<sup>[163-165]</sup> while some neutral macrocyclic AMPs can also exhibit host-guest complexations.<sup>[166]</sup> Furthermore, it can be distinguished between symmetric or non-symmetric azobenzophanes. While symmetric azobenzophanes show distinct spectroscopic features, it can be quite complex in <sup>1</sup>H NMR or UV-Vis spectroscopy, for example to characterize non-symmetric azobenzophanes. However, this is also the case for symmetrical AB when they lose their symmetry through isomerization.<sup>[155,167-169]</sup>

### 3.3 Hybrid-multinary Photoswitches Containing the Azobenzene Scaffold

By fusion of different photochromic systems, the advantages and properties of the respective photoswitches can be combined. Therefore, the number of so-called hybrid-multinary photosystems significantly increased within the last years, primarily in terms of multiaddressability.<sup>[150,170–177]</sup> Here, the different absorption maxima of the respective photoswitchable moieties are exploited. When combined by smart linkage or with non-conjugative linkers, their absorption maxima can be addressed separately and orthogonal switching is enabled. With the variety of syntheses and substitution possibilities (Section 2.2.1 and 2.3) along with their linkage dependent photo- as well as thermal isomerization behavior, ABs are promising candidates for hybrid-multinary photoswitches. However, due to their large absorption range between 300 and 500 nm, multiaddressability can be prevented by overlapping with absorption bands of other entities. Despite this, Feringa and co-workers designed multinary photoswitches **45** and **46** with different alkyl chains between AB and a DASA photoswitch (Figure 16).<sup>[171]</sup>

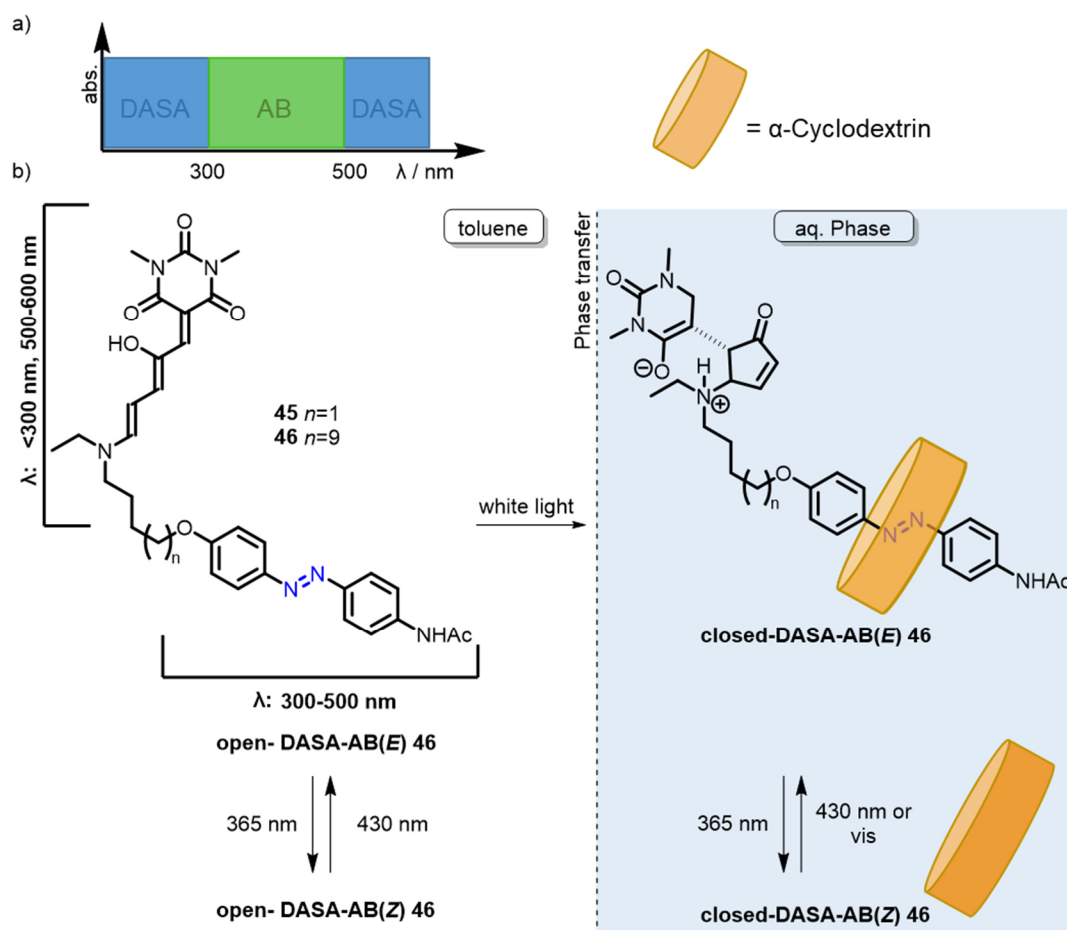
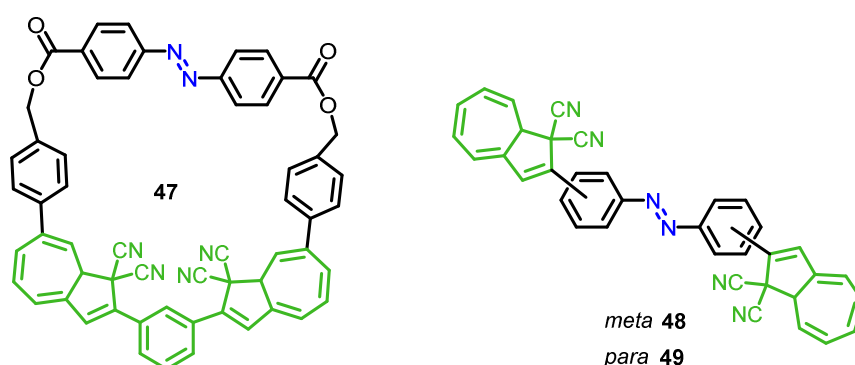


Figure 16: a) Absorption range of DASA (blue) and ABs (green). b) AB-DASA conjugates **45** and **46**. When **46** is irradiated with white light, ring closure of the DASA entity occurs and the compound acts like a phase transfer tag. In the aq. phase, host-guest binding to  $\alpha$ -cyclodextrin occurs in the closed-DASA-AB(E).

This difference in chain length affects the coupling between them so that in compound **45** ( $n=1$ ) by irradiation with 370 nm, not only the AB switches from (*E*)- to its (*Z*)-isomer, but also the DASA switch is slightly affected. This is not observed for the longer chain length in **46** ( $n=9$ ), enabling orthogonal switching to all four depicted isomers. By the significant change in polarity due to the ionic character of the DASA isomer in the closed form, the molecule can act as phase-transfer tag between toluene and the aqueous phase. Herein, the AB can be still isomerized in the aq. phase and act as a guest for  $\alpha$ -cyclodextrin in its (*E*)-form, while the binding is prohibited in its (*Z*)-isomer due to the change in geometry.<sup>[171]</sup> Another hybrid-multiphotoswitch consisting of DHA and AB was presented by Brøndsted Nielsen and co-workers, initially in a macrocyclic fashion **47**, and a few years later in a linear fashion with the AB as linker between two DHA units in *para*- and *meta*- connectivity **48** and **49** (Figure 17).<sup>[172,178]</sup> While it was not possible to assign the AB and DHA units separately in cyclic **47**, a more systematic study was performed by connecting AB and DHA in *para*- as well as in *meta*-position **48** and **49**. *Para*-**49** behaves more like one large chromophore rather than a system of individual photochromes due to conjugation between the entities. While it shows only minor conversion of the AB in *para*-**49**, the DHA as well as the AB moiety in *meta*-**48** are able to undergo photoisomerization (“*meta*”-rule). Although isomerization takes place stepwise and isomers can be detected in <sup>1</sup>H-NMR, orthogonal switching is not possible due to overlapping absorption bands.<sup>[178]</sup>

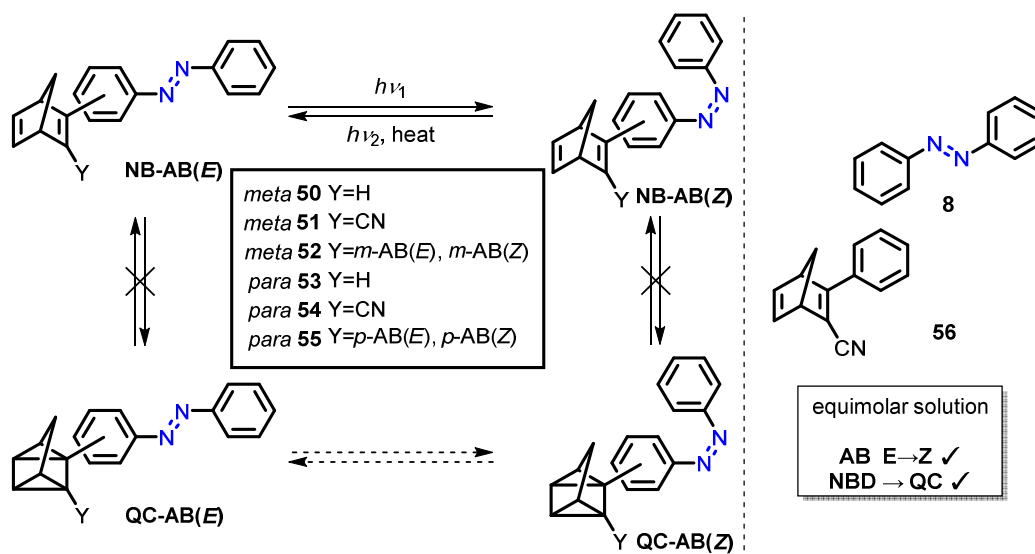
Brøndsted Nielsen and co-workers



**Figure 17: DHA-AB conjugates:** In cyclic **47** three different isomers can be addressed. In linear DHA-ABs, the AB as well as the DHA part can only be switched effectively in *meta*-connection (**48**), due to less conjugation.

To investigate the interplay of combined photoswitches further in this work, the AB scaffold was combined in *meta*- as well as *para*-position to the C<sub>2</sub> position of NBDs. Because unsubstituted AB-NBD switches **50** and **53** tend to decompose, nitrile-

substituted **51** and **54** as well as di-AB-NBDs **52** and **55** were synthesized and examined in terms of isomerization behavior and electronic communication. Even though in all synthesized compounds the ABs could be isomerized from (*E*)- to its (*Z*)-isomer, the [2+2]-cycloaddition of the NB-QC switch did not transpire due to energy transfer between the photoswitches. This assumption was supported by irradiating an equimolar solution of uncoupled **8** and **56**, where both photoswitches were isomerizable under the same conditions as the coupled system **54**.<sup>[147]</sup>



**Scheme 5:** a) Synthesized AB-NBD conjugates **50-55**. While AB isomerization in the NBD-AB form is possible, NBD→QC photoisomerization is prohibited due to energy transfer between the moieties. Therefore, also QC-AB(*E*) → QC-AB(*Z*) was not examined. b) In an equimolar solution of uncoupled AB **8** and NBD **56**, isomerization of AB, as well as NBD, is possible, substantiating energy coupling between the coupled AB-NBD conjugates.

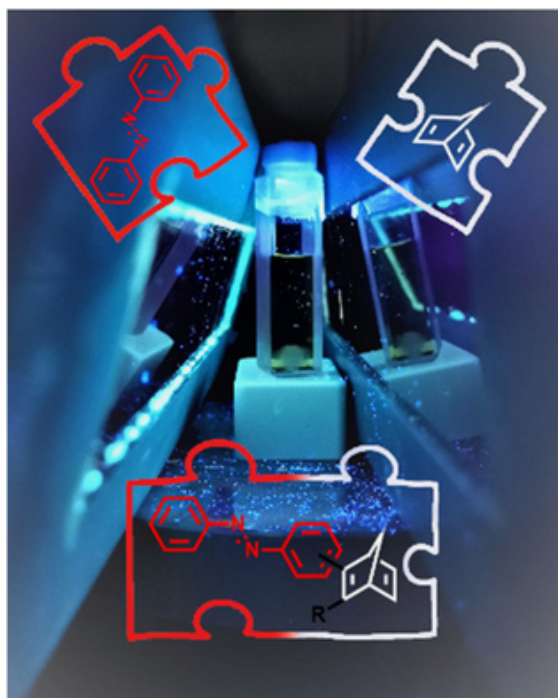
## 4 Contributions to the Literature

### 4.1 1+1 $\geq$ 2? Norbornadiene-Azobenzene Molecules as Multistate Photoswitches

Reference: A. Kunz, H. A. Wegner, *ChemSystemsChem* **2021**, 3, e200003.

DOI: 10.1002/syst.202000035

© 2022 Reproduced with permission from John Wiley & Sons.



“By combination of two photochromic molecules as multistate photoswitches new properties regarding to molecular solar thermal (MOST) energy storage systems and information storage capacity of smart materials are expected. By fusing the azobenzene with the norbornadiene system, new multinary photoswitches were designed. A successful synthesis towards different analogues was developed via Suzuki coupling reaction as key step. The isomerization behaviour of these norbornadiene-azobenzene fusions was studied by UV-Vis and  $^1\text{H}$  NMR spectroscopy in different solvents investigating the electronic communication within these multinary-photochromic systems.”

# 1 + 1 ≥ 2? Norbornadiene-Azobenzene Molecules as Multistate Photoswitches

Anne Kunz and Hermann A. Wegner\*<sup>[a]</sup>

By combination of two photochromic molecules as multistate photoswitches new properties regarding to molecular solar thermal (MOST) energy storage systems and information storage capacity of smart materials are expected. By fusing the azobenzene with the norbornadiene system, new multinary photoswitches were designed. A successful synthesis towards

different analogues was developed via Suzuki coupling reaction as key step. The isomerization behaviour of these norbornadiene-azobenzene fusions was studied by UV-Vis and <sup>1</sup>H NMR spectroscopy in different solvents investigating the electronic communication within these multinary-photochromic systems.

## 1. Introduction

Photochromic molecules are defined by the ability to undergo a light-induced reversible change between two forms with different absorption spectra.<sup>[1]</sup> Nowadays those photoswitches exhibit increasing attention due to their diverse and versatile applications for example in photobiology,<sup>[2]</sup> information storage<sup>[3]</sup> or solar fuel applications.<sup>[4–5]</sup> For the latter, azobenzenes (AB) as well as the norbornadiene-quadracyclane system (NB/QC) are both potent lead structures for molecular solar thermal energy storage (MOST) systems.<sup>[6–7]</sup> Upon irradiation with UV-light of around 350 nm the thermodynamically more stable *E*-isomer of ABs converts into the less stable *Z*-isomer.<sup>[8]</sup> The thermodynamically more stable NB can undergo a [2+2]-cycloaddition to its corresponding metastable QC also by irradiation of around 300 nm in the presence of a photosensitizer.<sup>[9]</sup> The differences in energy from parent to metastable photoisomer can be exploited to design versatile MOST systems.<sup>[5]</sup>

Herein, the combination of AB and NB as a new candidate for MOST applications is presented: One disadvantage of NBs is their absorption of light in the UV-region. Although the absorption maximum can be red-shifted by introducing different substituents, the energy density as a consequence decreases due to the increase of the molecular mass.<sup>[10]</sup> Moreover, the half-lives of the photoisomers are influenced.<sup>[7]</sup> By

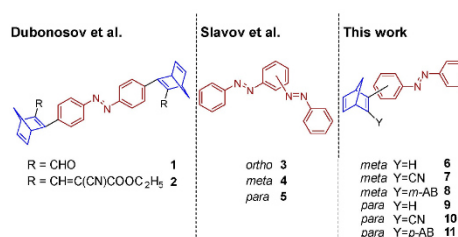
adding the AB scaffold as a substituent to the NB moiety, not only the absorption maximum might be shifted but also the storage density should be increased due to the additional energy storage capability in the AB-moiety. The combination of different photochromic units in one system in general bears special challenges, however, with the potential to create new or better properties for 'smart' materials.<sup>[11–13]</sup> In this fundamental study, the isomerization behavior and electronic communication of AB-NB switches are investigated. To the best of our knowledge there is only one report by Dubonosov *et al.* of combining an AB with a NB. In this study two substituted NBs were both connected to an AB moiety in *para*-position (Scheme 1, 1, 2). Although the authors mention successful switching of the norbornadiene as well as the azobenzene moiety, a detailed analysis has not been provided.<sup>[14]</sup> Previously, it could be shown that  $\pi$ -conjugation in *ortho*- and *para*-bis-ABs significantly influences the compounds isomerization behavior. In contrast to that, in bis-ABs connected in *meta*-position both photochromic moieties behave almost independently due to less  $\pi$ -conjugation (the "meta-rule", Scheme 1, 4).<sup>[15,16]</sup> Combining these observations, novel *meta*- and *para*-connected AB-NB were designed and their isomerization and energetic behavior of both photochromic moieties connected in one molecule were investigated (Scheme 1, 6–11).

These NB-AB dyads contain both, the AB and the NB scaffold, in either *meta*- or *para*-connection (Scheme 1, 6–11).

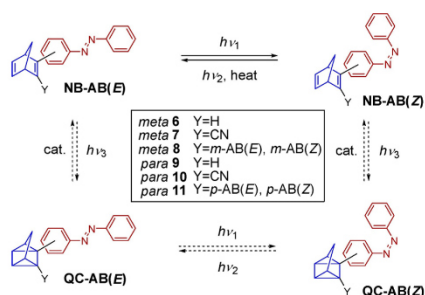
[a] A. Kunz, Prof. Dr. H. A. Wegner  
Institute of Organic Chemistry  
Justus Liebig University  
Heinrich-Buff-Ring 17, 35392 Giessen  
and  
Germany and Center for Materials Research (LaMa)  
Justus Liebig University  
Heinrich-Buff-Ring 16, 35392 Giessen (Germany)  
E-mail: Hermann.a.wegner@org.chemie.uni-giessen.de

Supporting information for this article is available on the WWW under <https://doi.org/10.1002/syst.202000035>

© 2020 The Authors. Published by Wiley-VCH GmbH. This is an open access article under the terms of the Creative Commons Attribution Non-Commercial License, which permits use, distribution and reproduction in any medium, provided the original work is properly cited and is not used for commercial purposes.



Scheme 1. Overview of previously reported NB-ABs 1 and 2, bis-azobenzenes sharing one phenyl ring 3–5, and NB-ABs investigated in this study 6–11.<sup>[14,16]</sup>



Scheme 2. Possible photoisomers of AB-NB compounds 6–11. QC-AB(E) and QC-AB(Z) were not observed in this study.

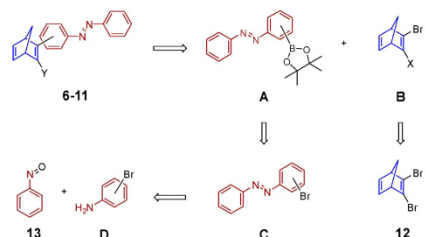
Because two photoswitchable moieties are combined, these compounds can be categorized as multinary-photoswitches. Therefore, molecules 6, 7, 9 and 10 can, in theory, adopt four different states [NB-AB(E), NB-AB(Z), QC-AB(E), QC-AB(Z)]; 8, 11 in principle can switch between six different states of isomerization [NB-AB(E,E), NB-AB(E,Z), NB-AB(Z,Z), QC-AB(E,E), QC-AB(E,Z), QC-AB(Z,Z)] (Scheme 2).

Challenges of combining two or more photochromic systems are the proper energy match of the absorption wavelength of both moieties to induce switching of either both chromophores at the same time, or only one selectively. The combinations of photoswitchable units can lead to energy transfer if the two scaffolds are energetically coupled inhibiting the switching.<sup>[17,18]</sup> Another obstacle can be a low quantum yield for each of the individual processes.

## 2. Results and Discussion

### 2.1. Synthesis

A synthetic route towards all NB-ABs 6–11 was developed as outlined in Scheme 3. As a key step, a Suzuki coupling reaction was envisioned to form the necessary AB-NB-connection.<sup>[19]</sup> The boronic esters **A** could be obtained by borylation via Miyaura reaction of mono-bromo-substituted ABs **C**.<sup>[20–21]</sup> Those inter-



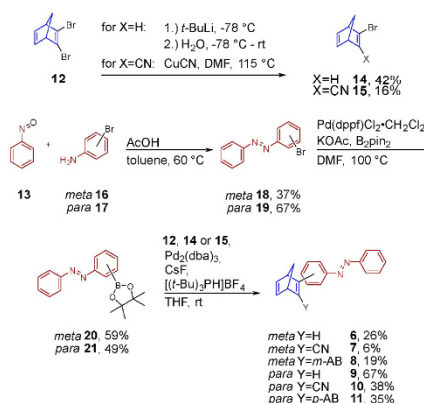
Scheme 3. Synthetic strategy towards AB-NBs 6–11.

mediates could be synthesized by Baeyer-Mills coupling of nitrosobenzene (**13**) with the respective bromo-anilines **D** (Scheme 3).<sup>[22]</sup>

To access *meta*-/*para*-bromo-substituted ABs **18/19**, Baeyer-Mills coupling with either *meta*- or *para*-bromoaniline **16** or **17** in acidic media was performed. All reactions were done under nitrogen atmosphere and the bromoanilines **16–17** were degassed in toluene prior to the addition of nitrosobenzene (**13**). As nitroso compounds in general tend to be unstable, 1.5 eq. of nitrosobenzene (**13**) were used. This reaction generated *meta*- and *para*-bromo-substituted ABs **18** and **19** as red solids. For the implementation of *meta*- and *para*-boronic esters **20** and **21** a Miyaura reaction was performed according to the literature.<sup>[20,23]</sup>

The borylation provided the starting material for the following Suzuki coupling in this route. Dissimilar from other Suzuki coupling reactions of NBs reported,<sup>[24]</sup> here, boronic esters instead of boronic acids were utilized. This choice was based on different advantages: Boronic esters are in general better soluble, more reactive and in most cases easily accessible via Miyaura coupling reaction of brominated aryl-compounds, while boronic acids tend to form anhydrides.<sup>[25]</sup> For the borylation bis(pinacolato)-diboron ( $B_2pin_2$ ) was applied generating the desired products as red solids.

The different substitution patterns of the second NB building block provide a combinatorial-like access to various AB-NBs. In the following Suzuki-coupling reaction di-bromo-NB **12**, mono-bromo-NB **14** as well as cyano-NB **15** were employed as starting materials. Mono-bromo-NB **14** was prepared from di-bromo-NB **12** by monolithium-halogen exchange with *t*-BuLi. Trapping of this organolithium intermediate with water gave mono-bromo-NB **14** as yellowish oil.<sup>[26]</sup> Cyano-NB **15** was obtained also as yellowish oil by nucleophilic attack of one equivalent of cyanide to di-bromo-NB **12** (Scheme 4).<sup>[27]</sup> With both building blocks, boronic esters **A** and NBs **B**, in hand Suzuki coupling reactions were performed. For this transformation, a catalyst system of  $CsF/Pd_2dba_3/[(t-Bu)_3PH]BF_4$  was utilized.<sup>[28]</sup> AB-NBs **6** and **9** turned out to be not very stable. Therefore, the reaction times in those cases were shortened to increase the yield of the products obtained as orange solids.



Scheme 4. Synthesis of AB-NBs 6–11.

Also, excess of NB starting material was avoided to prevent side reactions.

## 2.2. UV/Vis Absorption Spectroscopy

All AB-NBs 6–11 were investigated via UV-Vis spectroscopy. The spectra revealed a red-shift of the absorptions of *para*-connected compounds 9–11 compared to their *meta*-analogues and the parent AB and NB (Figure 1).<sup>[29]</sup> The absorption maximum of compound 8 is not shifted, while 6 shows a slight blue shift and 7 a slight red shift in comparison to unsubstituted AB in DMSO.<sup>[29]</sup> This observation can be explained by an elongated  $\pi$ -system due to higher  $\pi$ -conjugation of AB with NB in *para*- and less conjugation in *meta*-position (*meta*-rule).<sup>[16]</sup> The characteristic  $n$ - $\pi^*$  maximum of AB is located for *meta*-AB-NB 6, *meta*-cyano-AB-NB 7 and *meta*-AB<sub>2</sub>-NB 8 at around 450 nm, while for *para*-AB-NB 9, *para*-cyano-AB-NB 10 and *para*-AB<sub>2</sub>-NB 11 these maxima are not

or not fully visible. To examine the isomerization behavior of compounds 6–11, the samples were irradiated with light of different wavelengths. Exemplary, the isomerization behavior for *para*-AB-NB compound 10 will be discussed (for 6, 7, 8, 9 and 11 see SI). After irradiation with 365 nm in DMSO, the absorbance at around 364 nm decreased, while the  $n$ - $\pi^*$  absorption band showed a slight increase around 450 nm, representative for the *(E)*→*(Z)* isomerization of AB. After irradiation with 302 nm, the shoulder at 290 nm decreased and the absence of an isobestic point during the photoisomerization indicated decomposition.

For the isomerization of the other AB-NB compounds 6, 7, 8, 9 and 11 a similar behavior compared to in DMSO was observed. In contrast to that, the photoisomerization of AB-NB compound 10 in acetonitrile, methanol, and cyclohexane showed a clear isobestic point, but no signs of NB-QC isomerization could be observed (Figure 2, left). Changing the solvent to dimethyl formamide (DMF) or toluene, also decomposition was observed.

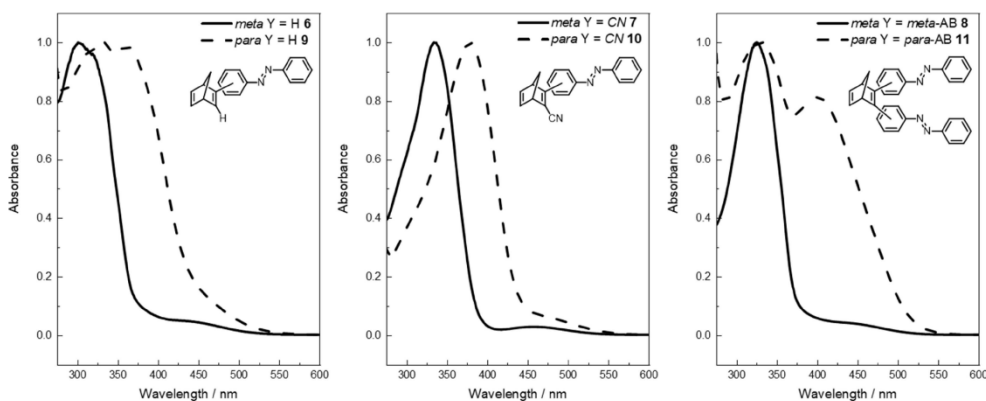


Figure 1. Normalized UV/Vis absorption spectra of compounds 6–11 in DMSO. (7,8,10:  $2 \times 10^{-5}$  mol/L; 11:  $2 \times 10^{-5}$  mol/L; 6,9:  $4 \times 10^{-5}$  mol/L, for detailed information see the Supporting Information).

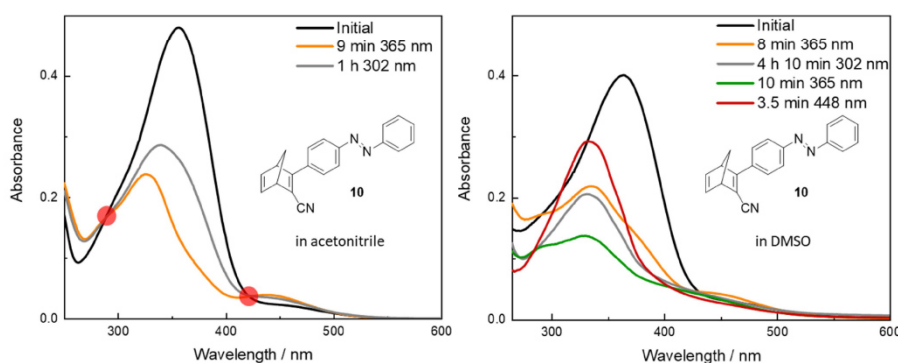


Figure 2. Isomerization behavior of AB-NB 10 [ $2 \times 10^{-5}$  mol/L in acetonitrile (left) and DMSO (right)]. Isobestic points are highlighted in red.

## 2.3. NMR Spectroscopy

$^1\text{H}$  NMR isomerization experiments were performed to further support these observations. AB-NB **10** was irradiated with light of 302 nm in  $\text{MeCN-}d_3$ , providing a mixture of AB(*E*)-NB and AB(*Z*)-NB [Figure 3, b)]. Subsequent irradiation with light of 365 nm preserved the AB moiety mostly as AB(*Z*) [Figure 3, c)]. By irradiation with light of 448 nm back isomerization occurred and as a consequence mostly AB(*E*)-NB was present [Figure 3, d)]. Those results in accordance to the UV-Vis analysis revealed only AB(*E*/*Z*) isomerization (Figure 3). Changing the solvent to  $\text{DMSO-}d_6$ , decomposition upon irradiation with 302 nm was observed (see  $^1\text{H}$ -NMR spectra in  $\text{DMSO-}d_6$  in SI). Additionally, the decomposition of compound **10** was supported by HPLC analysis. It has been shown before that the quantum yields of the NB-QC isomerization are solvent dependent and rather low in acetonitrile, but high in toluene.<sup>[30]</sup> In contrast, the isomerization-ability of AB is not as much affected by the solvent. Hence, both photoswitching units should be able to isomerize when changing the solvent to toluene. However, no isomerization of NB to QC was observed in toluene. Another explanation for the absent NB-QC isomerization could be an energy transfer between both photochromic units. Such a process as result of conjugation between the NB and AB moiety could inhibit the switching ability of NB to QC. This case of excitonic coupling was also observed in other cases of combined photochromic systems.<sup>[17]</sup> To support this assumption, an equimolar mixture of AB **22** and NB **23** was irradiated under the previous NMR isomerization conditions. It was found that both photoswitches isomerized in acetonitrile- $d_3$ , substantiating the proposal of intramolecular electronic coupling of AB-NB **6-11** preventing switching of the NB moiety (Figure 4).

## 3. Conclusion

Multinary photochromic systems consisting of AB and NB **6-11** have been successfully synthesized to investigate the interaction within switching processes. Isomerization experiments revealed that (*E*)→(*Z*) isomerization of AB can be induced, but the [2+2]-cycloaddition of the NB-QC switch does not occur due to energy transfer. In different solvents, DMSO, DMF, toluene, acetonitrile, cyclohexane and methanol it was only possible to isomerize the AB- but not the NB-moiety, accessing only two of the possible states. Concerning this, similar challenges of accessing the QC in other combined photochromic units were observed.<sup>[12,13]</sup> These fundamental results provide the basis for alternative designs so that in the future the molecules might be used as MOST systems or in data storage devices.

## Acknowledgements

The authors are indebted to the research group of K. Moth-Poulsen (Chalmers, Gothenburg), which provided an initial sample of 2,3-dibromo-norbornadiene (**12**). Financial support by the DFG is acknowledged. Open access funding enabled and organized by Projekt DEAL.

## Conflict of Interest

The authors declare no conflict of interest.

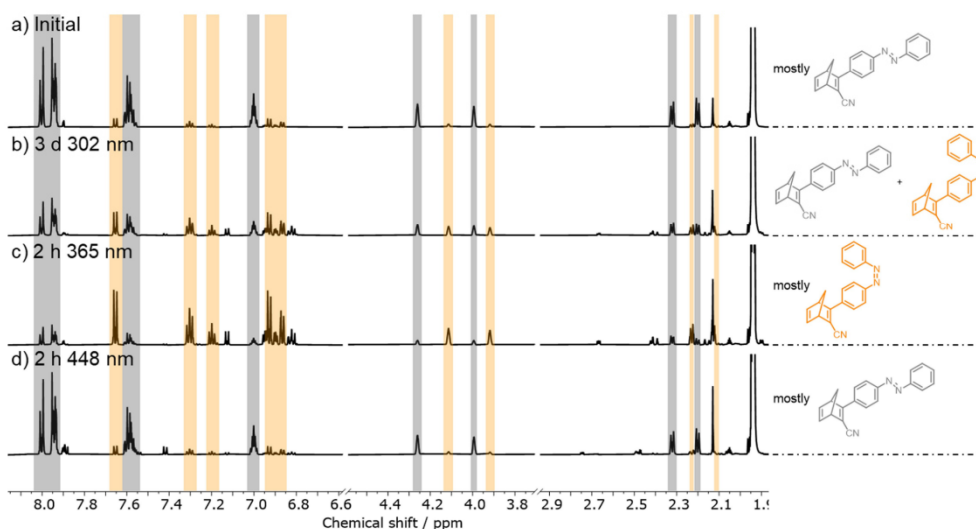
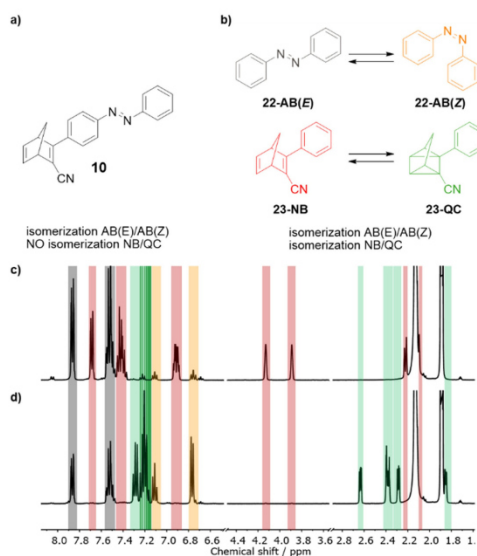


Figure 3. Isomerization of AB-NB **10** monitored by  $^1\text{H}$  NMR spectroscopy (600 MHz, acetonitrile- $d_3$ ,  $\text{N}_2$  atmosphere,  $-10^\circ\text{C}$ ). grey = AB(*E*)-NB, orange = AB(*Z*)-NB.



**Figure 4.** Top: a) Energetically coupled system NB-AB **10**, in which the AB moiety can be switched, but the NB-QC isomerization is prevented. b) Control system of a mixture of AB **22** together and cyano-phenyl-NB **23**, in which both separated molecules in one solution can be isomerized. Bottom: <sup>1</sup>H NMR isomerization experiment of equimolar solution of AB **22** together with cyano-phenyl-NB **23** (400 MHz, each  $8.5 \times 10^{-3}$  mol/L in acetonitrile-*d*<sub>4</sub>). grey = AB(E), orange = AB(Z), red = NB, green = QC. c) Initial spectrum, in which AB **22** is mostly present as AB(E) and cyano-phenyl-NB **23** as NB. d) After irradiation with light of 302 nm, AB(E/Z) isomerization as well as complete isomerization of cyano-phenyl-NB **23** from NB to QC could be observed.

**Keywords:** azo compounds · energy transfer · isomerization · norbornadiene · photoswitches

- [1] M. Nič, J. Jirát, B. Košata, A. Jenkins, A. McNaught, *IUPAC Compendium of Chemical Terminology*, IUPAC, Research Triangle Park, NC, 2009.  
 [2] a) A. A. Beharry, G. A. Woolley, *Chem. Soc. Rev.* **2011**, *40*, 4422–4437; b) J. P. van der Berg, W. A. Velema, W. Szymanski, A. J. M. Driessen, B. L. Feringa, *Chem. Sci.* **2015**, *6*, 3593–3598; c) J. Broichhagen, D. Trauner, *Curr. Opin. Chem. Biol.* **2014**, *21*, 121–127; d) M. M. Lerch, M. J. Hansen, G. M. van Dam, W. Szymanski, B. L. Feringa, *Angew. Chem. Int. Ed.* **2016**, *55*, 10978–10999; *Angew. Chem.* **2016**, *128*, 11140–11163; e) W. Szymański, D. Yilmaz, A. Koçer, B. L. Feringa, *Acc. Chem. Res.* **2013**, *46*, 2910–2923.

- [3] M. Irie, *Chem. Rev.* **2000**, *100*, 1685–1716.  
 [4] a) A. U. Petersen, A. I. Hofmann, M. Fillols, M. Manso, M. Jevric, Z. Wang, C. J. Sumby, C. Müller, K. Moth-Poulsen, *Adv. Sci.* **2019**, *6*, 1900367; b) Z. Wang, J. Udmark, K. Börjesson, R. Rodrigues, A. Roffey, M. Abrahamsson, M. B. Nielsen, K. Moth-Poulsen, *ChemSusChem* **2017**, *10*, 3049–3055; c) A. Kunz, A. H. Heindl, A. Dreos, Z. Wang, K. Moth-Poulsen, J. Becker, H. A. Wegner, *ChemPlusChem* **2019**, *84*, 1145–1148.  
 [5] A. Lennartson, A. Roffey, K. Moth-Poulsen, *Tetrahedron Lett.* **2015**, *56*, 1457–1465.  
 [6] L. Dong, Y. Feng, L. Wang, W. Feng, *Chem. Soc. Rev.* **2018**, *47*, 7339–7368.  
 [7] T. Nagai, K. Fujii, I. Takahashi, M. Shimada, *Bull. Chem. Soc. Jpn.* **2001**, *74*, 1673–1678.  
 [8] G. S. Hartley, *Nature* **1937**, *140*, 281.  
 [9] a) C. F. Wilcox, S. Winstein, W. G. McMillan, *J. Am. Chem. Soc.* **1960**, *82*, 5450–5454; b) G. S. Hammond, N. J. Turro, A. Fischer, *J. Am. Chem. Soc.* **1961**, *83*, 4674–4675.  
 [10] V. A. Bren, V. I. Minkin, A. D. Dubonosov, V. A. Chernoiyanov, V. P. Rybalkin, G. S. Borodkin, *Mol. Cryst. Liq. Cryst.* **1997**, *297*, 247–253.  
 [11] A. Fihey, A. Perrier, W. R. Browne, D. Jacquemin, *Chem. Soc. Rev.* **2015**, *44*, 3719–3759.  
 [12] M. D. Kilde, M. Manso, N. Ree, A. U. Petersen, K. Moth-Poulsen, K. V. Mikkelsen, M. B. Nielsen, *Org. Biomol. Chem.* **2019**, *17*, 7735.  
 [13] S. M. Büllmann, A. Jäschke, *Chem. Commun.* **2020**, *56*, 7124.  
 [14] A. D. Dubonosov, S. V. Galichev, V. A. Chernoiyanov, V. A. Bren, V. I. Minkin, *Russ. J. Org. Chem.* **2001**, *37*, 67–71.  
 [15] G. Floss, P. Saalfrank, *Am. J. Phys.* **2015**, *119*, 5026–5037.  
 [16] C. Slavov, C. Yang, L. Schweighauser, C. Boumirfak, A. Dreuw, H. A. Wegner, *J. Wachtveitl, Phys. Chem. Chem. Phys.* **2016**, *18*, 14795–14804.  
 [17] K. Uchida, G. Masuda, Y. Aoi, K. Nakayama, M. Irie, *Chem. Lett.* **1999**, *28*, 1071–1072.  
 [18] S. G. Telfer, T. M. McLean, M. R. Waterland, *Dalton Trans.* **2011**, *40*, 3097–3108.  
 [19] A. Suzuki, *J. Organomet. Chem.* **1999**, *576*, 147–168.  
 [20] T. Ishiyama, M. Murata, N. Miyaura, *J. Org. Chem.* **1995**, *60*, 7508–7510.  
 [21] J. Takagi, K. Takahashi, T. Ishiyama, N. Miyaura, *J. Am. Chem. Soc.* **2002**, *124*, 8001–8006.  
 [22] C. Mills, *J. Chem. Soc. Trans.* **1895**, *67*, 925–933.  
 [23] H. Qubaha, N. Demitri, J. Rault-Berthelot, P. Dubois, O. Coulembier, D. Bonifazi, *J. Org. Chem.* **2019**, *84*, 9101–9116.  
 [24] M. Quant, A. Lennartson, A. Dreos, M. Kuisma, P. Erhart, K. Börjesson, K. Moth-Poulsen, *Chem. Eur. J.* **2016**, *22*, 13265–13274.  
 [25] M. K. Smith, B. H. Northrop, *Chem. Mater.* **2014**, *26*, 3781–3795.  
 [26] G. K. Tranmer, C. Yip, S. Handerson, R. W. Jordan, W. Tam, *Can. J. Chem.* **2000**, *78*, 527–535.  
 [27] Y. Gunes, N. Arcelik, E. Sahin, F. F. Fleming, R. Altundas, *Eur. J. Org. Chem.* **2015**, 6679–6686.  
 [28] a) A. F. Littke, C. Dai, G. C. Fu, *J. Am. Chem. Soc.* **2000**, *122*, 4020–4028; b) A. F. Littke, G. C. Fu, *Angew. Chem. Int. Ed.* **1998**, *37*, 3387–3388; *Angew. Chem.* **1998**, *110*, 3586–3587.  
 [29] M. A. Strauss, H. A. Wegner, *ChemPhotoChem* **2019**, *3*, 392–395.  
 [30] M. Quant, A. Hamrin, A. Lennartson, P. Erhart, K. Moth-Poulsen, *J. Phys. Chem. C.* **2019**, *123*, 7081–7087.

Manuscript received: July 15, 2020  
Version of record online: September 9, 2020

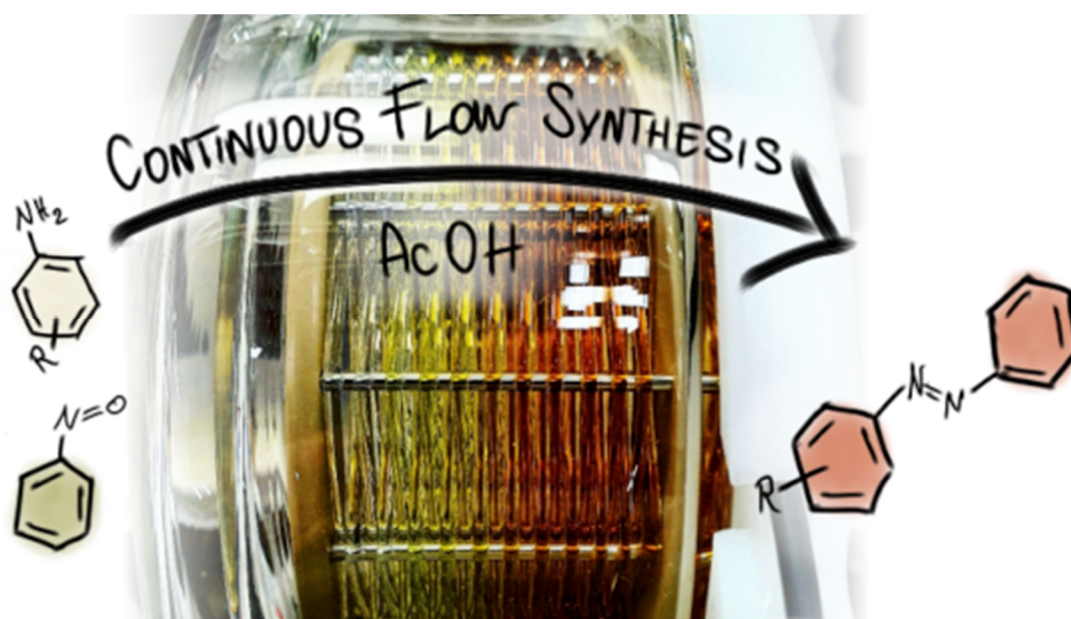
## 4.2 Continuous Flow Synthesis of Azobenzenes via Baeyer-Mills Reaction

Reference: A. Kunz<sup>‡</sup>, J. H. Griwatz<sup>‡</sup>, H. A. Wegner, *Beilstein J. Org. Chem.*  
**2022**, *18*, 781.

DOI: 10.3762/bjoc.18.78

<sup>‡</sup> equal contribution

© 2020 Kunz, Griwatz, Wegner, licensee Beilstein-Institut.



„Azobenzene, as one of the most prominent molecular switches, is featured in many applications ranging from photopharmacology to information or energy storage. In order to easily and reproducibly synthesize non-symmetric substituted azobenzenes in an efficient way, especially on a large scale, the commonly used Baeyer–Mills coupling reaction was adopted to a continuous flow setup. The versatility was demonstrated with a scope of 20 substances and the scalability of this method exemplified by the synthesis of >70 g of an azobenzene derivative applied in molecular solar thermal storage (MOST) systems.”

## Continuous flow synthesis of azobenzenes via Baeyer–Mills reaction

Jan H. Griwatz<sup>†1,2</sup>, Anne Kunz<sup>†1,2</sup> and Hermann A. Wegner<sup>\*1,2</sup>

### Full Research Paper

Open Access

#### Address:

<sup>1</sup>Institute of Organic Chemistry, Justus Liebig University, Heinrich-Buff-Ring 17, 35392 Giessen, Germany and <sup>2</sup>Center for Material Research (ZiM/LaMa), Justus Liebig University, Heinrich-Buff-Ring 16, 35392 Giessen, Germany

#### Email:

Hermann A. Wegner<sup>\*</sup> - hermann.a.wegner@org.chemie.uni-giessen.de

<sup>\*</sup> Corresponding author ‡ Equal contributors

#### Keywords:

azobenzenes; Baeyer–Mills reaction; continuous flow; molecular switches; solar fuel

*Beilstein J. Org. Chem.* **2022**, *18*, 781–787.  
<https://doi.org/10.3762/bjoc.18.78>

Received: 26 April 2022

Accepted: 15 June 2022

Published: 30 June 2022

This article is part of the thematic issue "Platform and enabling technologies in organic synthesis".

Guest Editor: P. Heretsch

© 2022 Griwatz et al.; licensee Beilstein-Institut.  
 License and terms: see end of document.

### Abstract

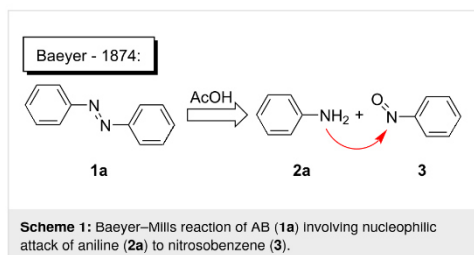
Azobenzene, as one of the most prominent molecular switches, is featured in many applications ranging from photopharmacology to information or energy storage. In order to easily and reproducibly synthesize non-symmetric substituted azobenzenes in an efficient way, especially on a large scale, the commonly used Baeyer–Mills coupling reaction was adopted to a continuous flow setup. The versatility was demonstrated with a scope of 20 substances and the scalability of this method exemplified by the synthesis of >70 g of an azobenzene derivative applied in molecular solar thermal storage (MOST) systems.

### Introduction

Although the red-colored azobenzenes (AB) have been known for years as dyes, their applications nowadays span from energy and information storage [1–5], organocatalysis [6], photobiology and photopharmacology [7], host–guest chemistry [8], molecular mechanics [9,10], to molecular machines [11]. This popularity is due to the ability of ABs to isomerize from their energetically more stable (*E*)- to the meta-stable (*Z*)-isomer by irradiation with light [12]. During this isomerization, not only the geometry is altered from the planar (*E*)-AB to its twisted (*Z*)-AB form, but also its properties change (e.g., dipole

moment and polarity) [13,14]. Furthermore, the (*Z*)-AB can be reversibly switched back by visible light or thermally [15]. To synthesize ABs a variety of reactions can be chosen from, each having both advantages and disadvantages. The best synthesis must be individually selected for the respective use [16]. There are various ways to access symmetric and non-symmetric AB compounds in a convenient way in batch size, as it has been summarized in detail [16]. One example is the reliable synthesis of symmetric ABs in high yields via a Cu-catalyzed oxidative coupling of aniline derivatives [17]. This synthesis can be

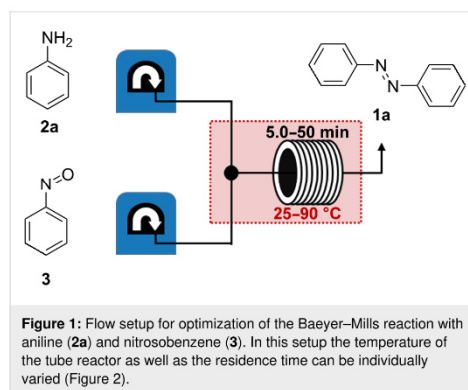
also used for the formation of non-symmetric AB, however, only for a selected set of anilines. One of the most applied methods to access non-symmetric azobenzenes is based on the condensation of nitrosobenzenes with anilines (Scheme 1). This so-called Baeyer–Mills reaction, which was first published by Baeyer in 1874 and further investigated by Mills, proceeds best for electron-rich anilines with electron-poor nitrosobenzenes. The reactivity can be rationalized by the proposed mechanism, which involves nucleophilic attack of the aniline on the nitrosobenzene derivatives in acidic or basic media (Scheme 1) [18–21]. However, in order to use azobenzenes as functional materials, access to a large-scale process is necessary. In this context continuous flow synthesis is frequently discussed as potential solution to address this challenge. This technique is neither limited by the size of the reaction vessel nor the stirring as the reagents are pumped continuously through the reactor. The set-up also allows precise control of the reaction time and temperature, which can lead to higher yields and purity [22]. Flow chemistry to prepare azobenzenes has been previously applied to the Cu-catalyzed synthesis of symmetric substituted AB derivatives [23,24]. However, non-symmetric substituted ABs are not accessible by this method in an efficient way. Herein, we report a continuous flow synthesis of non-symmetric AB compounds via the Baeyer–Mills reaction, which allows to obtain large quantities of products from different substrates in a fast and efficient manner.



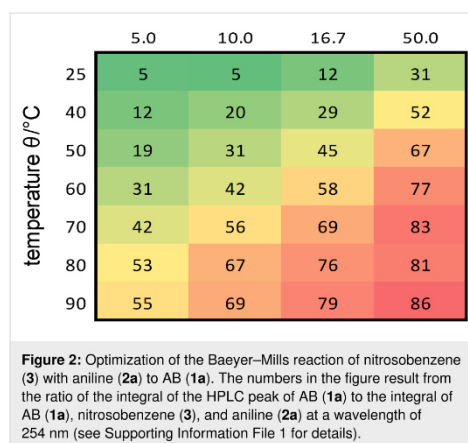
## Results and Discussion

For optimization of the Baeyer–Mills coupling in continuous flow the reaction to generate unsubstituted AB (**1a**) was performed with freshly distilled aniline (**2a**) and commercially available nitrosobenzene (**3**), dissolved separately in acetic acid. Both starting materials had the same concentration and were pumped by a Vapourtec E-Series system (for details, see experimental part in Supporting Information File 1). After mixing, the solution was passed through a tube reactor, in which the temperature as well as the residence time can be easily modified. Afterwards the respective reaction mixture was collected and analyzed (Figure 1). In order to optimize the reaction, both the temperature and the residence time were successively changed

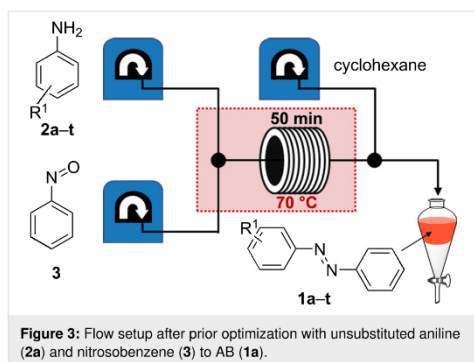
to achieve the highest conversion to AB. The residence time was increased from 5.0 to 50.0 min and the temperature was raised stepwise from 25 °C up to 90 °C (Figure 1). After the set residence time an aliquot was collected, diluted with acetonitrile, and subsequently examined by HPLC analysis (for details, see Supporting Information File 1).



At lower temperature, AB (**1a**) could be detected, but only a low conversion of the starting materials was observed (Figure 2). At higher temperature, the product/starting material ratio was improved but was still not satisfactory. Therefore, not only the temperatures, but also the residence time was gradually changed (Figure 2). At 70–90 °C and a residence time of 50.0 min the best results were observed. However, heating to 80–90 °C provided increasing amounts of azoxybenzene, which is a known side product of the Bayer–Mills reaction [25]. Hence, these parameters (70 °C, 50.0 min) were chosen to do



the synthesis on a preparative scale. The setup was slightly modified to include an aqueous workup and extraction of the organic phase. For this purpose, a third pump was implemented which adds cyclohexane to the reaction mixture after the tube reactor (Figure 3). The reaction solution with cyclohexane was continuously fed into a separating funnel containing brine. After phase separation, drying of the organic phase with  $\text{MgSO}_4$ , and evaporation of the solvent, AB (**1a**) could be obtained in 98% yield under the previously optimized conditions. By collection of the reactor output for 2 h, 582 mg of AB were obtained.



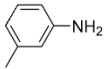
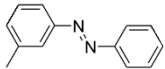
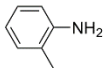
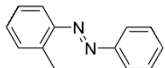
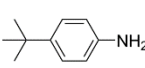
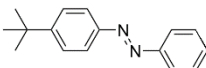
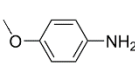
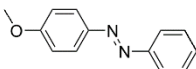
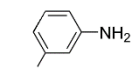
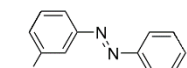
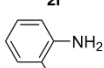
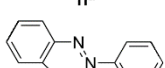
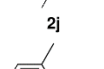
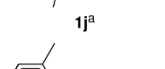
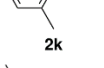
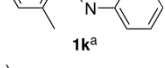
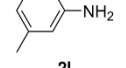
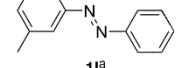
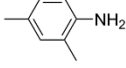
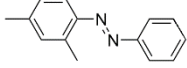
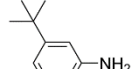
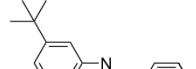
Further purification was not necessary as the product was satisfactorily pure with the described workup. After successful optimization of the synthesis of unsubstituted AB (**1a**) the setup was also tested for a large number of other azobenzene derivatives to determine the scope of the method (Table 1). All aniline derivatives **2a–s** were commercially available and the corresponding azobenzenes **1a–s** were synthesized according to the general procedure in continuous flow as described before. The optimized flow and workup conditions gave the products in high purity for most of the synthesized AB derivatives (see Supporting Information File 1 for details). Only in a few cases flash column chromatography was necessary to isolate the pure products (see Table 1). As expected, the method worked excellently for most of the electron-rich anilines due to their increased nucleophilicity.

A comparison of *ortho*-, *meta*- and *para*-substituted derivatives revealed that for electron-rich anilines, the *para*-substituted ABs are formed in better yields as their *ortho*- and *meta*-analogues. For example, the synthesis of AB **1i** from *m*-anisidine (**2i**) gave only 7% yield, due to the formation of large amounts of azoxybenzene and purification issues therefrom. The moderate product yields from the *ortho*-substituted aniline derivatives are presumably caused by the higher steric hindrance of the nucleophilic attack. Low yields in case of electron-poor aniline

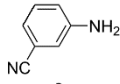
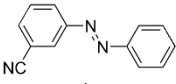
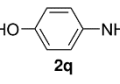
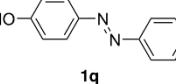
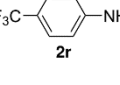
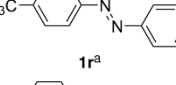
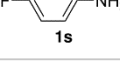
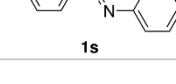
**Table 1:** Substrate scope of the Baeyer–Mills reaction under the optimized conditions in continuous flow.

entry	aniline <b>2</b>	product <b>1</b>	yield [%]
1			98
2			89
3			77
4			94

**Table 1:** Substrate scope of the Baeyer–Mills reaction under the optimized conditions in continuous flow. (continued)

5	 <b>2e</b>	 <b>1e<sup>a</sup></b>	79
6	 <b>2f</b>	 <b>1f<sup>a</sup></b>	67
7	 <b>2g</b>	 <b>1g</b>	>99
8	 <b>2h</b>	 <b>1h</b>	96
9	 <b>2i</b>	 <b>1i<sup>a</sup></b>	7
10	 <b>2j</b>	 <b>1j<sup>a</sup></b>	72
11	 <b>2k</b>	 <b>1k<sup>a</sup></b>	23
12	 <b>2l</b>	 <b>1l<sup>a</sup></b>	65
13	 <b>2m</b>	 <b>1m</b>	70
14	 <b>2n</b>	 <b>1n</b>	99
15	 <b>2o</b>	 <b>1o</b>	7

**Table 1:** Substrate scope of the Baeyer–Mills reaction under the optimized conditions in continuous flow. (continued)

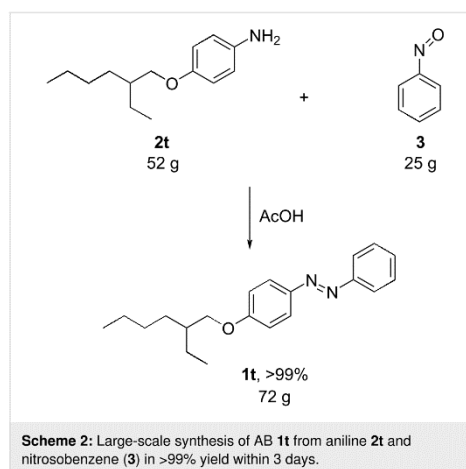
16			54
17			68
18			33
19			95

<sup>a</sup>Purified by chromatography.

derivatives can be explained by the reduced nucleophilicity. To exemplarily demonstrate the optimization for electron-poor derivatives, the synthesis of *p*-cyano-substituted AB **1o** was repeated at higher temperatures. Thereby the yield of **1o** could be increased to 17% (90 °C) and 19% (110 °C), respectively. However, since larger amounts of azoxybenzene were formed, column chromatography became necessary relativizing this improvement in yield (see Supporting Information File 1 for spectra). Substrates, which did not result in AB formation, were anilines with a nitro-substituent. Moreover, some further cases of *ortho*-substituted anilines were unsuccessful, for which steric effects could serve as an explanation (see Supporting Information File 1 for details). In comparison with published batch syntheses, the herein reported continuous flow synthesis usually gives similar or improved yields and eliminates the shortcomings in scalability.

For the applications of ABs as molecular materials often larger amounts are required, for example, as active compounds in molecular solar thermal energy storage (MOST) systems. Therefore, we utilized the set-up for the preparation of large amounts of AB **1t** (Scheme 2). This AB analogue was first synthesized by Masutani et al. in 2014 and was examined by them as well as in further studies by other groups regarding their potential for MOST applications, e.g., in a fluidic chip device by Wang et al. [1,26,27]. For the large-scale synthesis both, aniline **2t** as well as nitrosobenzene (**3**), were dissolved in acetic acid and, as described before, pumped through the flow setup (Figure 3). Every 12 h, the organic phase was separated from the aqueous phase, dried over MgSO<sub>4</sub>, and the solvent was subsequently re-

moved. The solvent was recycled to minimize waste. After a total runtime of 3 days 72 g of AB **1t** were obtained as pure red oil which corresponds to a yield of >99%. Therefore, the method should be suitable for the preparation of easily several 100 grams of azobenzene compounds.



## Conclusion

In summary, the Baeyer–Mills reaction was successfully transferred to a continuous flow setup. The method can be used for various anilines as starting materials to access the desired ABs. A scope of 20 different anilines (**2a–t**) resulting in the corre-

sponding azobenzenes **1a–t** was investigated and especially electron-rich azobenzenes were prepared in yields up to >99%. Furthermore, the setup was demonstrated to be applicable for a large-scale synthesis, where azobenzene **1t** was obtained in 72 g within 3 days without the need of further purification. With this process a large number of non-symmetric substituted azobenzenes can be prepared in high yields and large quantities which opens new possibilities for applications of AB as molecular materials in general.

### Supporting Information

#### Supporting Information File 1

General information, experimental data of all isolated products,  $^1\text{H}$  and  $^{13}\text{C}$  NMR spectra, and structures of unsuccessful substrates.

[<https://www.beilstein-journals.org/bjoc/content/supplementary/1860-5397-18-78-S1.pdf>]

### Acknowledgements

The authors thank Chiara Eleonora Campi for help with the graphical abstract.

### Funding

This project was partially funded by the European Regional Development Fund (ERDF), the Germans Research Council DFG (WE5601/12-1) and TCI.

### ORCID® iDs

Jan H. Griwatz - <https://orcid.org/0000-0003-2028-0938>

Anne Kunz - <https://orcid.org/0000-0002-2142-2689>

Hermann A. Wegner - <https://orcid.org/0000-0001-7260-6018>

### References

- Wang, Z.; Losantos, R.; Sampedro, D.; Morikawa, M.-a.; Börjesson, K.; Kimizuka, N.; Moth-Poulsen, K. *J. Mater. Chem. A* **2019**, *7*, 15042–15047. doi:10.1039/c9ta04905c
- Liu, Z. F.; Hashimoto, K.; Fujishima, A. *Nature* **1990**, *347*, 658–660. doi:10.1038/347658a0
- Ikeda, T.; Tsutsumi, O. *Science* **1995**, *268*, 1873–1875. doi:10.1126/science.268.5219.1873
- Gerkman, M. A.; Han, G. G. D. *Joule* **2020**, *4*, 1621–1625. doi:10.1016/j.joule.2020.07.011
- Dong, L.; Feng, Y.; Wang, L.; Feng, W. *Chem. Soc. Rev.* **2018**, *47*, 7339–7368. doi:10.1039/c8cs00470f
- Liu, H.-d.; Zheng, A.-x.; Gong, C.-b.; Ma, X.-b.; Hon-Wah Lam, M.; Chow, C.-f.; Tang, Q. *RSC Adv.* **2015**, *5*, 62539–62542. doi:10.1039/c5ra10343f
- Hüll, K.; Morstein, J.; Trauner, D. *Chem. Rev.* **2018**, *118*, 10710–10747. doi:10.1021/acs.chemrev.8b00037
- Liu, M.; Yan, X.; Hu, M.; Chen, X.; Zhang, M.; Zheng, B.; Hu, X.; Shao, S.; Huang, F. *Org. Lett.* **2010**, *12*, 2558–2561. doi:10.1021/ol100770j
- Konieczkowska, J.; Bujak, K.; Nocoń, K.; Schab-Balcerzak, E. *Dyes Pigm.* **2019**, *171*, 107659. doi:10.1016/j.dyepig.2019.107659
- Zhang, Y.; Sun, X.; An, X.; Sui, A.; Yi, J.; Song, X.-m. *Dyes Pigm.* **2021**, *186*, 109018. doi:10.1016/j.dyepig.2020.109018
- Norikane, Y.; Tamaoki, N. *Org. Lett.* **2004**, *6*, 2595–2598. doi:10.1021/ol049082c
- Hartley, G. S. *Nature* **1937**, *140*, 281. doi:10.1038/140281a0
- Harada, J.; Ogawa, K.; Tomoda, S. *Acta Crystallogr., Sect. B: Struct. Sci.* **1997**, *53*, 662–672. doi:10.1107/s0108768197002772
- Mostad, A.; Rømming, C. *Acta Chem. Scand.* **1971**, *25*, 3561–3561. doi:10.3891/acta.chem.scand.25-3561
- Bandara, H. M. D.; Burdette, S. C. *Chem. Soc. Rev.* **2012**, *41*, 1809–1825. doi:10.1039/c1cs15179g
- Merino, E. *Chem. Soc. Rev.* **2011**, *40*, 3835–3853. doi:10.1039/c0cs00183j
- Zhang, C.; Jiao, N. *Angew. Chem., Int. Ed.* **2010**, *49*, 6174–6177. doi:10.1002/anie.201001651
- Mills, C. J. *Chem. Soc., Trans.* **1895**, *67*, 925–933. doi:10.1039/ct8956700925
- Baeyer, A. *Ber. Dtsch. Chem. Ges.* **1874**, *7*, 1638–1640. doi:10.1002/cber.187400702214
- Ueno, K.; Akiyoshi, S. *J. Am. Chem. Soc.* **1954**, *76*, 3670–3672. doi:10.1021/ja01643a021
- Dommaschk, M.; Peters, M.; Gutzeit, F.; Schütt, C.; Näther, C.; Sönnichsen, F. D.; Tiwari, S.; Riedel, C.; Boretius, S.; Herges, R. *J. Am. Chem. Soc.* **2015**, *137*, 7552–7555. doi:10.1021/jacs.5b00929
- Plutschack, M. B.; Pleber, B.; Gilmore, K.; Seeberger, P. H. *Chem. Rev.* **2017**, *117*, 11796–11893. doi:10.1021/acs.chemrev.7b00183
- Qin, H.; Liu, C.; Lv, N.; He, W.; Meng, J.; Fang, Z.; Guo, K. *Dyes Pigm.* **2020**, *174*, 108071. doi:10.1016/j.dyepig.2019.108071
- Georgiades, Á.; Ötvös, S. B.; Fülöp, F. *ACS Sustainable Chem. Eng.* **2015**, *3*, 3388–3397. doi:10.1021/acssuschemeng.5b01096
- Tombari, R. J.; Tuck, J. R.; Yardeny, N.; Gingrich, P. W.; Tantillo, D. J.; Olson, D. E. *Org. Biomol. Chem.* **2021**, *19*, 7575–7580. doi:10.1039/d1ob01450a
- Masutani, K.; Morikawa, M.-a.; Kimizuka, N. *Chem. Commun.* **2014**, *50*, 15803–15806. doi:10.1039/c4cc07713j
- Wang, Z.; Moise, H.; Cacciarini, M.; Nielsen, M. B.; Morikawa, M.-a.; Kimizuka, N.; Moth-Poulsen, K. *Adv. Sci.* **2021**, *8*, 2103060. doi:10.1002/advs.202103060

### License and Terms

This is an open access article licensed under the terms of the Beilstein-Institut Open Access License Agreement (<https://www.beilstein-journals.org/bjoc/terms>), which is identical to the Creative Commons Attribution 4.0 International License (<https://creativecommons.org/licenses/by/4.0>). The reuse of material under this license requires that the author(s), source and license are credited. Third-party material in this article could be subject to other licenses (typically indicated in the credit line), and in this case, users are required to obtain permission from the license holder to reuse the material.

The definitive version of this article is the electronic one which can be found at:

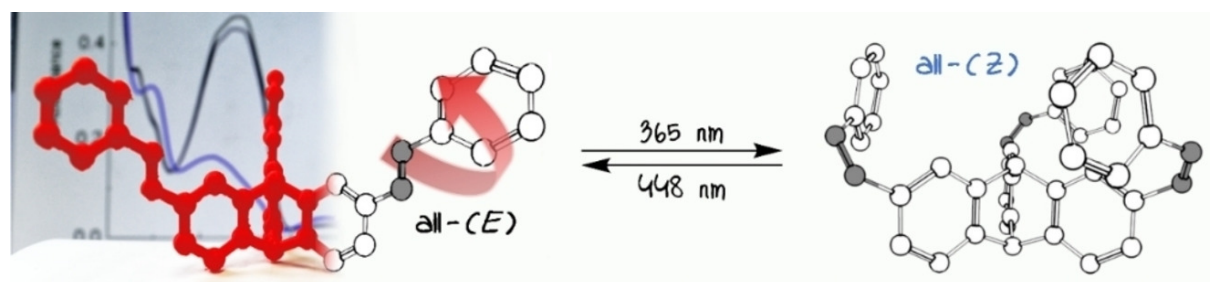
<https://doi.org/10.3762/bjoc.18.78>

### 4.3 Azobenzene Substituted Triptycenes – Understanding Exciton Coupling of Molecular Switches in Close Proximity

Reference: A. Kunz, N. Oberhof, F. Scherz, L. Martins, A. Dreuw, H. A. Wegner, *Chem. Eur. J.*, **2022**, *28*, e202200972.

DOI: 10.1002/chem.202200972

© 2022 Reproduced with permission from John Wiley & Sons.



“Herein, we report a series of azobenzene-substituted triptycenes. In their design, these switching units were placed in close proximity, but electronically separated by a  $sp^3$  center. The azobenzene switches were prepared by Baeyer–Mills coupling as key step. The isomerization behavior was investigated by  $^1\text{H}$  NMR spectroscopy, UV/Vis spectroscopy, and HPLC. It was shown that all azobenzene moieties are efficiently switchable. Despite the geometric decoupling of the chromophores, computational studies revealed excitonic coupling effects between the individual azobenzene units depending on the connectivity pattern due to the different transition dipole moments of the  $\pi \rightarrow \pi^*$  excitations. Transition probabilities for those excitations are slightly altered, which is also revealed in their absorption spectra. These insights provide new design parameters for combining multiple photoswitches in one molecule, which have high potential as energy or information storage systems, or, among others, in molecular machines and supramolecular chemistry.”



## Azobenzene-Substituted Triptycenes: Understanding the Exciton Coupling of Molecular Switches in Close Proximity

Anne Kunz,<sup>[a, b]</sup> Nils Oberhof,<sup>[c]</sup> Frederik Scherz,<sup>[c]</sup> Leon Martins,<sup>[c]</sup> Andreas Dreuw,<sup>[c]</sup> and Hermann A. Wegner<sup>\*[a, b]</sup>

**Abstract:** Herein, we report a series of azobenzene-substituted triptycenes. In their design, these switching units were placed in close proximity, but electronically separated by a  $sp^3$  center. The azobenzene switches were prepared by Baeyer–Mills coupling as key step. The isomerization behavior was investigated by  $^1\text{H}$  NMR spectroscopy, UV/Vis spectroscopy, and HPLC. It was shown that all azobenzene moieties are efficiently switchable. Despite the geometric decoupling of the chromophores, computational studies revealed exci-

tonic coupling effects between the individual azobenzene units depending on the connectivity pattern due to the different transition dipole moments of the  $\pi \rightarrow \pi^*$  excitations. Transition probabilities for those excitations are slightly altered, which is also revealed in their absorption spectra. These insights provide new design parameters for combining multiple photoswitches in one molecule, which have high potential as energy or information storage systems, or, among others, in molecular machines and supramolecular chemistry.

### Introduction

In recent years, azobenzenes (ABs) have turned out to be truly multitalented. They are no longer just used as dyes.<sup>[1]</sup> Their ability to isomerize between the planar, energetically more stable (*E*)-AB to the twisted, metastable *Z* isomer makes them useful protagonists in energy and information storage,<sup>[2]</sup> organocatalysis,<sup>[3]</sup> photobiology and photopharmacology,<sup>[4]</sup> host–guest chemistry,<sup>[5]</sup> molecular mechanics,<sup>[6]</sup> molecular machines<sup>[7]</sup> and other areas of research.<sup>[8]</sup> The reason for this multitude of application possibilities is the large change in geometry and length by the isomerization from (*E*)- to (*Z*)-AB.<sup>[9]</sup> This *E*→*Z* isomerization can be triggered photochemically with light of around 300–360 nm. The AB can be conveniently switched back from *Z*→*E* with light of 450 nm or thermally.<sup>[9]</sup> Moreover, it can also be isomerized by electrochemical stimulation as well as by mechanical stress.<sup>[10]</sup> Despite this

versatility in properties and applications, the ideal connection of AB switches with other functional entities and their inter- and intramolecular interaction is still not fully understood; this can also be observed for other photoswitches.<sup>[11]</sup> When combining the AB scaffold with (photo-)systems in general, these units can have an influence on the photochemical properties depending on the linkage.<sup>[11a,d]</sup> By connecting, for example, two ABs in the *ortho*, *meta* or *para* position on the same phenyl ring, not only their absorption maximum is changed, but also their half-life and quantum yield differ drastically.<sup>[11a]</sup>

To minimize the influence of joined photosystems on each other it is possible to spatially separate them by fixing them at a suitable distance.<sup>[12]</sup> Moreover, connecting photosystems in the *meta* position (“*meta* rule”) often leads to less  $\pi$ -conjugation and, therefore, to practically independent behavior of the individual systems.<sup>[11a,b,13]</sup> However, photochromic entities in close proximity, even if not directly conjugated, can influence each other. One option is the incorporation in cycles, in which upon isomerization a drastic conformational change is induced that alters the switching behavior of the other parts.<sup>[14]</sup> One example of this behavior is the incorporation of two AB moieties in a ring system separated by a methylene linker. In this case, the expected stability order was overturned with the *Z,Z* isomer being most stable conformer because of ring strain.<sup>[15]</sup> Less obvious and controllable are influences like for example energy transfer through space with distance being the crucial parameter.<sup>[16]</sup>

To study the interaction of multiple, spatially close azobenzene units but electronically separated by a  $sp^3$  center without influences like ring strain, one, two and three azobenzene moieties were attached to a triptycene scaffold in *meta* connection. Triptycene (1) as spacer unit is a bridgehead system with  $D_{3h}$  symmetry, which was first synthesized by Bartlett et al.<sup>[17]</sup> Due to their high symmetry and rigidity,

[a] A. Kunz, Prof. Dr. H. A. Wegner  
Institute of Organic Chemistry, Justus Liebig University  
Heinrich-Buff-Ring 17, 35392 Giessen (Germany)  
E-mail: Hermann.a.wegner@org.chemie.uni-giessen.de

[b] A. Kunz, Prof. Dr. H. A. Wegner  
Center of Material Research (LaMa/ZfM)  
Justus Liebig University  
Heinrich-Buff-Ring 16, 35392 Giessen (Germany)

[c] N. Oberhof, F. Scherz, L. Martins, Prof. Dr. A. Dreuw  
Interdisciplinary Center for Scientific Computing  
Heidelberg University  
Im Neuenheimer Feld 205, 69120 Heidelberg (Germany)

Supporting information for this article is available on the WWW under <https://doi.org/10.1002/chem.202200972>

© 2022 The Authors. Chemistry – A European Journal published by Wiley-VCH GmbH. This is an open access article under the terms of the Creative Commons Attribution Non-Commercial License, which permits use, distribution and reproduction in any medium, provided the original work is properly cited and is not used for commercial purposes.

tritycene derivatives have been studied inter alia in the fields of molecular machines, supramolecular chemistry as well as material science.<sup>[18]</sup> Besides the fundamental insights these switchable compounds offer application as molecular grippers as the all-*Z* form of a threefold substituted azobenzene triptycene exhibits a close cavity that can be reversibly opened with light (Figure 1).<sup>[19]</sup>

Triptycene offers different connection patterns. Besides the number of azobenzenes connected, constitutional isomers also exist (*ortho* vs. *meta* and up vs. down, relatively). Herein, we present a systematic study comprising synthesis and photochemical characterization of all different *meta*-isomers. The study was supported by computations to reveal any interaction of the individual switches in detail.

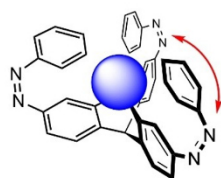
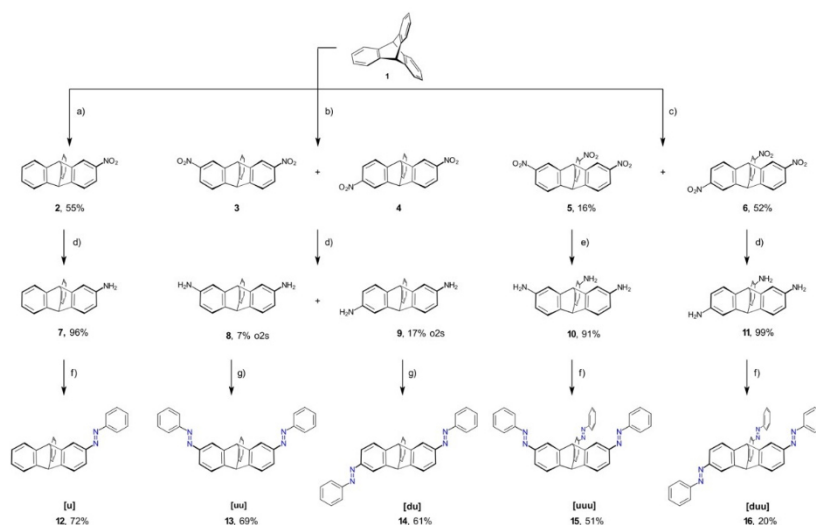


Figure 1. Azobenzene-triptycene as model for through-space interactions and potential molecular gripper.

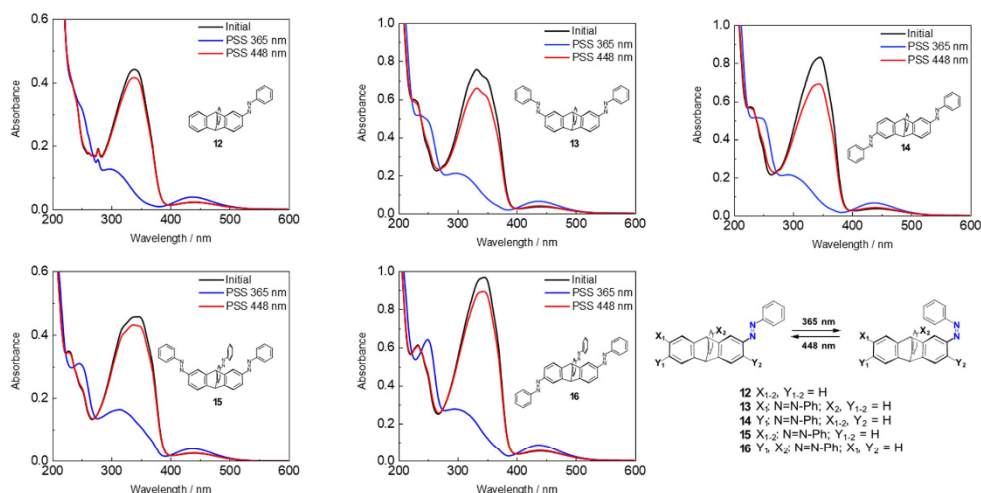
## Results and Discussion

### Synthesis

A synthetic route starting from commercially available unsubstituted triptycene (**1**) was developed to access the desired *meta*-azobenzene-substituted triptycenes (*meta*-TrpABs) **12–16**. The Baeyer–Mills coupling reaction as key step was the method of choice to install the azobenzene moiety from the aminotriptycenes **7–11** with nitrosobenzene. This reaction has been proven to be reliable in various azobenzene syntheses by others as well as by us.<sup>[11f,14b,20]</sup> The aminotriptycenes **7–11** required should be prepared by hydrogenation of nitrotriptycenes **2–6**, which can be synthesized by nitration of unsubstituted triptycene (**1**). As the first step, triptycene **1** was nitrated under various conditions (Scheme 1). Optimization was required to provide satisfactory yields for the desired substitution patterns. For the triple *meta*-nitration nitrotriptycene **6** is always preferably formed in relation to nitrotriptycene **5**. In this process excess of fuming nitric acid in acetic acid was applied to yield the nitrotriptycene **6** in 52% and nitrotriptycene **5** in yields of 16%, respectively.<sup>[21]</sup> For double nitration best yields were achieved with  $\text{KNO}_3$  and trifluoroacetic anhydride (TFAA), providing mostly **3** and **4** as mixture of isomers.<sup>[22]</sup> This mixture of **3** and **4** was used without further purification in the following hydrogenation reaction, after which the two isomers could be separated by column chromatography as aminotriptycenes **8** and **9**.<sup>[23]</sup> For single *meta* nitration, concentrated nitric acid was used.<sup>[24]</sup> After hydrogenation, the obtained aminotriptycenes **7–11** were condensed in a Baeyer–Mills coupling reaction with nitrosobenzene to obtain the target



Scheme 1. Synthesis route towards *meta*-TrpABs **12–16**. a) conc.  $\text{HNO}_3$ , 75 °C, 24 h; b)  $\text{KNO}_3$ , TFAA, ACN, RT, 24 h; c) fuming  $\text{HNO}_3$ , AcOH, 0 °C, 1 h; d)  $\text{H}_2$ , Pd/C, MeOH, overnight; e)  $\text{H}_2$ , Pd/C, MeOH, 2 h; f) nitrosobenzene, AcOH, toluene, 60 °C, 24 h; g) nitrosobenzene, AcOH, toluene, 60 °C, 48 h. o:2 s: over two steps.



**Scheme 2.** UV-Vis spectroscopy of (*meta*-TrpABs 12–16 in acetonitrile/H<sub>2</sub>O (90:10) at a concentration of  $2 \times 10^{-5}$  mol L<sup>-1</sup>. The solutions were irradiated with light of 365 nm (purple) and subsequently with light of 448 nm (blue) until the PSS was reached.

TrpABs 12–16 in yields up to 72%. TrpAB 14 is chiral and was accordingly obtained as a mixture of enantiomers. The enantiomeric ratio was not examined, but is subject of future research.

#### Isomerization studies

After successful synthesis the photochemical properties of all synthesized *meta*-TrpABs 12–16 were studied by UV/Vis spectroscopy in acetonitrile (see the Supporting Information for acetonitrile and Scheme 2 for acetonitrile/water 90:10). The proportion of water had no noticeable influence on the switching properties (see the Supporting Information). In comparison to the parent AB, the TrpABs exhibited slightly redshifted  $\pi \rightarrow \pi^*$  transitions at around 340 nm. For all *meta*-TrpABs 12–16 the decrease in the absorption maxima of the  $\pi \rightarrow \pi^*$  transition after irradiation of 365 nm indicating  $E \rightarrow Z$  photoisomerization.

Although the initial absorbance of the all-*E* spectra (black spectra, Scheme 2) could not be reached, irradiation at 448 nm initiated  $Z \rightarrow E$  back photoisomerization (purple spectra, Scheme 2). Additionally, the isomerization of the *meta*-TrpABs 12–16 was followed by <sup>1</sup>H NMR spectroscopy in [D<sub>3</sub>]acetonitrile, which confirmed the results of the UV-Vis experiments. Furthermore, all possible isomers (for 12 *E* and *Z*, for 13 and 14 *EE*, *EZ*, *ZZ* and for 15 and 16, *EEE*, *EEZ*, *EZZ*, *ZZZ*) could be detected after irradiation with different wavelength in the <sup>1</sup>H NMR spectra (see the Supporting Information). The exact compositions of isomers present in the PSSs were also determined by HPLC. The spectroscopic and photoisomerization results are summarized in Table 1. For all compounds an overall percentage of azobenzene moieties in the *Z* state after

**Table 1.** Irradiation wavelengths of the *E* isomers and photostationary state (PSS) compositions for AB moieties in *E* or *Z* in (*meta*-TrpABs 12–16 determined by HPLC at the corresponding isosbestic points of the spectra.

TrpAB	$E \rightarrow Z$ 365 nm PSS composition [%]		$Z \rightarrow E$ PSS composition [%]	
	<i>E</i> <sup>[c]</sup>	<i>Z</i> <sup>[c]</sup>	<i>E</i> <sup>[c]</sup>	<i>Z</i> <sup>[c]</sup>
12 <sup>[a]</sup>	6	94	80	20
13 <sup>[b]</sup>	8	92	78	22
14 <sup>[b]</sup>	6	94	78	22
15 <sup>[a]</sup>	31	69	80	20
16 <sup>[a]</sup>	16	84	79	21

[a] For  $Z \rightarrow E$  isomerization, samples were irradiated at 448 nm. [b] For  $Z \rightarrow E$  isomerization, samples were irradiated at 425–430 nm. [c] Percentage of AB units in *E* or *Z*. Ratios of the individual isomers can be found in the Supporting Information.

irradiation with light of 365 nm was over 80%, except for *meta*-TrpAB 15. In this case, the increased steric demand could be a reason for the lower overall (*Z*)-AB concentration. Back isomerization to ~80% (*E*)-AB moieties was possible for all *meta*-TrpAB 12–16 by irradiation of light into the  $n \rightarrow \pi^*$  transition bands, located at around 430 nm (Scheme 2) and to ~100% (*E*)-AB by heating to 70 °C.

#### Computation

The molecular geometry of TrpAB 12 has *C*<sub>s</sub> point group symmetry. The first excited electronic *S*<sub>1</sub> state possesses the well-known  $n\pi^*$  character of azobenzenes and has an excitation energy of 2.86 eV (calculated with linear-response time-dependent density functional theory, TDDFT;<sup>[25]</sup> for details see the Supporting Information). The  $\pi \rightarrow \pi^*$  excitation corresponds to

the  $S_2$  state and is slightly red-shifted with an excitation energy of 4.17 eV compared to standard AB, whose  $S_2$  state is at 4.37 eV at the same level of theory. The transition dipole moment of the  $\pi$ - $\pi^*$  absorption is oriented along the longitudinal axis (Figure 2) of the AB moiety.

Introducing a second AB moiety at the triptycene unit parallel to the existing one results in TrpAB 13 (Figure 2), which also has  $C_2$  point group symmetry. The  $n$ - $\pi^*$  excitations (now  $S_1$  and  $S_2$ ) are localized at each AB branch, are basically unaffected by each other and possess excitation energies of 2.84 and 2.85 eV, respectively. In contrast, the  $\pi$ - $\pi^*$  excitations of the individual AB branches change significantly due to excitonic coupling effects between them.

As a consequence, the two corresponding states  $S_3$  and  $S_4$  are red and blue shifted by approximately 0.15 to 4.01 and 4.32 eV, respectively. The excitonic coupling can be understood in terms of vector sums or phase combinations of the two transition dipole moment vectors of the individual  $\pi$ - $\pi^*$  excitations (Figure 2). The out-of-phase combination leads to stabilizing interaction introducing a red shift whereas the in-phase combination gives a destabilizing interaction causing a blue shift of the excitation. As neither interaction is parallel or in-line, both excited states retain reasonable oscillator strengths. This manifests as peak broadening within the theoretical spectrum (Figure S14) and can also be seen in the experimental spectrum comparing TrpABs 12 and 13 (Scheme 2).

When the second azobenzene moiety is introduced at the "down" position of the triptycene unit leading to TrpAB 14, the excitonic coupling is reduced. This can be rationalized as the two interacting transition dipole moments are further apart, because they are positioned on opposite sides of the triptycene core. This leads to smaller shifts of the excitation energies of the  $\pi$ - $\pi^*$  states now being found at 4.07 and 4.28 eV. Due to the more linear orientation of the transition dipole moments, the difference in oscillator strength between the  $\pi$ - $\pi^*$  states, however, becomes larger than in TrpAB 13, as the out-of-phase

and in-phase combinations of the transition dipole moments become more constructive and more destructive, respectively. Therefore, the blue shifted in-phase transition retains very low oscillator strength and does not manifest as peak broadening in the calculated spectrum (Figure S15).

Introducing a third AB unit to the remaining phenyl ring of the triptycene unit such that the whole molecule exhibits  $C_{3v}$  point group symmetry yields TrpAB 15. The  $n$ - $\pi^*$  excitations ( $S_{1-3}$ ) still remain largely unaffected and stay localized at the individual azobenzene branches with excitation energies of 2.84, 2.85 and 2.85 eV. In this highly symmetric molecule TrpAB 15, the pattern of the excitonic coupling between the three individual  $\pi$ - $\pi^*$  excitations reflects the molecular point group symmetry and exhibits two degenerate stabilized states  $S_4$  and  $S_5$  at 4.02 eV and one destabilized state  $S_6$  at 4.50 eV. The out-of-phase degenerate combinations herein correspond to the E irreducible representation, whereas the in-phase combination has  $A_2$  symmetry (Figure 3). Due to the diagonal orientation of the transition dipole moments all states retain significant oscillator strength.

When the third AB group is introduced in the "down" position of the remaining phenyl ring of the central triptycene unit, the resulting system TrpAB 16 exhibits  $C_s$  symmetry leading to non-degenerate out-of-phase combinations of the  $A'$  and  $A''$  symmetry of the  $\pi$ - $\pi^*$  states (Figure 4). The corresponding excitation energies are now 4.03, 4.07 and 4.40 eV for  $S_4$ ,  $S_5$ , and  $S_6$ , respectively. The now more linear orientation of the transition dipole moments leads again also to different oscillator strengths with the in-phase combination having a significantly reduced transition probability. This then substantiates with the absence of the blue shifted shoulder in the calculated spectrum of TrpAB 16 compared to that of TrpAB 15. This is in agreement with the experimental spectra, since the  $\pi$ - $\pi^*$  band of TrpAB 15 is clearly broader than the  $\pi$ - $\pi^*$  band of TrpAB 16 (see the Supporting Information for superimposed absorption spectra of 15 and 16).

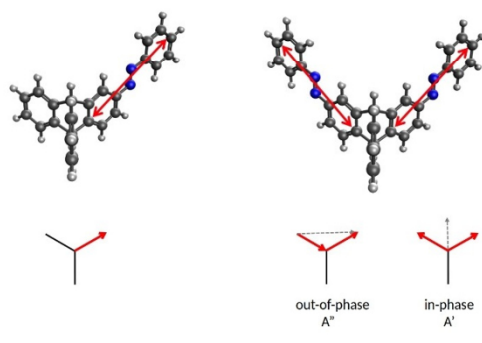


**Figure 2.** Vector representation of the transition dipole moments of the  $\pi$ - $\pi^*$  excitations in TrpAB 12 (right) and TrpAB 13 (left) and the respective out-of-phase and in-phase combinations in 13, which represent the excitonically coupled states  $S_3$  and  $S_4$  in 13.

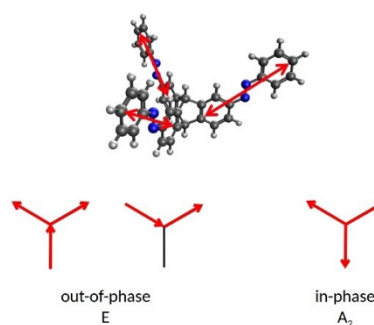


**Figure 3.** Vector representation of the transition dipole moments of the  $\pi$ - $\pi^*$  excitations in TrpAB 15 and the respective out-of-phase and in-phase combinations representing  $S_4$  to  $S_6$ .

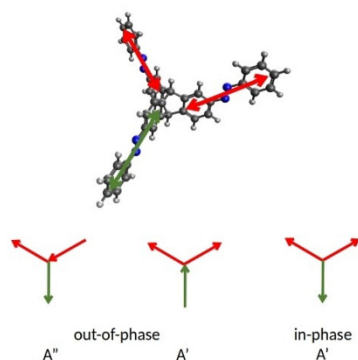


**Figure 4.** Vector representation of the transition dipole moments of the  $\pi$ - $\pi^*$  excitations in [duu] TrpAB **16** and the respective out-of-phase and in-phase combinations representing  $S_4$  to  $S_6$ . The reduced symmetry leads to three non-degenerate excitonically coupled excited states.

## Conclusion

In summary, five different combinations of TrpABs in the *meta* position **12–16** were successfully synthesized with a Baeyer–Mills coupling reaction as the key step. UV/Vis and  $^1\text{H}$  NMR spectroscopy confirmed that **12–16** are able to photoisomerize. Their exact compositions of isomers in the photostationary states at different excitation wavelength were determined by HPLC at their specific isosbestic points. All compounds were able to isomerize to an *E* composition of ~80%. Photochemical back-isomerization to an *E* composition of ~80% was achieved in all cases; this makes the substances not only interesting as switchable hosts, but also as possible information and energy storage systems. Moreover, calculations revealed the  $n$ - $\pi^*$  excitations to be practically unaffected by the neighboring AB units. In contrast, the  $\pi$ - $\pi^*$  excitations of the individual AB units in the TrpAB derivatives change significantly due to excitonic coupling effects obeying, like textbook examples, the molecular point group symmetry.

## Acknowledgements

Financial support by the DFG is acknowledged, and we thank J. H. Griwatz for help with the graphical abstract. Open Access funding enabled and organized by Projekt DEAL.

## Conflict of Interest

The authors declare no conflict of interest.

## Data Availability Statement

The data that support the findings of this study are available in the supplementary material of this article.

**Keywords:** azo compounds · computational chemistry · excitonic coupling · isomerization · photochemistry

- [1] K. Hunger, P. Mischke, W. Rieper, S. Zhang in *Ullmann's Encyclopedia of Industrial Chemistry*, Wiley-VCH, Weinheim, **2000**, p. 1–24.
- [2] a) Z. Wang, R. Losantos, D. Sampedro, M. Morikawa, K. Börjesson, N. Kimizuka, K. Moth-Poulsen, *J. Mater. Chem. A* **2019**, *7*, 15042–15047; b) L. Dong, Y. Feng, L. Wang, W. Feng, *Chem. Soc. Rev.* **2018**, *47*, 7339–7368; c) Z. F. Liu, K. Hashimoto, A. Fujishima, *Nature* **1990**, *347*, 658–660; d) T. Ikeda, O. Tsutsumi, *Science* **1995**, *268*, 1873–1875; e) M. A. Gerkman, G. G. Han, *Joule* **2020**, *4*, 1621–1625.
- [3] H. Liu, A. Zheng, C. Gong, X. Ma, M. Hon-Wah Lam, C. Chow, Q. Tang, *RSC Adv.* **2015**, *5*, 62539–62542.
- [4] K. Hüll, J. Morstein, D. Trauner, *Chem. Rev.* **2018**, *118*, 10710–10747.
- [5] M. Liu, X. Yan, M. Hu, X. Chen, M. Zhang, B. Zheng, X. Hu, S. Shao, F. Huang, *Org. Lett.* **2010**, *12*, 2558–2561.
- [6] a) J. Konieczkowska, K. Bujak, K. Nocoń, E. Schab-Balcerzak, *Dyes Pigm.* **2019**, *171*, 107659; b) Y. Zhang, X. Sun, X. An, A. Sui, J. Yi, X. Song, *Dyes Pigm.* **2021**, *186*, 109018.
- [7] Y. Norikane, N. Tamaoki, *Org. Lett.* **2004**, *6*, 2595–2598.
- [8] a) H. M. D. Bandara, S. C. Burdette, *Chem. Soc. Rev.* **2012**, *41*, 1809–1825; b) J. Boelke, S. Hecht, *Adv. Opt. Mater.* **2019**, *7*, 1900404.
- [9] G. S. Hartley, *Nature* **1937**, *140*, 281.
- [10] a) R. Turanský, M. Konópka, N. L. Doltsinis, I. Stich, D. Marx, *Phys. Chem. Chem. Phys.* **2010**, *12*, 13922–13932; b) J. Henzl, M. Mehlhorn, H. Gawronski, K.-H. Rieder, K. Morgenstern, *Angew. Chem. Int. Ed.* **2006**, *45*, 603–606; *Angew. Chem.* **2006**, *118*, 617–621; c) A. Goulet-Hanssens, M. Utecht, D. Mutruc, E. Titov, J. Schwarz, L. Grubert, D. Bléger, P. Saalfrank, S. Hecht, *J. Am. Chem. Soc.* **2017**, *139*, 335–341.
- [11] a) C. Slavov, C. Yang, L. Schweighauser, C. Boumrifak, A. Dreuw, H. A. Wegner, J. Wachtveitl, *Phys. Chem. Chem. Phys.* **2016**, *18*, 14795–14804; b) A. U. Petersen, S. L. Broman, S. T. Olsen, A. S. Hansen, L. Du, A. Kadziola, T. Hansen, H. G. Kjaergaard, K. V. Mikkelsen, M. B. Nielsen, *Chem. Eur. J.* **2015**, *21*, 3968–3977; c) A. Perrier, F. Maurel, D. Jacquemin, *J. Phys. Chem. C* **2011**, *115*, 9193–9203; d) A. Kunz, H. A. Wegner, *ChemSystemsChem* **2021**, *3*, e2000035; e) M. A. Strauss, H. A. Wegner, *Angew. Chem. Int. Ed.* **2021**, *60*, 779–786; *Angew. Chem.* **2021**, *133*, 792–799; f) A. Kunz, A. H. Heindl, A. Dreos, Z. Wang, K. Moth-Poulsen, J. Becker, H. A. Wegner, *ChemPlusChem* **2019**, *84*, 1145–1148; g) R. Reuter, H. A. Wegner, *Chem. Commun.* **2013**, *49*, 146–148.
- [12] D. Bléger, J. Dokić, M. V. Peters, L. Grubert, P. Saalfrank, S. Hecht, *J. Phys. Chem.* **2011**, *115*, 9930–9940.
- [13] A. Mengots, A. Erbs Hillers-Bendtsen, S. Doria, F. Ørsted Kjeldal, N. Machholdt Høyer, A. Ugleholdt Petersen, K. V. Mikkelsen, M. Di Donato, M. Cacciarini, M. Brøndsted Nielsen, *Chem. Eur. J.* **2021**, *27*, 12437–12446.
- [14] a) T. J. Kucharski, N. Ferralis, A. M. Kolpak, J. O. Zheng, D. G. Nocera, J. C. Grossman, *Nat. Chem.* **2014**, *6*, 441–447; b) A. H. Heindl, J. Becker, H. A. Wegner, *Chem. Sci.* **2019**, *10*, 7418–7425.
- [15] a) A. Heindl, L. Schweighauser, C. Logemann, H. Wegner, *Synthesis* **2017**, *49*, 2632–2639; b) Y. Norikane, K. Kitamoto, N. Tamaoki, *J. Org. Chem.* **2003**, *68*, 8291–8304.
- [16] a) R. Ziessel, P. Stachelek, A. Harriman, G. J. Hedley, T. Roland, A. Ruseckas, I. D. W. Samuel, *J. Phys. Chem. A* **2018**, *122*, 4437–4447; b) F. M. Raymo, M. Tomasulo, *Chem. Soc. Rev.* **2005**, *34*, 327–336.
- [17] P. D. Bartlett, M. J. Ryan, S. G. Cohen, *J. Am. Chem. Soc.* **1942**, *64*, 2649–2653.
- [18] a) J. H. Chong, M. J. MacLachlan, *Chem. Soc. Rev.* **2009**, *38*, 3301–3315; b) T. M. Swager, *Acc. Chem. Res.* **2008**, *41*, 1181–1189; c) C.-F. Chen, *Chem. Commun.* **2011**, *47*, 1674–1688; d) Z. Meng, J.-F. Xiang, C.-F. Chen, *Chem. Sci.* **2014**, *5*, 1520; e) T. R. Kelly, H. de Silva, R. A. Silva, *Nature* **1999**, *401*, 150–152; f) Y. Han, Z. Meng, Y.-X. Ma, C.-F. Chen, *Acc. Chem. Res.* **2014**, *47*, 2026–2040; g) X.-Y. Hu, W.-S. Zhang, F. Rominger, I. Wacker, R. R. Schröder, M. Mastalerz, *Chem. Commun.* **2017**, *53*, 8616–8619.
- [19] a) T. Gottschalk, B. Jaun, F. Diederich, *Angew. Chem. Int. Ed.* **2007**, *46*, 260–264; *Angew. Chem.* **2007**, *119*, 264–268; b) J. V. Milić, F. Diederich,

- Chem. Eur. J.* **2019**, *25*, 8440–8452; c) J. R. Moran, S. Karbach, D. J. Cram, *J. Am. Chem. Soc.* **1982**, *104*, 5826–5828.
- [20] a) R. Reuter, N. Hostettler, M. Neuburger, H. A. Wegner, *Eur. J. Org. Chem.* **2009**, *2009*, 5647–5652; b) R. Reuter, H. A. Wegner, *Chem. Eur. J.* **2011**, *17*, 2987–2995; c) C. Mills, *J. Chem. Soc. Trans.* **1895**, *67*, 925–933.
- [21] X. Hu, *Synthesis and Modification of [2 + 3] Imine Cage Based on 2,7,14-Triaminotriptycene*, Heidelberg University Library, **2019**.
- [22] Z. Zhu, J. Zhu, J. Li, X. Ma, *Macromolecules* **2020**, *53*, 1573–1584.
- [23] J. M. Granda, J. Grabowski, J. Jurczak, *Org. Lett.* **2015**, *17*, 5882–5885.
- [24] C. Zhang, C.-F. Chen, *J. Org. Chem.* **2006**, *71*, 6626–6629.
- [25] A. Dreuw, M. Head-Gordon, *Chem. Rev.* **2005**, *105*, 4009–4037.

Manuscript received: March 29, 2022  
Accepted manuscript online: May 2, 2022  
Version of record online: June 3, 2022

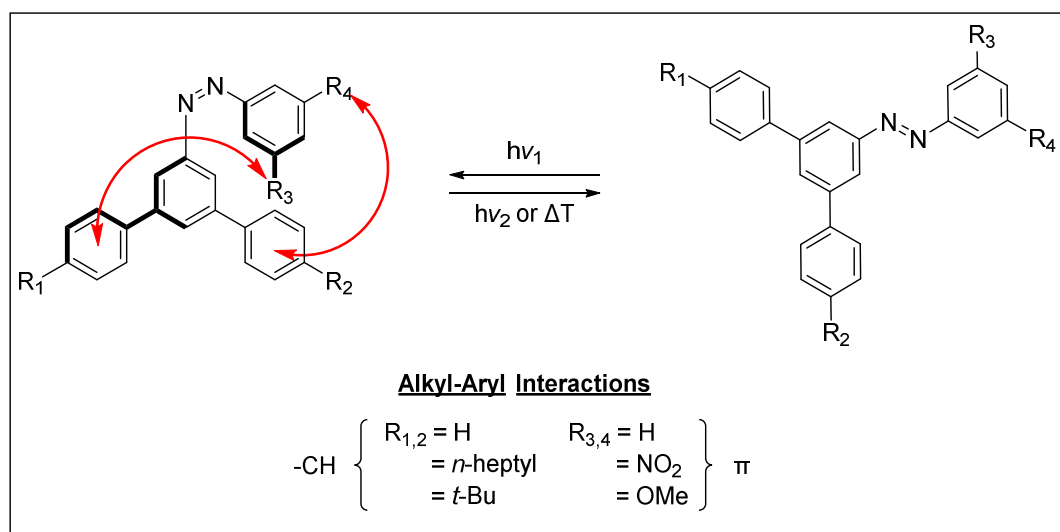
#### 4.4 Investigation of Alkyl-Aryl Interactions using the Azobenzene Switch – The Influence of the Electronic Nature of Aromatic London Dispersion Donors

Reference: A. Kunz<sup>‡</sup>, D. Schatz<sup>‡</sup>, A. R. Raab, H. A. Wegner, *Synlett* **2022**, 33, A-F.

DOI: 10.1055/a-1951-2833

<sup>‡</sup> equal contribution

© 2022 Reproduced with permission from Georg Thieme Verlag KG.



“Herein we report the synthesis of non-symmetrically substituted azobenzene derivatives with meta-alkyl substituents on one side and meta-aryl moieties with electron donating or electron withdrawing groups on the other side. The half-lives for the thermal (Z)- to (E)-isomerization of these molecules were measured in n-octane, which allows investigation of the strength of the aryl-alkyl interactions between their substituents. It was found that the London dispersion donor strength of the alkyl substrate is the deciding factor in the observed stabilization, whereas the electronic structure of the aryl fragment does not influence the isomerization in a significant way.”

A

Synlett

D. Schatz and A. Kunz et al.

Cluster

# Investigation of Alkyl–Aryl Interactions Using the Azobenzene Switch – The Influence of the Electronic Nature of Aromatic London Dispersion Donors

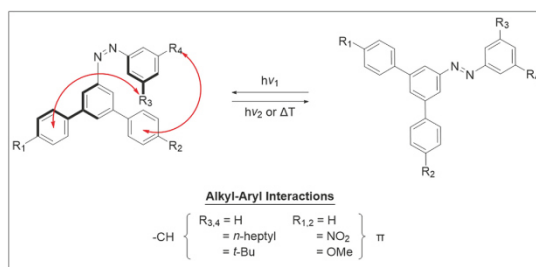
Dominic Schatz<sup>a,b</sup>Anne Kunz<sup>a,b</sup>Aileen R. Raab<sup>a,b</sup>Hermann A. Wegner<sup>a,b</sup><sup>a</sup> Institute of Organic Chemistry, Justus Liebig University, Heinrich-Buff-Ring 17, 35392 Giessen, Germany

Hermann.A.Wegner@org.chemie.uni-giessen.de

<sup>b</sup> Center of Material Research (LaMa/ZIM), Justus Liebig University, Heinrich-Buff-Ring 16, 35392 Giessen, Germany<sup>c</sup> These authors contributed equally

Published as part of the Cluster

Dispersion Effects



Received: 12.08.2022

Accepted after revision: 27.09.2022

Published online: 27.09.2022 (Accepted Manuscript), 28.10.2022 (Version of Record)

DOI: 10.1055/a-1951-2833; Art ID: ST-2022-08-0360-C

**Abstract** Herein we report the synthesis of nonsymmetrically substituted azobenzene derivatives with *meta*-alkyl substituents on one side and *meta*-aryl moieties with electron-donating or electron-withdrawing groups on the other side. The half-lives for the thermal (*Z*) to (*E*) isomerization of these molecules were measured in *n*-octane, which allows investigation of the strength of the aryl–alkyl interactions between their substituents. It was found that the London dispersion donor strength of the alkyl substrate is the decisive factor in the observed stabilization, whereas the electronic structure of the aryl fragment does not influence the isomerization in a significant way.

**Key words** London dispersion, azobenzenes, kinetics, molecular switches, CH– $\pi$  interactions

One important parameter for the geometry and conformation of molecules are inter- and intramolecular noncovalent interactions. In this regard, the van der Waals force describes repulsive interactions, often referred to as steric hindrance, and an attractive part including dipole–dipole, dipole-induced dipole, as well as London dispersion forces.<sup>1</sup> In recent years the decisive role of these relatively small stabilizing interactions has been demonstrated by, for example, enabling long C–C bonds in adamantly dimers,<sup>2</sup> stabilizing DNA helices,<sup>3</sup> or aiding in the aggregation of rhodium complexes.<sup>4</sup> Stabilizing interactions can arise between polarizable surfaces that are in close proximity to each other, usually between 2.5–5 Å, allowing alkyl–alkyl, alkyl–aryl, and aryl–aryl interactions (or combinations of those) to influence the three-dimensional structure of compounds.<sup>5–7</sup>

As a single dispersive interaction is small from an energetically viewpoint, but grows with the number of interactions between atoms, they need to be viewed as a holistic system.<sup>8</sup> The small contribution to stability of a single interaction makes quantifying London dispersion forces challenging. In recent years, a variety of different molecular balances were introduced to allow measuring and comparing such small interactions. These balances are usually based on a thermodynamic equilibrium of a substrate, in which the ratio of two conformers or an equilibrium between an aggregated and nonaggregated state can be precisely measured. By placing a substituent at a position, which can engage in interactions in only one conformer or state, stabilizing effects can be observed by a change in the equilibrium. By precise construction of such a molecular balance, alkyl–aryl,<sup>9</sup> alkyl–alkyl,<sup>10,11</sup> aryl–aryl,<sup>12</sup> as well as competing interactions with solvent molecules were studied.<sup>11,13,14</sup> The effects of London dispersion are an extensively studied field, and there have been a number of comprehensive reviews in recent years, indicating the importance of noncovalent interactions.<sup>14,15</sup> Stabilizing interactions with aromatic scaffolds have also been extensively explored.<sup>16</sup> The *N*-arylimide balance, established by Shimizu, was used for observing the effect of face-to-face aryl, halogen–aryl, OH–aryl, *n*-aryl, as well as CH–aryl interactions.<sup>17,18</sup>

We established a different molecular system that allows quantification of intramolecular forces based on the azobenzenes (AB) switch. Unlike the previous described balances, AB does not exist in an equilibrium of energetically close conformers but can be switched photochemically to a metastable (*Z*)-state. Upon isomerization, the end-to-end distance decreases drastically (from 9.1 Å to 6.2 Å at the *para* position)<sup>19</sup> allowing substituents at the *meta* position

B

Synlett

D. Schatz and A. Kunz et al.

Cluster

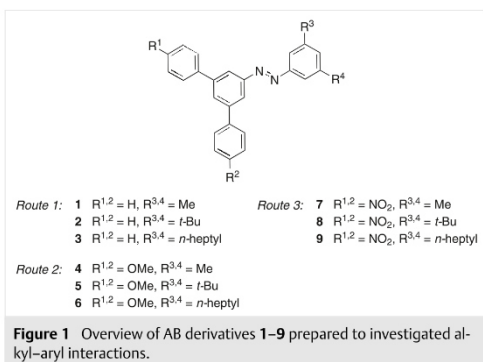
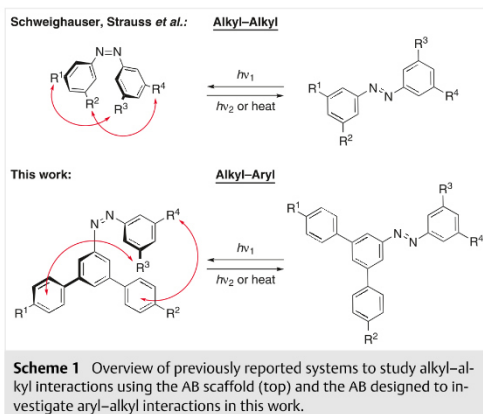
to engage in through-space interactions. For small-to-medium-sized substituents, these intramolecular interactions are only present in the (*Z*)-state and no stabilizing effects in the (*E*)-state or the transition state via an inversion mechanism occur.<sup>7</sup> This allows the correlation of the kinetically controlled (*Z*)→(*E*)-isomerization to thermodynamic quantities. Additionally, by placing substituents in the *meta* position the influence of electronical effects on the mechanism of isomerization is minimized ('*meta*' rule).<sup>20</sup> Schweighauser as well as Strauss *et al.* investigated the photochemical properties of different alkyl-substituted AB derivatives and established that even flexible alkyl chains such as *n*-butyl can cause increased half-lives of the (*Z*)-isomers, which are up to five times prolonged in comparison to their *meta*-Me-substituted AB-derivatives (*n*-decane as solvent, Scheme 1).<sup>6,7</sup>

In the work of Schweighauser and Strauss, mostly alkyl-alkyl interactions have been established as the reason for the increased half-life. However, alkyl-aryl interactions are

also contributors.<sup>6,7,14,21</sup> To disbar the alkyl-alkyl interactions and put a focus on the aryl-alkyl interactions, nine different AB derivatives were designed, which are substituted in *meta* position with Me, *t*-Bu, and *n*-heptyl on one phenyl ring and with electron-donating (*p*-OMe), electron-withdrawing (*p*-NO<sub>2</sub>), and unsubstituted (*p*-H) phenyl rings in *meta* position on the opposite phenyl ring relative to the corresponding azo unit (Figure 1). For synthesizing the all-*meta*-substituted ABs of interest with two aryl substituents on one side and two *meta*-alkyl substituents on the other side (1–9), three different synthetic routes were implemented (Figure 1, Scheme 2): route 1 was applied for Me-, *t*-Bu-, and *n*-heptyl-substituted ABs with unsubstituted phenyl rings (1–3), route 2 for Me-, *t*-Bu-, and *n*-heptyl-substituted ABs with OMe-substituted phenyl groups in *meta* position (4–6), and route 3 for ABs with bis-*para*-NO<sub>2</sub>-substituted phenyl rings in *meta* position (7–9, Scheme 2). For route 1, anilines 15 and 16 were commercially available; only bis-*n*-heptyl-aniline (14) had to be synthesized starting from 5-nitroisophthalic acid (10). After reduction to 5-nitro-1,3-benzenedimethanol (11) and subsequent oxidation to 5-nitro-1,3-benzenedicarboxaldehyde (12), a Wittig reaction to nitrobenzene 13 was performed.<sup>6</sup> To yield bis-*n*-heptyl-aniline (14), nitrobenzene 13 was hydrogenated with palladium on activated charcoal under hydrogen atmosphere.<sup>6</sup> Afterwards, anilines 14–16 were condensed in a Baeyer–Mills coupling reaction with nitrosobenzene 20 to the corresponding ABs 1–3. Nitroso compound 20 was synthesized by Suzuki coupling reaction of dibromoaniline (17) with boronic ester 18, followed by oxidation with Oxone® in a biphasic system of DCM/H<sub>2</sub>O (Scheme 2, top).

Route 2 is also based on a Baeyer–Mills coupling reaction as key step to yield ABs 4–6 as final products. The first building block, bis-*meta*-substituted nitrosobenzenes 24–26, were synthesized by oxidation of the corresponding anilines 14–16 with Oxone®. As second building block, OMe-phenyl-aniline 23 was synthesized by Suzuki coupling reaction of dibromoaniline 17 with boronic ester 22, which was obtained by Miyaura coupling reaction of 4-iodoanisole (21) with bis(pinacolato)diboron (Scheme 2, middle). Route 3 generated the desired ABs 7–9 by Suzuki coupling reaction of ABs 29–31 together with nitro-boronic ester 28, which was synthesized by Miyaura reaction of iodonitrobenzene 27. Before, ABs 29–31 were prepared by Baeyer–Mills coupling reaction of dibromoaniline (17) with the corresponding nitrosobenzenes 24–26 (Scheme 2, bottom).

After successful synthesis of AB derivatives 1–9 (Scheme 2) their rates of the thermal (*Z*)→(*E*) isomerization were determined by temperature-controlled UV/Vis spectroscopy at 40 °C in *n*-octane (Figure 2, Table S3, Table S4). As expected from previous research,<sup>7</sup> *meta*-di-Me-substituted ABs 1, 4, and 7 exhibit the shortest half-life (11.9 h, 11.8 h, 10.3 h for R<sup>3,4</sup> = H, OMe or NO<sub>2</sub>, respectively). The *meta*-di-*n*-heptyl-substituted ABs 3, 6, and 9 exhibit half-

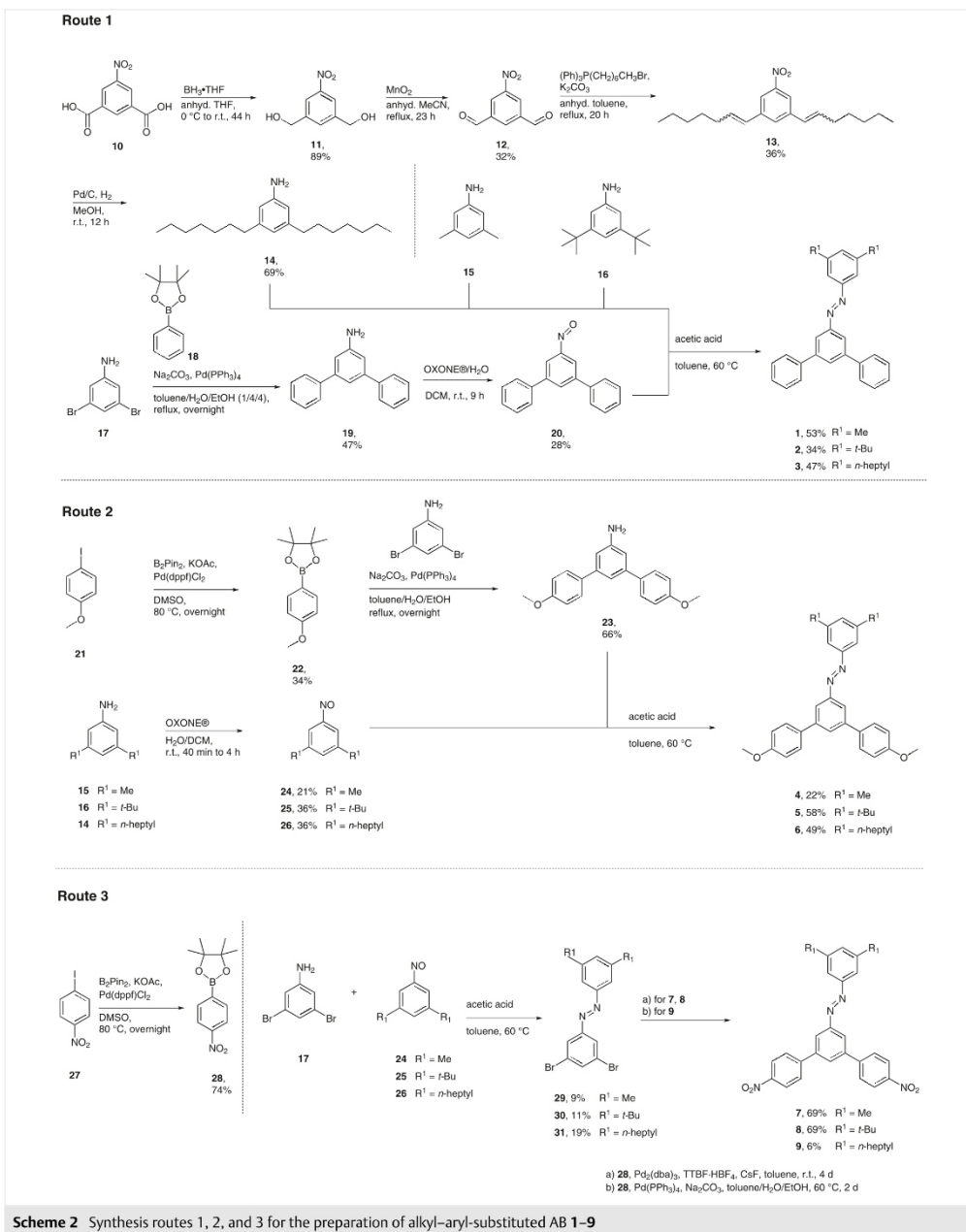


C

Synlett

D. Schatz and A. Kunz et al.

Cluster



D

Synlett

D. Schatz and A. Kunz et al.

Cluster

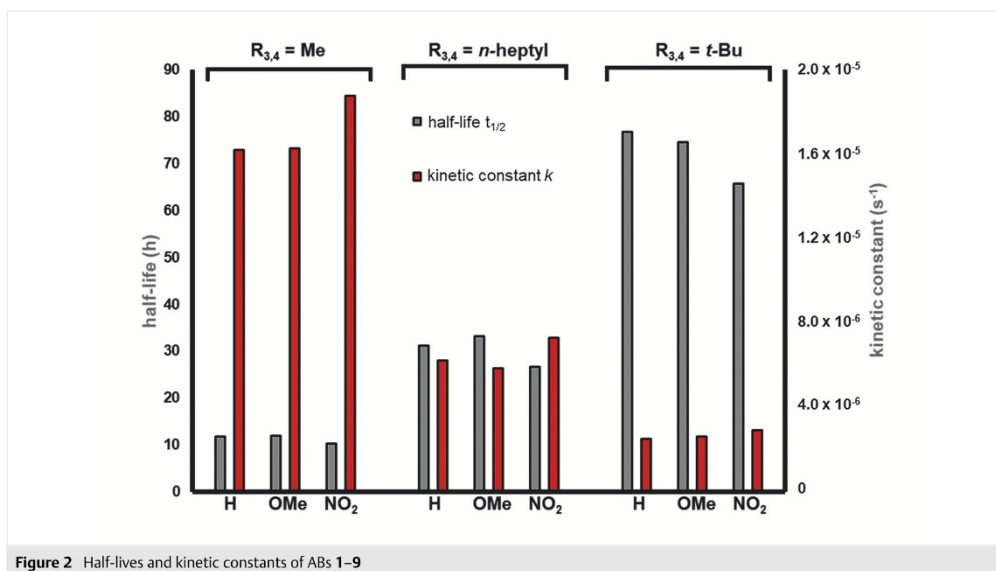


Figure 2 Half-lives and kinetic constants of ABs 1–9

lives almost three times longer than the *meta*-di-Me ABs (31.0 h, 33.0 h, 25.9 h). Among all tested AB derivatives, *meta*-*tert*-butyl-substituted ABs **2**, **5**, and **8** were found to exhibit the longest half-lives (76.5 h, 71.4 h, 64.9 h). ABs with unsubstituted rings **1–3** show similar isomerization kinetics in comparison to ABs with OMe-substituted phenyl rings (**4–6**). The NO<sub>2</sub>-substituted ABs **7–9** exhibit a slightly faster isomerization behavior (ca. 15%, independent of the alkyl group attached) compared to their unsubstituted analogues. This effect might be based on the difference in their electronic structure, as ABs with push–pull configurations are generally showing faster isomerization kinetics.<sup>22</sup> However, a uniform mechanism has been previously established for similar *meta*-substituted ABs confirmed by Exner plot analysis.<sup>7,23</sup>

In addition, <sup>1</sup>H NOESY NMR spectra were performed exemplary for OMe-substituted ABs **4–6** (Figure 2, full spectra can be found in the Supporting Information). As this technique allows to identify protons which are in close proximity (up to 5 Å) even when they are not covalently bound, it is predestinated to study London dispersion interactions which operate in exactly this range. Therefore, ABs **4**, **5**, and **6** were irradiated with light of 365 nm to enrich the (*Z*)-isomer before the <sup>1</sup>H NOESY-NMR spectra were recorded (Figure 3).

As expected for compound **4** no interactions of the methyl groups with the opposite phenyl rings were observed neither in their (*Z*)- nor in the (*E*)-state. For the *t*-Bu-

substituted AB **5**, though, distinct cross-peaks to the protons of phenyl ring in *ortho* position, as well as cross-peaks to the protons of the substituted phenyl rings in *ortho* position can be observed when switched to its (*Z*)-state, demonstrating the attractive interactions resulting in the longer half-life. Similarly, the <sup>1</sup>H NOESY spectrum of the *n*-heptyl-substituted AB **6** in its (*Z*)-isomer shows also cross-peaks to the opposite phenyl ring as well as to the protons of the substituted phenyl rings in *ortho* as well as in *meta* position. As expected, AB **6** has a shorter half-life than its *t*-Bu-substituted AB analogue **7**. One reason for this observation can be found in the unfavorable contributions of entropy that grow with increasing the flexible alkyl chain. In a previously study, *n*-Bu chains showed the strongest stabilizing effects, whereas the addition of more methylene groups resulted in lower half-lives.<sup>21</sup> Furthermore, *n*-heptyl substituents show a higher anisotropic behavior than *t*-Bu groups, resulting in a in average closer distance, explaining the larger stabilization in the *t*-Bu derivatives.<sup>24</sup>

Interestingly, the influence of electron-donating or electron-withdrawing substituents on the aryl side is comparatively small on the alkyl–aryl interaction. Besides the small consistent shorter half-life for the NO<sub>2</sub> analogues as discussed above, the OMe and H derivatives behave rather uniform. We therefore conclude that the electronic structure of the aromatic London dispersion acceptor in the AB scaffold does not significantly affect the strength of the attractive interactions.

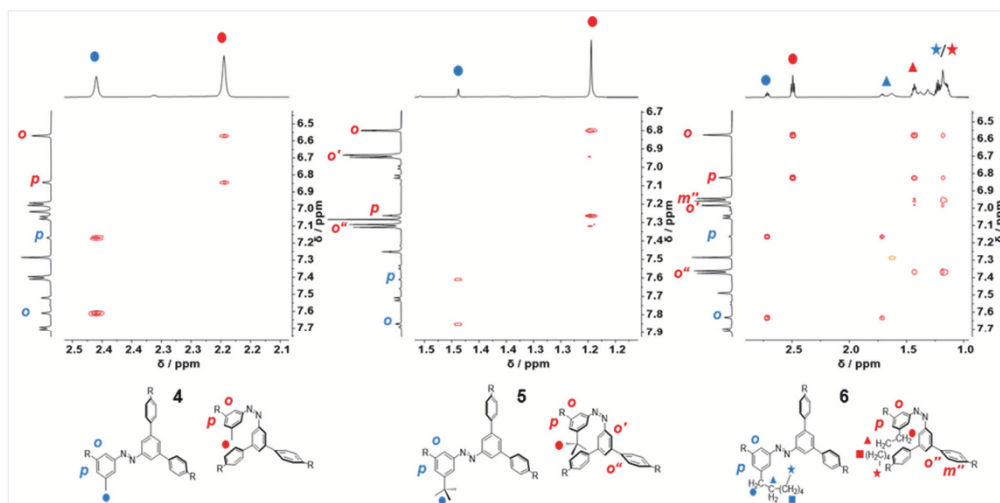


**Figure 3**  $^1\text{H}$  NOESY NMR spectra of an enriched concentration of (Z)-isomer of ABs **4**, **5**, and **6** in  $\text{CDCl}_3$ . The cross-peaks in the enlarged area indicate close proximity of *t*-Bu and *n*-heptyl among the protons of the same phenyl ring with the phenyl rings on the opposite side for the (Z)-isomer (middle and right spectra) and only close proximity of Me with the phenyl ring on the same side (left).

This is in analogy to other studies: Computational studies of CH- $\pi$  interactions of substituted benzenes with (halo)methanes revealed that the benzene-methane complex showed dispersive forces similar to those of the 1,3,5-trifluorobenzene-methane complex, whereas the dimer of benzene and fluoroform is more stable.<sup>25</sup> Methane-benzene, methane-phenol, and methane-indole also form energetically very similar T-shaped CH- $\pi$  dimers.<sup>26</sup> Shimidzu and co-workers established via an *N*-arylimide molecular balance that aryl ethers with different sized and branched carbon chains show only small influence of stabilizing dispersion effects with increasing chain size. However, the observed stabilization is masked by entropy effects, as well as by lone-pair- $\pi$  interactions of the oxygen.<sup>18</sup> Theoretically, as well as experimentally, the interaction of ethyl or methoxy substituents showed similar dispersive interactions with heterocyclic and nonheterocyclic aromatic compounds, confirming further that the electronic nature of the aryl system does not influence CH- $\pi$  interactions in a significant way.<sup>27</sup> Furthermore,  $-\text{CH}_3$  and  $-\text{CD}_3$  do not show a measurable difference in their interaction with aromatic rings in the experiment or in silico.<sup>28</sup> Our described AB system follows this trend, supporting that the size and shape of the alkyl London dispersion donor is much more important than the electronic properties of the aryl fragment.

In conclusion ABs **1–9** were successfully synthesized via three different synthetic strategies to obtain di-*meta*-Me-, *t*-Bu- and *n*-heptyl-substituted ABs with H-, OMe-, and

$\text{NO}_2$ -substituted phenyl rings on the other benzene moiety.<sup>29</sup> Kinetic data revealed elongated half-lives of the *t*-Bu-substituted ABs up to six times compared to Me- and *n*-heptyl-substituted derivatives as expected from previous studies. In accordance with  $^1\text{H}$  NOESY NMR experiments, the increased half-lives of *n*-heptyl- and *t*-Bu-substituted ABs can be attributed to alkyl-aryl interactions, which were not observed for Me-substituted AB derivatives. Altering the electronic structure of the  $\pi$ -donor has no significant effect on the London dispersion interactions, though. Therefore, no drastic change in the isomerization kinetics of OMe- or  $\text{NO}_2$ -substituted aromatic systems was observed in comparison to unsubstituted analogues.

### Conflict of Interest

The authors declare no conflict of interest.

### Funding Information

This project was partially funded by the Deutsche Forschungsgemeinschaft (DFG, WE5601/8-1).

### Acknowledgment

We thank Heike Hausmann for NMR support.

## Supporting Information

Supporting information for this article is available online at <https://doi.org/10.1055/a-1951-2833>.

## References and Notes

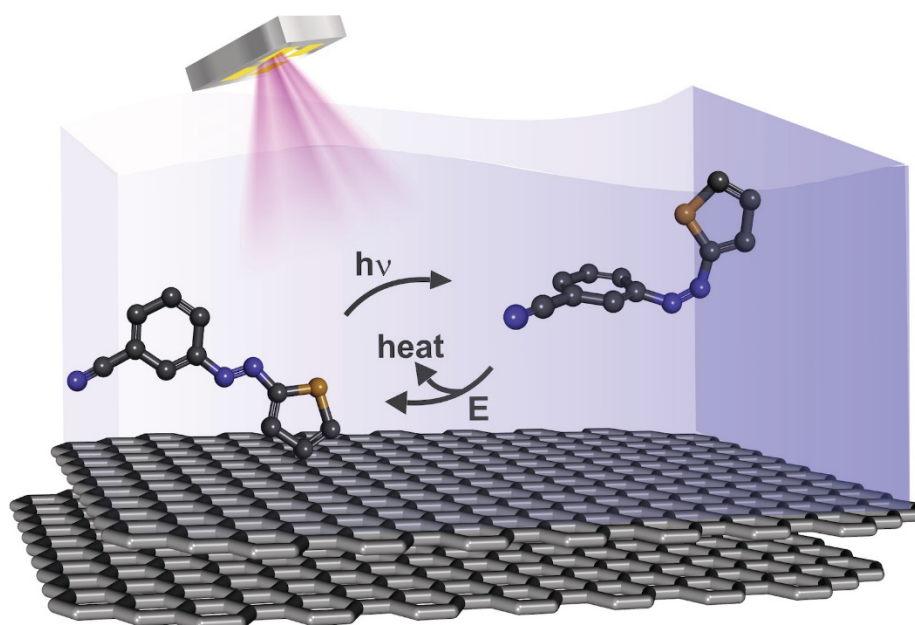
- (1) London, F. *Trans. Faraday Soc.* **1937**, *33*, 8b.
- (2) Fokin, A. A.; Chernish, L. V.; Gunchenko, P. A.; Tikhonchuk, E. Y.; Hausmann, H.; Serafin, M.; Dahl, J. E. P.; Carlson, R. M. K.; Schreiner, P. R. *J. Am. Chem. Soc.* **2012**, *134*, 13641.
- (3) Cerný, J.; Kabelác, M.; Hobza, P. *J. Am. Chem. Soc.* **2008**, *130*, 16055.
- (4) Grimme, S.; Djukic, J.-P. *Inorg. Chem.* **2011**, *50*, 2619.
- (5) (a) Grimm, L. M.; Spicher, S.; Tkachenko, B.; Schreiner, P. R.; Grimme, S.; Biedermann, F. *Chem. Eur. J.* **2022**, *28*, e202200529. (b) Mears, K. L.; Power, P. P. *Acc. Chem. Res.* **2022**, *55*, 1337. (c) Rummel, L.; Domanski, M. H. J.; Hausmann, H.; Becker, J.; Schreiner, P. R. *Angew. Chem. Int. Ed.* **2022**, e202204393. (d) McCrea-Hendrick, M. L.; Bursch, M.; Gullett, K. L.; Maurer, L. R.; Fettingner, J. C.; Grimme, S.; Power, P. P. *Organometallics* **2018**, *37*, 2075. (e) Linnemannstons, M.; Schwabedissen, J.; Schultz, A. A.; Neumann, B.; Stammler, H.-G.; Berger, R. J. F.; Mitzel, N. W. *Chem. Commun.* **2020**, 56, 2252. (f) Zou, W.; Fettingner, J. C.; Vasko, P.; Power, P. P. *Organometallics* **2022**, *41*, 794. (g) Giese, M.; Albrecht, M. *ChemPlusChem* **2020**, *85*, 715.
- (6) Strauss, M. A.; Wegner, H. A. *Angew. Chem. Int. Ed.* **2019**, *58*, 18552.
- (7) Schweighauser, L.; Strauss, M. A.; Bellotto, S.; Wegner, H. A. *Angew. Chem. Int. Ed.* **2015**, *54*, 13436.
- (8) Wagner, J. P.; Schreiner, P. R. *Angew. Chem. Int. Ed.* **2015**, *54*, 12274.
- (9) (a) Kim, E.; Paliwal, S.; Wilcox, C. S. *J. Am. Chem. Soc.* **1998**, *120*, 11192. (b) Paliwal, S.; Geib, S.; Wilcox, C. S. *J. Am. Chem. Soc.* **1994**, *116*, 4497.
- (10) Yang, L.; Adam, C.; Nichol, G. S.; Cockroft, S. L. *Nat. Chem.* **2013**, *5*, 1006.
- (11) Adam, C.; Yang, L.; Cockroft, S. L. *Angew. Chem. Int. Ed.* **2015**, *54*, 1164.
- (12) Hwang, J.; Dial, B. E.; Li, P.; Kozik, M. E.; Smith, M. D.; Shimizu, K. D. *Chem. Sci.* **2015**, *6*, 4358.
- (13) (a) Pollice, R.; Bot, M.; Kobylanskii, I. J.; Shenderovich, I.; Chen, P. *J. Am. Chem. Soc.* **2017**, *139*, 13126. (b) Schümann, J. M.; Wagner, J. P.; Eckhardt, A. K.; Quanz, H.; Schreiner, P. R. *J. Am. Chem. Soc.* **2021**, *143*, 41.
- (14) Strauss, M. A.; Wegner, H. A. *Eur. J. Org. Chem.* **2018**, 295.
- (15) (a) Li, P.; Vik, E. C.; Shimizu, K. D. *Acc. Chem. Res.* **2020**, *53*, 2705. (b) Elmi, A.; Cockroft, S. L. *Acc. Chem. Res.* **2021**, *54*, 92.
- (16) (a) Aliev, A. E.; Motherwell, W. B. *Chemistry* **2019**, *25*, 10516. (b) Yamada, M.; Narita, H.; Maeda, Y. *Angew. Chem. Int. Ed.* **2020**, *132*, 16267.
- (17) (a) Carroll, W. R.; Pellechia, P.; Shimizu, K. D. *Org. Lett.* **2008**, *10*, 3547. (b) Sun, H.; Horatscheck, A.; Martos, V.; Bartetzko, M.; Uhrig, U.; Lentz, D.; Schmieder, P.; Nazaré, M. *Angew. Chem. Int. Ed.* **2017**, *56*, 6454. (c) Maier, J. M.; Li, P.; Vik, E. C.; Yehl, C. J.; Strickland, S. M. S.; Shimizu, K. D. *J. Am. Chem. Soc.* **2017**, *139*, 6550. (d) Vik, E. C.; Li, P.; Madukwe, D. O.; Karki, I.; Tibbetts, G. S.; Shimizu, K. D. *Org. Lett.* **2021**, *23*, 8179.
- (18) Carroll, W. R.; Zhao, C.; Smith, M. D.; Pellechia, P. J.; Shimizu, K. D. *Org. Lett.* **2011**, *13*, 4320.
- (19) Harada, J.; Ogawa, K.; Tomoda, S. *Acta Crystallogr., Sect. B: Struct. Sci.* **1997**, *53*, 662.
- (20) (a) Slavov, C.; Yang, C.; Schweighauser, L.; Boumrifak, C.; Dreuw, A.; Wegner, H. A.; Wachtveitl, J. *Phys. Chem. Chem. Phys.* **2016**, *18*, 14795. (b) Kunz, A.; Wegner, H. A. *ChemSystemsChem* **2021**, *3*, e2000035. (c) Petersen, A. U.; Broman, S. L.; Olsen, S. T.; Hansen, A. S.; Du, L.; Kadziola, A.; Hansen, T.; Kjaergaard, H. G.; Mikkelsen, K. V.; Nielsen, M. B. *Chemistry* **2015**, *21*, 3968.
- (21) Strauss, M. A.; Wegner, H. A. *Angew. Chem. Int. Ed.* **2021**, *60*, 779.
- (22) García-Amorós, J.; Velasco, D. *Beilstein J. Org. Chem.* **2012**, *8*, 1003.
- (23) (a) Robertus, J.; Reker, S. F.; Pijper, T. C.; Deuzeman, A.; Browne, W. R.; Feringa, B. L. *Phys. Chem. Chem. Phys.* **2012**, *14*, 4374. (b) Exner, O. *Prog. Phys. Org. Chem.*; Streitwieser, A. Jr.; Traft, R. W., Ed.; Wiley: Hoboken, **1973**, 411–482. (c) Dokić, J.; Gothe, M.; Wirth, J.; Peters, M. V.; Schwarz, J.; Hecht, S.; Saalfrank, P. *J. Phys. Chem. A* **2009**, *113*, 6763. (d) Asano, T.; Okada, T.; Shinkai, S.; Shigematsu, K.; Kusano, Y.; Manabe, O. *J. Am. Chem. Soc.* **1981**, *103*, 5161.
- (24) Di Berardino, C.; Strauss, M. A.; Schatz, D.; Wegner, H. A. *Chemistry* **2022**, *28*, e202104284.
- (25) Dey, R. C.; Seal, P.; Chakrabarti, S. *J. Phys. Chem. A* **2009**, *113*, 10113.
- (26) Ringer, A. L.; Figgs, M. S.; Sinnokrot, M. O.; Sherrill, C. D. *J. Phys. Chem. A* **2006**, *110*, 10822.
- (27) Li, P.; Parker, T. M.; Hwang, J.; Deng, F.; Smith, M. D.; Pellechia, P. J.; Sherrill, C. D.; Shimizu, K. D. *Org. Lett.* **2014**, *16*, 5064.
- (28) Zhao, C.; Parrish, R. M.; Smith, M. D.; Pellechia, P. J.; Sherrill, C. D.; Shimizu, K. D. *J. Am. Chem. Soc.* **2012**, *134*, 14306.
- (29) **General Procedures**  
**Route 1:** 1,3-Diphenyl-5-nitrosobenzene (**20**, 1.0 equiv.) was dissolved in toluene and degassed with a nitrogen stream. The corresponding aniline (**14**, **15** or **16**, 1.0–1.6 equiv.) and acetic acid were added, and the mixture was stirred at 60 °C for the time given in the Supporting Information. The solvent was subsequently removed under reduced pressure, and the residue was purified by column chromatography.  
**Route 2:** Under nitrogen atmosphere the corresponding nitrosobenzene (**24**, **25**, or **26**, 1.0 equiv.) was dissolved in toluene and was degassed with a nitrogen stream. Acetic acid and a solution of aniline **23** (1.0 equiv.) in toluene were added. The reaction mixture was stirred at 60 °C for the time given in the Supporting Information. The solvent was subsequently removed under reduced pressure, and the residue was purified by column chromatography.  
**Route 3 for 7, 8:** Corresponding dibromoazobenzene (**29** or **30**, 1.0 equiv.) was dissolved in dry THF (transferred under inert conditions), boronic ester **28** (2.1 equiv.), CsF (6.7 equiv.), as well as tris(dibenzylideneacetone)dipalladium(0) (3 mol%) and tri-*tert*-(butyl)phosphonium tetrafluoroborate (10–14 mol%) were added and stirred for the time given in the Supporting Information. The solvent was subsequently removed under reduced pressure, and the residue was purified by column chromatography.  
**Route 3 for 9:** See the Supporting Information.

## 5 Additional Contributions

### 5.1 Electrochemically Triggered Energy Release from an Azothiophene-Based Molecular Solar Thermal System

Reference: E. Franz, A. Kunz, N. Oberhof, A. H. Heindl, M. Bertram, L. Fusek, N. Taccardi, P. Wasserscheid, A. Dreuw, H. A. Wegner, O. Brummel, J. Libuda, *ChemSusChem* **2022**, *15*, e202200958.

DOI: 10.1002/cssc.202200958



„Molecular solar thermal (MOST) systems combine solar energy conversion, storage, and release in simple one-photon one-molecule processes. Here, we address the electrochemically triggered energy release from an azothiophene-based MOST system by photoelectrochemical infrared reflection absorption spectroscopy (PEC-IRRAS) and density functional theory (DFT). Specifically, the electrochemically triggered back-reaction from the energy rich (*Z*)-3-cyanophenylazothiophene to its energy lean (*E*)-isomer using highly oriented pyrolytic graphite (HOPG) as the working electrode was studied. Theory predicts that two reaction channels are accessible, an oxidative one (hole-catalyzed) and a reductive one (electron-catalyzed). Experimentally it was found that the photo-isomer decomposes during hole-catalyzed energy release. Electrochemically triggered back-conversion was possible, however,

through the electron-catalyzed reaction channel. The reaction rate could be tuned by the electrode potential within two orders of magnitude. It was shown that the MOST system withstands 100 conversion cycles without detectable decomposition of the photoswitch. After 100 cycles, the photochemical conversion was still quantitative and the electrochemically triggered back-reaction reached 94 % of the original conversion level.”

## Abbreviations

A	Parent molecule
Ad	Adamantyl-
AB	Azobenzene
AMP	Azobenzene Multinary Photoswitch
aq.	Aqueous
Ar	Aryl-
B	photoisomer
Bu	Butyl-
Cy	Cyclohexyl-
d	Day
DASA	Donor–acceptor Stenhouse adduct
DHA	Dihydroazulene
DNA	Deoxyribonucleic acid
DTE	Dithienylethene
e.g.	exempli gratia
ESIPT	Excited-State Intramolecular Proton Transfer
Et	Ethyl-
g	Gram
h	Hour
Hex	Hexyl-
Hept	Heptyl-
ICT	Intermolecular charge transfer
L	Liter
<i>m</i>	<i>meta</i>
Me	Methyl-
MC	Merocyanine
min	Minute

mol	Mole
MOST	Molecular solar thermal energy storage
NBD	Norbornadiene
nm	Nanometer
NMR	Nuclear magnetic resonance
NOESY	Nuclear Overhauser Enhancement Spectroscopy
<i>o</i>	<i>ortho</i>
Oct	Octyl-
<i>p</i>	<i>para</i>
Pent	Pentyl-
Ph	Phenyl-
Pr	Propyl-
PSS	Photostationary State
QC	Quadricyclane
s	Second
SP	Spiropyran
<i>t</i>	<i>tert</i>
$t_{1/2}$	half-life
UV	Ultraviolet
VHF	Vinylheptafulvene
VIS	Visible

## Acknowledgement

Zuerst möchte ich mich herzlich bei meinem Doktorvater Prof. Dr. Hermann A. Wegner bedanken, bei dem ich die Möglichkeit hatte diese interessante Arbeit, die mir bis zum Ende Freude bereitet hat, anzufertigen. Es ist nicht selbstverständlich, dass ich von ihm immer durch Ideen unterstützt wurde, er immer ein offenes Ohr für Fragen und Probleme hatte, er mich zwar wissenschaftlich stets gefordert hat und mir aber gleichermaßen viel Freiraum in meiner Forschung gelassen hat. All dies hat maßgeblich zum Erfolg dieser Arbeit beigetragen.

Des Weiteren möchte ich Prof. Dr. R. Göttlich für die Anfertigung des Zweitgutachtens herzlich danken.

Außerdem möchte ich mich unglaublich bei meinen Eltern bedanken. Durch ihre beständige Unterstützung haben sie mir das Studium und Promotion erst ermöglicht und ich konnte mich zu jeder Zeit auf ihre Hilfe und Unterstützung verlassen. Ihr habt mir gezeigt, dass man alles schaffen kann, wenn man es nur wirklich will und dafür arbeitet.

Vielen Dank außerdem an meinen Bruder Simon, der mich nicht nur im privaten immer unterstützt und mir Halt gegeben hat, sondern der mir auch seit Beginn des Studiums mit Rat und Tat zur Seite stand und es ihm nie zu viel wurde mir etwas Chemisches oder Physikalisches noch einmal zu erklären.

Ein großes Dankeschön geht an all meine Freunde, auf die ich mich immer verlassen konnte und bei denen ich den Stress, den die Promotion mit sich brachte, jedes einzelne Mal vergessen konnte. Ohne euch hätte ich es niemals geschafft. Insbesondere danke ich hier meinen Mitbewohnern, von denen ich immer unterstützt wurde.

Ich danke von Herzen der gesamten Arbeitsgruppe Wegner. Besonders bedanken möchte ich mich hier bei den ehemaligen Doktoranden Dr. Andreas H. Heindl und Dr. Sebastian Ahles. Durch ihr Wissen und ihre praktischen Tipps und Erklärungen habe ich so viel lernen können, was mich zu der Chemikerin macht, die ich heute bin und sie waren dadurch am Erfolg dieser Arbeit maßgeblich beteiligt. Ich möchte mich außerdem bei meinen Laborpartner:innen bedanken, die zu Freunden geworden sind; nicht nur für die dauerhaft freundliche und schöne Atmosphäre, sowohl im Labor als

auch in der Kaffeeküche und allen AG Ausflügen, sondern auch für die immer wissenschaftliche hilfsbereite Art aller. Die wissenschaftlichen Diskussionen und Ideen haben mir viel geholfen. Hier bedanke ich mich daher bei Jan Griwatz, Julia Ruhl, Dominic Schatz, Jannis Volkmann, Daniel Kohrs, Mari Janse van Rensburg, Michel Große, Conrad Averdunk, Felix Bernt, Christopher Leonhardt, Kai Hanke, Sebastian Beeck, Dr. Marcel Strauß, Dr. Longcheng Hong und Nathaniel Ukah.

Außerdem möchte ich mich bei unseren Chemielaborant:innen Katinka Grimmeisen und Finn Schneider bedanken, die mir mit Synthesen zur Seite standen.

Ich möchte auch den anderen Arbeitsgruppen des Instituts, AG Schreiner, der AG Gellrich sowie der AG Göttlich für die gute Zusammenarbeit, Hilfsbereitschaft und freundschaftliche Atmosphäre danken.

Des Weiteren gilt ein großer Dank allen Mitarbeiter:innen des organischen Instituts der JLU, die mir mit technischen und administrativer Hilfe zur Seite standen und die diese Arbeit mit ihrer Hilfe und ihren Messungen erst möglich gemacht haben. Dabei danke ich Dr. Heike Hausmann, Anika Bernhardt, Anja Platt und Inna Klein für die Messung aller NMR-Spektren und dass sie immer so flexibel waren, wenn ich mal spontan mit meinen bestrahlten Proben bei ihnen aufgetaucht bin. Außerdem danke ich Dr. Raffael Wende, Dr. Dennis Gerbig, Stefan Bernhardt, Steffen Wagner, Brigitte Wein-Boulakhrouf und Edgar Reitz.

Außerdem danke ich dem Team der Chemikalienausgabe: Eike Santowski und Mario Dauber, sowie dem Team der Materialenausgabe und Glasbläserei: Anja Beneckenstein, Dr. Wolfgang Herrendorf, Hans-Jürgen Wolf, Michaela Jäkel und Petra Grundmann für die Bereitstellung und Bestellungen von Chemikalien und Laborausstattung. Vielen Dank auch an Dr. Jörg Neudert, der bei der allgemeinen Organisation des Instituts sowie der OC-Praktika immer zuvorkommend und unterstützend handelte.

Zuletzt geht ein großer Dank an Anika Jäger, Michaela Richter und Doris Verch, die mir bei organisatorischen und verwaltungstechnischen Fragen und Abläufen immer helfend zur Seite standen.

## References

- [1] H. Bouas-Laurent, H. Dürr, *Pure Appl. Chem.* **2001**, *73*, 639.
- [2] M. Irie, *Chem. Rev.* **2000**, *100*, 1685.
- [3] S. Crespi, N. A. Simeth, B. König, *Nat. Rev. Chem.* **2019**, *3*, 133.
- [4] V. Gold, *The IUPAC Compendium of Chemical Terminology*, International Union of Pure and Applied Chemistry (IUPAC), Research Triangle Park, NC, **2019**.
- [5] H. M. D. Bandara, S. C. Burdette, *Chem. Soc. Rev.* **2012**, *41*, 1809.
- [6] M. A. Strauss, H. A. Wegner, *Angew. Chem. Int. Ed.* **2019**, *58*, 18552.
- [7] S. Chen, Y. Zhang, K. Chen, Y. Yin, C. Wang, *ACS Appl. Mater. Interfaces* **2017**, *9*, 13778.
- [8] B. L. Feringa, W. R. Browne, *Molecular switches*, Wiley, Weinheim, **2011**.
- [9] J. Orrego-Hernández, A. Dreos, K. Moth-Poulsen, *Acc. Chem. Res.* **2020**, *53*, 1478.
- [10] R. S. Becker, W. F. Richey, *J. Am. Chem. Soc.* **1967**, *89*, 1298.
- [11] R. Nakagaki, T. Kobayashi, J. Nakamura, S. Nagakura, *Bull. Chem. Soc. Jpn.* **1977**, *50*, 1909.
- [12] E. Hadjoudis, M. Vittorakis, I. Moustakali-Mavridis, *Tetrahedron* **1987**, *43*, 1345.
- [13] V. I. Minkin, *Chem. Rev.* **2004**, *104*, 2751.
- [14] V. I. Minkin, *Russ. Chem. Rev.* **2013**, *82*, 1.
- [15] R. Klajn, *Chem. Soc. Rev.* **2014**, *43*, 148.
- [16] S. L. Broman, M. B. Nielsen, *Phys. Chem. Chem. Phys.* **2014**, *16*, 21172.
- [17] J. Ern, M. Petermann, T. Mrozek, J. Daub, K. Kuldová, C. Kryschi, *Chem. Phys.* **2000**, *259*, 331.
- [18] V. de Waele, M. Beutter, U. Schmidhammer, E. Riedle, J. Daub, *Chem. Phys. Lett.* **2004**, *390*, 328.
- [19] S. L. Broman, M. Jevric, M. B. Nielsen, *Chem. Eur. J* **2013**, *19*, 9542.
- [20] M. Å. Petersen, S. L. Broman, A. Kadziola, K. Kilså, M. B. Nielsen, *Eur. J. Org. Chem.* **2009**, 2733.
- [21] S. L. Broman, M. A. Petersen, C. G. Tortzen, A. Kadziola, K. Kilså, M. B. Nielsen, *J. Am. Chem. Soc.* **2010**, *132*, 9165.
- [22] N. Mallo, P. T. Brown, H. Iranmanesh, T. S. C. MacDonald, M. J. Teusner, J. B. Harper, G. E. Ball, J. E. Beves, *Chem. Commun.* **2016**, *52*, 13576.

- [23] S. Helmy, F. A. Leibfarth, S. Oh, J. E. Poelma, C. J. Hawker, J. Read de Alaniz, *J. Am. Chem. Soc.* **2014**, *136*, 8169.
- [24] J. R. Hemmer, S. O. Poelma, N. Treat, Z. A. Page, N. D. Dolinski, Y. J. Diaz, W. Tomlinson, K. D. Clark, J. P. Hooper, C. Hawker, J. Read de Alaniz, *J. Am. Chem. Soc.* **2016**, *138*, 13960.
- [25] M. Irie, T. Fukaminato, K. Matsuda, S. Kobatake, *Chem. Rev.* **2014**, *114*, 12174.
- [26] G. S. Hammond, N. J. Turro, A. Fischer, *J. Am. Chem. Soc.* **1961**, *83*, 4674.
- [27] S. J. Cristol, R. L. Snell, *J. Am. Chem. Soc.* **1958**, *80*, 1950.
- [28] W. G. Dauben, R. L. Cargill, *Tetrahedron* **1961**, *15*, 197.
- [29] O. Brummel, D. Besold, T. Döpfer, Y. Wu, S. Bochmann, F. Lazzari, F. Waidhas, U. Bauer, P. Bachmann, C. Papp, H.-P. Steinrück, A. Görling, J. Libuda, J. Bachmann, *ChemSusChem* **2016**, *9*, 1424.
- [30] M. Jevric, A. U. Petersen, M. Mansø, S. Kumar Singh, Z. Wang, A. Dreos, C. Sumbly, M. B. Nielsen, K. Börjesson, P. Erhart, K. Moth-Poulsen, *Chem. Eur. J.* **2018**, *24*, 12767.
- [31] X. An, Y. Xie, *Thermochim. Acta* **1993**, *220*, 17.
- [32] P. R. Khoury, J. D. Goddard, W. Tam, *Tetrahedron* **2004**, *60*, 8103.
- [33] D. S. Kabakoff, J. C. G. Buenzli, J. F. M. Oth, W. B. Hammond, J. A. Berson, *J. Am. Chem. Soc.* **1975**, *97*, 1510.
- [34] E. Haselbach, T. Bally, Z. Lanyiova, P. Baertschi, *Helv. Chim. Acta* **1979**, *62*, 583.
- [35] V. A. Bren', A. D. Dubonosov, V. I. Minkin, V. A. Chernoiyanov, *Russ. Chem. Rev.* **1991**, *60*, 451.
- [36] U. Bauer, L. Fromm, C. Weiß, P. Bachmann, F. Späth, F. Düll, J. Steinhauer, W. Hieringer, A. Görling, A. Hirsch, H.-P. Steinrück, C. Papp, *J. Phys. Chem. C* **2019**, *123*, 7654.
- [37] Z. Wang, P. Erhart, T. Li, Z.-Y. Zhang, D. Sampedro, Z. Hu, H. A. Wegner, O. Brummel, J. Libuda, M. B. Nielsen, K. Moth-Poulsen, *Joule* **2021**, *5*, 3116.
- [38] T. Luchs, P. Lorenz, A. Hirsch, *ChemPhotoChem* **2020**, *4*, 52.
- [39] F. Waidhas, M. Jevric, M. Bosch, T. Yang, E. Franz, Z. Liu, J. Bachmann, K. Moth-Poulsen, O. Brummel, J. Libuda, *J. Mater. Chem. A* **2020**, *8*, 15658.
- [40] R. Eschenbacher, T. Xu, E. Franz, R. Löw, T. Moje, L. Fromm, A. Görling, O. Brummel, R. Herges, J. Libuda, *Nano Energy* **2022**, *95*, 107007.

- [41] T. Akioka, Y. Inoue, A. Yanagawa, M. Hiyamizu, Y. Takagi, A. Sugimori, *J. Mol. Catal.* **2003**, *202*, 31.
- [42] A. Cuppoletti, J. P. Dinnocenzo, J. L. Goodman, I. R. Gould, *J. Phys. Chem. A* **1999**, *103*, 11253.
- [43] A. A. Gorman, R. L. Leyland, M. Rodgers, P. G. Smith, *Tetrahedron Lett.* **1973**, *14*, 5085.
- [44] R. R. Hautala, J. Little, E. Sweet, *Solar Energy* **1977**, *19*, 503.
- [45] A. Ikeda, A. Kameyama, T. Nishikubo, T. Nagai, *Macromolecules* **2001**, *34*, 2728.
- [46] V. Gray, A. Lennartson, P. Ratanalert, K. Börjesson, K. Moth-Poulsen, *Chem. Commun.* **2014**, *50*, 5330.
- [47] S. Miki, Y. Asako, Z. Yoshida, *Chem. Lett.* **1987**, *16*, 195.
- [48] Z. Yoshida, *J. Photochem.* **1985**, *29*, 27.
- [49] E. Mitscherlich, *Ann. Phys. Chem.* **1834**, *108*, 225.
- [50] P. J. T. Morris, A. S. Travis, *Am. Dyestuff Rep.* **1992**, 11.
- [51] Z. Wang, R. Losantos, D. Sampedro, M. Morikawa, K. Börjesson, N. Kimizuka, K. Moth-Poulsen, *J. Mater. Chem. A* **2019**, *7*, 15042.
- [52] L. Dong, Y. Feng, L. Wang, W. Feng, *Chem. Soc. Rev.* **2018**, *47*, 7339.
- [53] Z. F. Liu, K. Hashimoto, A. Fujishima, *Nature* **1990**, *347*, 658.
- [54] T. Ikeda, O. Tsutsumi, *Science* **1995**, *268*, 1873.
- [55] H. Liu, A. Zheng, C. Gong, X. Ma, M. Hon-Wah Lam, C. Chow, Q. Tang, *RSC Adv.* **2015**, *5*, 62539.
- [56] K. Hüll, J. Morstein, D. Trauner, *Chem. Rev.* **2018**, *118*, 10710.
- [57] M. Liu, X. Yan, M. Hu, X. Chen, M. Zhang, B. Zheng, X. Hu, S. Shao, F. Huang, *Org. Lett.* **2010**, *12*, 2558.
- [58] J. Konieczkowska, K. Bujak, K. Nocoń, E. Schab-Balcerzak, *Dyes Pigm.* **2019**, *171*, 107659.
- [59] Y. Zhang, X. Sun, X. An, an Sui, J. Yi, X. Song, *Dyes Pigm.* **2021**, *186*, 109018.
- [60] Y. Norikane, N. Tamaoki, *Org. Lett.* **2004**, *6*, 2595.
- [61] M. A. Gerkman, G. G. Han, *Joule* **2020**, *4*, 1621.
- [62] R. Liu, X. Zhang, F. Xia, Y. Dai, *J. Catal.* **2022**, *409*, 33.
- [63] G. S. HARTLEY, *Nature* **1937**, *140*, 281.
- [64] H. Rau, E. Lueddecke, *J. Am. Chem. Soc.* **1982**, *104*, 1616.

- [65] A. Goulet-Hanssens, M. Utecht, D. Mutruc, E. Titov, J. Schwarz, L. Grubert, D. Bléger, P. Saalfrank, S. Hecht, *J. Am. Chem. Soc.* **2017**, *139*, 335.
- [66] A. Goulet-Hanssens, C. Rietze, E. Titov, L. Abdullahu, L. Grubert, P. Saalfrank, S. Hecht, *Chem* **2018**, *4*, 1740.
- [67] C. J. Brown, *Acta Crystallogr.* **1966**, *21*, 146.
- [68] A. Mostad, C. Rømming, S. Hammarström, R. J. J. C. Lousberg, U. Weiss, *Acta Chem. Scand.* **1971**, *25*, 3561.
- [69] J. Henzl, M. Mehlhorn, H. Gawronski, K.-H. Rieder, K. Morgenstern, *Angew. Chem. Int. Ed.* **2006**, *45*, 603.
- [70] M. Ishikawa, T. Ohzono, T. Yamaguchi, Y. Norikane, *Sci. Rep.* **2017**, *7*, 6909.
- [71] G. S. HARTLEY, R. J. W. Le Fèvre, *J. Chem. Soc.* **1939**, 531.
- [72] J. Harada, K. Ogawa, S. Tomoda, *Acta Crystallogr. B. Struct. Sci., Cryst. Eng. Mater.* **1997**, *53*, 662.
- [73] K. S. Schanze, T. F. Mattox, D. G. Whitten, *J. Org. Chem.* **1983**, *48*, 2808.
- [74] N. Nishimura, T. Sueyoshi, H. Yamanaka, E. Imai, S. Yamamoto, S. Hasegawa, *Bull. Chem. Soc. Jpn.* **1976**, *49*, 1381.
- [75] P. Haberfield, P. M. Block, M. S. Lux, *J. Am. Chem. Soc.* **1975**, *97*, 5804.
- [76] L. Schweighauser, M. A. Strauss, S. Bellotto, H. A. Wegner, *Angew. Chem. Int. Ed.* **2015**, *54*, 13436.
- [77] J. Dokić, M. Gothe, J. Wirth, M. V. Peters, J. Schwarz, S. Hecht, P. Saalfrank, *J. Phys. Chem. A* **2009**, *113*, 6763.
- [78] T. Asano, T. Okada, S. Shinkai, K. Shigematsu, Y. Kusano, O. Manabe, *J. Am. Chem. Soc.* **1981**, *103*, 5161.
- [79] T. Halicioğlu, O. Sinanoğlu, *Ann. N. Y. Acad. Sci.* **1969**, *158*, 308.
- [80] D. Schulte-Frohlinde, *Justus Liebigs Ann. Chem.* **1958**, *612*, 131.
- [81] C. D. Hall, P. D. Beer, *J. Chem. Soc., Perkin Trans. 2* **1991**, 1947.
- [82] A. Nakamura, K. Doi, K. Tatsumi, S. Otsuka, *J. Mol. Catal.* **1976**, *1*, 417.
- [83] S. Yamashita, *Bull. Chem. Soc. Jpn.* **1961**, *34*, 842.
- [84] R. Arnaud, J. Lemaire, *Can. J. Chem.* **1974**, *52*, 1868.
- [85] J. L. Greenfield, M. A. Gerkman, R. S. L. Gibson, G. G. D. Han, M. J. Fuchter, *J. Am. Chem. Soc.* **2021**, *143*, 15250.
- [86] E. Franz, A. Kunz, N. Oberhof, A. H. Heindl, M. Bertram, L. Fusek, N. Taccardi, P. Wasserscheid, A. Dreuw, H. A. Wegner, O. Brummel, J. Libuda, *ChemSusChem* **2022**, *15*, e202200958.

- [87] J. Isokuortti, K. Kuntze, M. Virkki, Z. Ahmed, E. Vuorimaa-Laukkanen, M. A. Filatov, A. Turshatov, T. Laaksonen, A. Priimagi, N. A. Durandin, *Chem. Sci.* **2021**, *12*, 7504.
- [88] P. Bortolus, S. Monti, *J. Phys. Chem.* **1979**, *83*, 648.
- [89] D. G. Whitten, P. D. Wildes, J. G. Pacifici, G. Irick, *J. Am. Chem. Soc.* **1971**, *93*, 2004.
- [90] H. Rau, *Photochemistry and photophysics (Ed: J. F. Rabek)*, CRC Pr, Boca Raton, Fl., **1990**, 119.
- [91] H. Rau, G. Greiner, G. Gauglitz, H. Meier, *J. Phys. Chem.* **1990**, *94*, 6523.
- [92] A. Albin, E. Fasani, S. Pietra, *J. Chem. Soc., Perkin Trans. 2* **1983**, 1021.
- [93] R. Tahara, T. Morozumi, H. Nakamura, M. Shimomura, *J. Phys. Chem. B* **1997**, *101*, 7736.
- [94] R. Siewertsen, J. B. Schönborn, B. Hartke, F. Renth, F. Temps, *Phys. Chem. Chem. Phys.* **2011**, *13*, 1054.
- [95] Q. Ya, X.-Z. Dong, W.-Q. Chen, X.-M. Duan, *Dyes Pigm.* **2008**, *79*, 159.
- [96] F. Aleotti, A. Nenov, L. Salvigni, M. Bonfanti, M. M. El-Tahawy, A. Giunchi, M. Gentile, C. Spallacci, A. Ventimiglia, G. Cirillo, L. Montali, S. Scurti, M. Garavelli, I. Conti, *J. Phys. Chem. A* **2020**, *124*, 9513.
- [97] V. Marturano, V. Ambrogio, N. A. G. Bandeira, B. Tylkowski, M. Giamberini, P. Cerruti, *Phys. Sci. Rev.* **2017**, *2*, 20170138.
- [98] C. R. Crecca, A. E. Roitberg, *J. Phys. Chem. A* **2006**, *110*, 8188.
- [99] S. Yamada, J. Bessho, H. Nakasato, O. Tsutsumi, *Dyes Pigm.* **2018**, *150*, 89.
- [100] J. Liu, Z. Chen, S. Yuan, *J. Zhejiang Univ. Sci. B* **2005**, *6*, 584.
- [101] L. Antonov, K. Kamada, K. Ohta, F. S. Kamounah, *Phys. Chem. Chem. Phys.* **2003**, *5*, 1193.
- [102] J. Yong Lee, K. S. Kim, B. Jin Mhin, *J. Chem. Phys.* **2001**, *115*, 9484.
- [103] C. Slavov, C. Yang, L. Schweighauser, C. Boumrifak, A. Dreuw, H. A. Wegner, J. Wachtveitl, *Phys. Chem. Chem. Phys.* **2016**, *18*, 14795.
- [104] D. Bléger, J. Schwarz, A. M. Brouwer, S. Hecht, *J. Am. Chem. Soc.* **2012**, *134*, 20597.
- [105] N. Nishimura, S. Kosako, Y. Sueishi, *Bull. Chem. Soc. Jpn* **1984**, *57*, 1617.
- [106] A. Heindl, L. Schweighauser, C. Logemann, H. Wegner, *Synthesis* **2017**, *49*, 2632.

- [107] R. Siewertsen, H. Neumann, B. Buchheim-Stehn, R. Herges, C. Näther, F. Renth, F. Temps, *J. Am. Chem. Soc.* **2009**, *131*, 15594.
- [108] Y. Norikane, R. Katoh, N. Tamaoki, *Chem. Commun.* **2008**, 1898.
- [109] C. Slavov, C. Yang, A. H. Heindl, T. Stauch, H. A. Wegner, A. Dreuw, J. Wachtveitl, *J. Phys. Chem. Lett.* **2018**, *9*, 4776.
- [110] F. London, *Z. Physik* **1930**, *63*, 245.
- [111] J. P. Wagner, P. R. Schreiner, *Angew. Chem. Int. Ed.* **2015**, *54*, 12274.
- [112] A. A. Fokin, L. V. Chernish, P. A. Gunchenko, E. Y. Tikhonchuk, H. Hausmann, M. Serafin, J. E. P. Dahl, R. M. K. Carlson, P. R. Schreiner, *J. Am. Chem. Soc.* **2012**, *134*, 13641.
- [113] J. Cerný, M. Kabelác, P. Hobza, *J. Am. Chem. Soc.* **2008**, *130*, 16055.
- [114] S. Grimme, J.-P. Djukic, *Inorg. Chem.* **2011**, *50*, 2619.
- [115] M. A. Strauss, H. A. Wegner, *ChemPhotoChem* **2019**, *3*, 392.
- [116] M. A. Strauß, Universitätsbibliothek Gießen, **2021**.
- [117] A. Kunz, D. Schatz, A. R. Raab, H. A. Wegner, *Synlett* **2022**, A-F.
- [118] E. Merino, *Chem. Soc. Rev.* **2011**, *40*, 3835.
- [119] C. Zhang, N. Jiao, *Angew. Chem. Int. Ed.* **2010**, *49*, 6174.
- [120] R. O. Hutchins, D. W. Lamson, L. Rua, C. Milewski, B. Maryanoff, *J. Org. Chem.* **1971**, *36*, 803.
- [121] R. F. NYSTROM, W. G. BROWN, *J. Am. Chem. Soc.* **1948**, *70*, 3738.
- [122] W. Tadros, M. S. Ishak, E. Bassili, *J. Chem. Soc.* **1959**, 627.
- [123] S. Wada, M. Urano, H. Suzuki, *J. Org. Chem.* **2002**, *67*, 8254.
- [124] D. D. Laskar, D. Prajapati, J. S. Sandhu, *J. Chem. Soc., Perkin Trans. 1* **2000**, 67.
- [125] M. B. Sridhara, R. Suhas, D. G. C. Gowda, *Eur. J. Chem.* **2013**, *4*, 61.
- [126] N. A. Noureldin, *Synthesis* **1999**, 939.
- [127] A. R. Patel, G. Patel, G. Maity, S. P. Patel, S. Bhattacharya, A. Putta, S. Banerjee, *ACS omega* **2020**, *5*, 30416.
- [128] Y.-K. Lim, K.-S. Lee, C.-G. Cho, *Org. Lett.* **2003**, *5*, 979.
- [129] B. Haag, Z. Peng, P. Knochel, *Org. Lett.* **2009**, *11*, 4270.
- [130] K. Haghbeen, E. W. Tan, *J. Org. Chem.* **1998**, *63*, 4503.
- [131] M. Wang, K. Funabiki, M. Matsui, *Dyes Pigm.* **2003**, *57*, 77.
- [132] C. Mills, *J. Chem. Soc., Trans.* **1895**, *67*, 925.
- [133] A. Baeyer, *Ber. Dtsch. Chem. Ges.* **1874**, *7*, 1638.

- [134] M. Dommaschk, M. Peters, F. Gutzeit, C. Schütt, C. Näther, F. D. Sönnichsen, S. Tiwari, C. Riedel, S. Boretius, R. Herges, *J. Am. Chem. Soc.* **2015**, *137*, 7552.
- [135] K. Ueno, S. Akiyoshi, *J. Am. Chem. Soc.* **1954**, *76*, 3670.
- [136] B.-C. Yu, Y. Shirai, J. M. Tour, *Tetrahedron* **2006**, *62*, 10303.
- [137] M. B. Plutschack, B. Pieber, K. Gilmore, P. H. Seeberger, *Chem. Rev.* **2017**, *117*, 11796.
- [138] H. Qin, C. Liu, N. Lv, W. He, J. Meng, Z. Fang, K. Guo, *Dyes Pigm.* **2020**, *174*, 108071.
- [139] Á. Georgiádes, S. B. Ötvös, F. Fülöp, *ACS Sustainable Chem. Eng.* **2015**, *3*, 3388.
- [140] R. J. Tombari, J. R. Tuck, N. Yardeny, P. W. Gingrich, D. J. Tantillo, D. E. Olson, *Org. Biomol. Chem.* **2021**, *19*, 7575.
- [141] A. Lennartson, A. Roffey, K. Moth-Poulsen, *Tetrahedron Lett.* **2015**, *56*, 1457.
- [142] H.-D. Scharf, J. Fleischhauer, H. Leismann, I. Ressler, W. Schleker, R. Weitz, *Angew. Chem. Int. Ed.* **1979**, *18*, 652.
- [143] T. J. Kucharski, Y. Tian, S. Akbulatov, R. Boulatov, *Energy Environ. Sci.* **2011**, *4*, 4449.
- [144] A. Fihey, A. Perrier, W. R. Browne, D. Jacquemin, *Chem. Soc. Rev.* **2015**, *44*, 3719.
- [145] S. G. Telfer, T. M. McLean, M. R. Waterland, *Dalton trans.* **2011**, *40*, 3097.
- [146] K. Uchida, G. Masuda, Y. Aoi, K. Nakayama, M. Irie, *Chem. Lett.* **1999**, *28*, 1071.
- [147] A. Kunz, H. A. Wegner, *ChemSystemsChem* **2021**, *3*, e200003.
- [148] A. Perrier, F. Maurel, D. Jacquemin, *J. Phys. Chem. C* **2011**, *115*, 9193.
- [149] F. M. Raymo, M. Tomasulo, *Chem. Soc. Rev.* **2005**, *34*, 327.
- [150] A. U. Petersen, J. Kirschner Solberg Hansen, E. Sperling Andreassen, S. Peder Christensen, A. Tolstrup, A. Bo Skov, A. Vlasceanu, M. Cacciarini, M. Brøndsted Nielsen, *Chem. Eur. J* **2020**, *26*, 13419.
- [151] P. Kumar, D. Gupta, S. Grewal, A. Srivastava, A. Kumar Gaur, S. Venkataramani, *Chem. Rec.* **2022**, e202200074.
- [152] M. Li, S. Yang, W. Liang, X. Zhang, D. Qu, *Dyes and Pigments* **2019**, *166*, 239.
- [153] A. Perrier, F. Maurel, D. Jacquemin, *Acc. Chem. Res.* **2012**, *45*, 1173.
- [154] F. Zhao, L. Grubert, S. Hecht, D. Bléger, *Chem. Commun.* **2017**, *53*, 3323.

- [155] A. H. Heindl, J. Becker, H. A. Wegner, *Chem. Sci.* **2019**, *10*, 7418.
- [156] F. Cisnetti, R. Ballardini, A. Credi, M. T. Gandolfi, S. Masiero, F. Negri, S. Pieraccini, G. P. Spada, *Chem. Eur. J* **2004**, *10*, 2011.
- [157] Y.-K. Lim, S. Choi, K. B. Park, C.-G. Cho, *J. Org. Chem.* **2004**, *69*, 2603.
- [158] C. Yang, C. Slavov, H. A. Wegner, J. Wachtveitl, A. Dreuw, *Chem. Sci.* **2018**, *9*, 8665.
- [159] A. H. Heindl, H. A. Wegner, *Beilstein J. Org. Chem.* **2020**, *16*, 22.
- [160] D. Bléger, J. Dokić, M. V. Peters, L. Grubert, P. Saalfrank, S. Hecht, *J. Phys. Chem. B* **2011**, *115*, 9930.
- [161] T. J. Kucharski, N. Ferralis, A. M. Kolpak, J. O. Zheng, D. G. Nocera, J. C. Grossman, *Nat. Chem.* **2014**, *6*, 441.
- [162] A. Kunz, N. Oberhof, F. Scherz, L. Martins, A. Dreuw, H. A. Wegner, *Chem. Eur. J* **2022**, *28*, e202200972.
- [163] S. T. J. Ryan, J. del Barrio, R. Suardíaz, D. F. Ryan, E. Rosta, O. A. Scherman, *Angew. Chem. Int. Ed.* **2016**, *55*, 16096.
- [164] X. Chi, W. Cen, J. A. Queenan, L. Long, V. M. Lynch, N. M. Khashab, J. L. Sessler, *J. Am. Chem. Soc.* **2019**, *141*, 6468.
- [165] J. Wei, T.-T. Jin, J.-X. Yang, X.-M. Jiang, L.-J. Liu, T.-G. Zhan, K.-D. Zhang, *Tetrahedron Lett.* **2020**, *61*, 151389.
- [166] Y. Liu, H. Wang, P. Liu, H. Zhu, B. Shi, X. Hong, F. Huang, *Angew. Chem. Int. Ed.* **2021**, *60*, 5766.
- [167] M. Müri, K. C. Schuermann, L. de Cola, M. Mayor, *Eur. J. Org. Chem.* **2009**, 2562.
- [168] X. Xu, N. Zhou, J. Zhu, Y. Tu, Z. Zhang, Z. Cheng, X. Zhu, *Macromol. Rapid Commun.* **2010**, *31*, 1791.
- [169] R. Reuter, H. A. Wegner, *Chem. Commun.* **2011**, *47*, 12267.
- [170] L. Gobbi, P. Seiler, F. Diederich, *Angew. Chem. Int. Ed.* **1999**, *38*, 674.
- [171] M. M. Lerch, M. J. Hansen, W. A. Velema, W. Szymanski, B. L. Feringa, *Nat. Commun.* **2016**, *7*, 12054.
- [172] A. Vlasceanu, M. Koerstz, A. B. Skov, K. V. Mikkelsen, M. B. Nielsen, *Angew. Chem.* **2018**, *130*, 6177.
- [173] M. W. H. Hoorens, M. Medved', A. D. Laurent, M. Di Donato, S. Fanetti, L. Slappendel, M. Hilbers, B. L. Feringa, W. Jan Buma, W. Szymanski, *Nat. Commun.* **2019**, *10*, 2390.

- 
- [174] T. Mrozek, J. Daub, H. Görner, *Chem. Commun.* **1999**, 1487.
- [175] T. Mrozek, H. Görner, J. Daub, *Chem. Eur. J.* **2001**, *7*, 1028.
- [176] H. Nie, J. L. Self, A. S. Kuenstler, R. C. Hayward, J. Read de Alaniz, *Adv. Optical Mater.* **2019**, *7*, 1900224.
- [177] A. D. Dubonosov, S. V. Galichev, V. A. Chernov, V. A. Bren', V. I. Minkin, *Russ. J. Org. Chem.* **2001**, *37*, 67.
- [178] A. Mengots, A. Erbs Hillers-Bendtsen, S. Doria, F. Ørsted Kjeldal, N. Machholdt Høyer, A. Ugleholdt Petersen, K. V. Mikkelsen, M. Di Donato, M. Cacciarini, M. Brøndsted Nielsen, *Chem. Eur. J.* **2021**, *27*, 12437.